АВТОМАТИКА
И
ТЕЛЕМЕХАНИКА

Vol. 21, No. 11, November, 1960

Translation Published May, 1961

SOVIET INSTRUMENTATION AND
CONTROL TRANSLATION SERIES

Automation and Remote Control

(The Soviet Journal *Avtomatika i Telemekhanika* in English Translation)

■ This translation of a Soviet journal on automatic control is published as a service to American science and industry. It is sponsored by the Instrument Society of America under a grant in aid from the National Science Foundation, continuing a program initiated by the Massachusetts Institute of Technology.

SOVIET INSTRUMENTATION AND CONTROL TRANSLATION SERIES

■ This translation of the Soviet Journal *Avtomatika i Telemekhanika* is published and distributed at nominal subscription rates under a grant in aid to the Instrument Society of America from the National Science Foundation. This translated journal, and others in the Series (see back cover), will enable American scientists and engineers to be informed of work in the fields of instrumentation, measurement techniques, and automatic control reported in the Soviet Union.

The original Russian articles are translated by competent technical personnel. The translations are on a cover-to-cover basis and the Instrument Society of America and its translators propose to translate faithfully all of the scientific material in *Avtomatika i Telemekhanika*, permitting readers to appraise for themselves the scope, status, and importance of the Soviet work. All views expressed in the translated material are intended to be those of the original authors and not those of the translators nor the Instrument Society of America.

Publication of *Avtomatika i Telemekhanika* in English translation started under the present auspices in April, 1958, with Russian Vol. 18, No. 1 of January, 1957. The program has been continued with the translation and printing of the 1958, 1959, and 1960 issues.

Transliteration of the names of Russian authors follows the system known as the British Standard. This system has recently achieved wide adoption in the United Kingdom, and is currently being adopted by a large number of scientific journals in the United States.

Readers are invited to submit communications on the quality of the translations and the content of the articles to ISA headquarters. Pertinent correspondence will be published in the "Letters" section of the ISA Journal. Space will also be made available in the ISA Journal for such replies as may be received from Russian authors to comments or questions by American readers.

1960 Volume 21 Subscription Prices:

Per year (12 issues), starting with Vol. 21, No. 1

General: United States and Canada	$35.00
Elsewhere	38.00
Libraries of nonprofit academic institutions:	
United States and Canada	$17.50
Elsewhere	20.50
Single issues to everyone, each	$ 6.00

1957 Volume 18, 1958 Volume 19, and 1959 Volume 20 issues also available. Prices upon request.

See back cover for combined subscription to entire Series.

Subscriptions and requests for information on back issues should be addressed to the:

Instrument Society of America
313 Sixth Avenue, Pittsburgh 22, Penna.

Translated and printed by Consultants Bureau Enterprises, Inc.

Automation and Remote Control

A translation of Avtomatika i Telemekhanika, a publication of the Academy of Sciences of the USSR

Vol. 21, No. 11 Russian Original Dated November, 1960 May, 1961

CONTENTS

DUAL CONTROL THEORY. II

A. A. Fel'dbaum

Moscow

Translated from Avtomatika i Telemekhanika, Vol. 21, No. 11,
pp. 1453-1464 , November, 1960
Original article submitted March 23, 1960

Basic formulas are derived and the optimum control algorithm is determined in the general case, first for an open-loop and then for a closed-loop nonlinear system of dual control [1].

Similarities and differences between the solutions for open and closed systems are indicated.

1. Derivation of the Risk Formula in Open-Loop Systems

We start first by deriving the formulas for an open system shown in Fig. 1. This is done to demonstrate certain methods which have led to the obtained results; also to compare certain characteristics of the open and closed systems. The open system is basically more simple than the closed one, and this makes the derivation of the formulas easier in the former case.

The problem is stated as follows [1]: all quantities are functions of discrete time at the time moments 0, 1, ..., s, ..., n, where n is fixed. The input is

$$x_s^* = x_s^*(s, \lambda), \tag{1}$$

where λ is the parameter vector

$$\lambda = (\lambda_1, \ldots, \lambda_q) \tag{2}$$

with an a priori probability density $P_0(\lambda) = P(\lambda)$. The input x^* becomes mixed with noise h^* in the channel or system H^*, at whose output y^* is obtained. Statistical properties of the noise, and the method of combining the signal and the noise in H^* are known. Consequently the conditional probability $P(y_s^*/x_s^*)$ is also known, being identical for all s , as the probability density $P(h_s^*)$ of the noise is assumed as not varying with s*.

The characteristic of the controlled object B is given by the formula

$$x_s = F_0(z_s, v_s), \tag{3}$$

where F_0 is a known function, and

$$z_s = z_s(s, \mu), \tag{4}$$

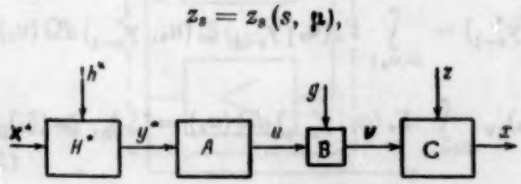

Fig. 1

in which μ is the parameter vector

$$\mu = (\mu_1, \mu_2, \ldots, \mu_m) \tag{5}$$

with given a priori probability density $P_0(\mu) = P(\mu)$. The quantity v_s is obtained at the output of the channel G, in which quantity u_s is mixed in a known manner with the noise g_s, whose probability density $P(g_s)$ does not vary with s. Thus, the conditional probability density $P(v_s|\, u_s)$ is also known. It is now required to find such a sequence of probability densities $\Gamma_s(u_s|\mathbf{y}_{s-1}^*)$, that the average risk, that is, the mathematical expectation of the quantity

$$W = \sum_{s=0}^{s=n} W_s(s, x_s^*, x_s), \tag{6}$$

will be minimum.

Therefore, the minimum of the quantity

$$R = M\{W\} = \sum_{s=0}^{s=n} M\{W_s\} = \sum_{s=0}^{s=n} R_s \tag{7}$$

is required. The function Γ_s is the required algorithm of the controlling member A.

Further notation is introduced. Let $P(x_s|\, u_s)$ be the conditional probability density of x_s with given u_s. This function can be computed from the formulas (3) and (4), when the probability density $P(\mu)$ is known. In addition, let $P(\mathbf{y}_{s-1}^*|\, \mathbf{x}_{s-1}^*)$ be the conditional probability density of the vector

$$\mathbf{y}_{s-1}^* = (y_0^*, y_1^*, \ldots, y_{s-1}^*) \tag{8}$$

when the vector

$$\mathbf{x}_{s-1}^* = (x_0^*, x_1^*, \ldots, x_{s-1}^*) \tag{9}$$

is known.

It follows from the properties of the channel H^* that

$$P(\mathbf{y}_{s-1}^*|\mathbf{x}_{s-1}^*) = \prod_{i=0}^{i=s-1} P(y_i^*|\, x_i^*). \tag{10}$$

* All external noises are regarded as independent.

The vector $\mathbf{x}^*_{s-1}$ depends on s and $\boldsymbol{\lambda}$, and therefore $P(\mathbf{y}^*_{s-1}|\,\mathbf{x}^*_{s-1})$ depends also on s and $\boldsymbol{\lambda}$.

We denote by $\Omega(x_s, v_s, u_s, \mathbf{y}^*_{s-1})$ the region of variation of the parameters x_s, v_s, u_s, $\mathbf{y}^*_{s-1}$. An infinitely small element of this region is denoted by

$$d\Omega(x_s, v_s, u_s, \mathbf{y}^*_{s-1}) = dx_s\, dv_s\, du_s\, dy^*_0 \ldots dy^*_{s-1} \quad (11)$$

At first we shall write down the expression for the conditional partial risk r_s at the sth moment, understanding by the latter the magnitude of the risk R_s when the vector $\mathbf{x}^*_s$ is kept fixed or, what amounts to the same, when the vector $\boldsymbol{\lambda}$ remains fixed. Then

$$r_s = M\{W_s|\,\mathbf{x}^*_s\} =$$

$$= \int\limits_{\Omega(x_s, v_s, u_s, \mathbf{y}^*_{s-1})} W_s(s, x^*_s, x_s)\, P(x_s|v_s) \times \quad (12)$$

$$\times P(v_s|u_s)\, \Gamma_s(u_s|\,\mathbf{y}^*_{s-1})$$

$$P(\mathbf{y}^*_{s-1}|\,\mathbf{x}^*_{s-1})\, d\Omega(x_s, v_s, u_s, \mathbf{y}^*_{s-1}).$$

Let $\Omega(\boldsymbol{\lambda})$ be the region of variation of the vector $\boldsymbol{\lambda}$ and $d\Omega(\boldsymbol{\lambda})$ an infinitely small element of it. The partial risk R_s is given by the formula

$$R_s = \int\limits_{\Omega(\lambda)} r_s P(\boldsymbol{\lambda})\, d\Omega(\boldsymbol{\lambda}) =$$

$$= \int\limits_{\Omega(x_s, u_s, v_s, \mathbf{y}^*_{s-1}, \lambda)} W_s(s, x^*_s, x_s)\, P(x_s|v_s) \times$$

$$\times P(v_s|u_s)\, \Gamma_s(u_s|\,\mathbf{y}^*_{s-1})\, P(\mathbf{y}_{s-1}|\,\mathbf{x}^*_{s-1})$$

$$P(\boldsymbol{\lambda})\, d\Omega(x_s, u_s, v_s, \mathbf{y}_{s-1}, \boldsymbol{\lambda}) =$$

$$= \int\limits_{\Omega(x_s, u_s, v_s, \mathbf{y}_{s-1})} P(x_s|v_s)\, P(v_s|u_s)\, \Gamma_s(u_s|\,\mathbf{y}^*_{s-1})$$

$$\Big\{ \int\limits_{\Omega(\lambda)} W_s[s, x^*_s(s, \boldsymbol{\lambda}), x_s] \times$$

$$\times P(\mathbf{y}^*_{s-1}|\,\mathbf{x}^*_{s-1})\, P(\boldsymbol{\lambda})\, d\Omega(\boldsymbol{\lambda}) \Big\}\, d\Omega(x_s, u_s, v_s, \mathbf{y}^*_{s-1}). \quad (13)$$

The expression in the braces represents an integral over the region $\Omega(\boldsymbol{\lambda})$, as W_s and $P(\mathbf{y}^*_{s-1}|\,\mathbf{x}^*_{s-1})$ generally depend on $\boldsymbol{\lambda}$. Having performed the integration, we obtain a function ρ_s in the braces depending on x_s, s, $\mathbf{y}^*_{s-1}$. The dependence on s is shown in the index s, and therefore one can write

$$\rho_s = \rho_s(x_s, \mathbf{y}^*_{s-1}) = \int\limits_{\Omega(\lambda)} W_s[s, x^*_s(s, \boldsymbol{\lambda}), x_s] \cdot$$

$$\cdot P(\mathbf{y}^*_{s-1}|\,\mathbf{x}^*_{s-1})\, P(\boldsymbol{\lambda})\, d\Omega(\boldsymbol{\lambda}). \quad (14)$$

Then

$$R_s = \int\limits_{\Omega(x_s, v_s, u_s, \mathbf{y}^*_{s-1})} P(x_s|v_s)\, P(v_s|u_s)\, \Gamma_s(u_s|\,\mathbf{y}^*_{s-1}) \times$$

$$\times \rho_s(x_s, \mathbf{y}^*_{s-1})\, d\Omega(x_s, v_s, u_s, \mathbf{y}^*_{s-1}). \quad (15)$$

From (7) the total risk R is determined from the expression

$$R = \sum_{s=0}^{s=n} R_s = \sum_{s=0}^{s=n} \int\limits_{\Omega(x_s, v_s, u_s, \mathbf{y}^*_{s-1})} P(x_s|v_s)\, P(v_s|u_s) \times$$

$$\times \Gamma_s(u_s|\,\mathbf{y}^*_{s-1})\, \rho_s(x_s, \mathbf{y}^*_{s-1})\, d\Omega(x_s, v_s, u_s, \mathbf{y}^*_{s-1}). \quad (16)$$

The functions Γ_s are to be selected in such a way that the value of R is a minimum.

2. Determination of Optimum Strategy for Open-Loop Systems

It can be seen from the formula (16) that the selection of functions Γ_s for fixed s only affects the component R_s corresponding to the sth time moment. In this way the total risk is identical with action risk and one is allowed to select Γ_s such that it minimizes a single R_s in (15). As the function Γ_s represents probability density, we have

$$\int\limits_{\Omega(u_s)} \Gamma_s(u_s)\, d\Omega(u_s) = 1. \quad (17)$$

The expression for R(s) is rewritten as follows:

$$R_s = \int\limits_{\Omega(u_s, \mathbf{y}^*_{s-1})} \Gamma_s(u_s|\,\mathbf{y}^*_{s-1}) \Big\{ \int\limits_{\Omega(x_s, v_s)} P(x_s|v_s)\, P(v_s|u_s) \times$$

$$\times \rho_s(x_s, \mathbf{y}^*_{s-1})\, d\Omega(x_s, v_s) \Big\}\, d\Omega(u_s, \mathbf{y}^*_{s-1}). \quad (18)$$

The integral in the braces represents a function of u_s and $\mathbf{y}^*_{s-1}$ which we shall denote by $\xi_s(u_s, \mathbf{y}^*_{s-1})$, that is,

$$\xi_s(u_s, \mathbf{y}^*_{s-1}) =$$

$$= \int\limits_{\Omega(x_s, v_s)} P(x_s|v_s)\, P(v_s|u_s)\, \rho_s(x_s, \mathbf{y}^*_{s-1})\, d\Omega(x_s, v_s). \quad (19)$$

Then

$$R_s = \int\limits_{\Omega(\mathbf{y}^*_{s-1})} I(\mathbf{y}^*_{s-1})\, d\Omega(\mathbf{y}^*_{s-1}),$$

where

$$I(\mathbf{y}^*_{s-1}) = \int\limits_{\Omega(u_s)} \Gamma_s(u_s|\,\mathbf{y}^*_{s-1})\, \xi_s(u_s, \mathbf{y}^*_{s-1})\, d\Omega(u_s) =$$

$$= (\xi_s)_{av} \int\limits_{\Omega(u_s)} \Gamma_s(u_s|\,\mathbf{y}^*_{s-1})\, d\Omega(u_s) = (\xi_s)_{av} \geqslant (\xi_s)_{min}. \quad (20)$$

One can take the average value $(\xi_s)_{av}$ outside the integration in accordance with the integral mean value

theorem. The function Γ_s represents probability density and hence its integral over the region $\Omega(u_s)$ equals unity.

It follows from the expression (20) that a minimum value of $I(\mathbf{y}^*_{s-1})$ is $(\xi_s)_{min}$. It is not difficult to show that I attains this value if the function Γ_s is chosen accordingly. In fact, let u^*_s be the value of u_s corresponding to the minimum (for instance, the least of all local minima) of the function $\xi_s(u_s)$ in the region $\Omega(u_s)$. We assume that such a value exists either within or on the boundary of the region.

Consider the function

$$\Gamma_s(u_s) = \delta(u_s - u^*_s), \tag{21}$$

where δ is the unit impulse function (otherwise Dirac's δ-function). Formula (21) provides the optimum algorithm of the member A, as substituting (21) into the left-hand side of (20) and using a well-known property of δ-function, we find

$$I = \int_{\Omega(u_s)} \Gamma_s(u_s \mid \mathbf{y}^*_{s-1})\, \xi_s(u_s, \mathbf{y}^*_{s-1})\, d\Omega(u_s) =$$

$$= \int_{\Omega(u_s)} \delta(u_s - u^*_s)\, \xi_s(u_s, \mathbf{y}^*_{s-1})\, d\Omega(u_s) =$$

$$= \xi_s(u^*_s) = \min_{u_s \in \Omega(u_s)} \xi_s(u_s) = (I)\ \min^* \tag{22}$$

The minimum values of I for each $\mathbf{y}^*_{s-1}$ provide also the minimum of R_s.

Thus, the optimum strategy, as seen from the formula (21), does not prove random but regular. The value of u_s should be taken as equal to a u^*_s. As seen from the formula (20), the value u^*_s which minimizes the function $\xi_s(u_s, \mathbf{y}^*_{s-1})$ depends on $\mathbf{y}^*_{s-1}$. In other words, as

$$\xi_s(u^*_s, \mathbf{y}^*_{s-1}) = \min, \tag{23}$$

the quantity u^*_s is a function of $\mathbf{y}^*_{s-1}$:

$$u^*_s = u^*_s(\mathbf{y}^*_{s-1}). \tag{24}$$

This makes also the function Γ_s in the formula (21) depend on $\mathbf{y}^*_{s-1}$:

$$\Gamma_s = \delta(u_s - u^*_s) = \delta[u_s - u^*_s(\mathbf{y}^*_{s-1})]. \tag{25}$$

Thus, the optimum strategy proves regular; it is determined in the general case from all the preceding values of y^*_i ($i = 0, \ldots, s-1$). It should be shown that the regularity of the optimum decisions occurs in a wide group of problems in Wald's general theory of statistical decisions.

The integral $\xi_s(u_s, \mathbf{y}^*_{s-1})$ can be evaluated with the aid of a computer CO (Fig. 2). The block diagram of the optimum controlling member can then be represented as shown in Fig. 2. The automatic optimizer AO selects a value u_s such that ξ_s becomes least. This value is now sent to the output of the block A. Were it possible to determine the value of u^*_s analytically as a function of $\mathbf{y}^*_{s-1}$, the block A could be constructed differently. However, the formula for $\xi_s(u_s, \mathbf{y}^*_{s-1})$ is as a rule most difficult to obtain explicitly and that is why the computer CO must perform automatically the integrations with respect to x_s and v_s, as shown in the formula (18). In this way the minimization of the integral ξ_s can be achieved directly.

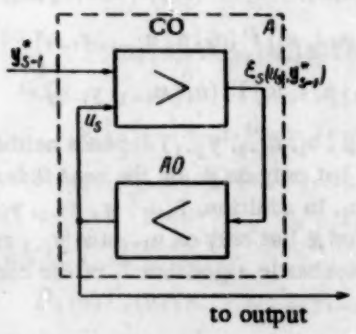

Fig. 2

3. Derivation of Risk Formula for Closed-Loop Systems

Consider now a block diagram of a closed system shown in Fig. 3. In order to simplify the exposition we neglect the interference h^* in the channel H^* (see, for example, Fig. 1 or Fig. 3 of [1]); x^* is thus assumed known. It was shown previously how the interference h^* should be taken into consideration, and should such a need arise, this can be done without any real difficulties. Our notation remains the same. In addition, there is also the feedback channel H with interference h_s which has a constant in time density distribution $P(h_s)$.

The way in which the signal and noise combine in the channel H is given and the conditional probability density $P(y_s \mid x_s)$ can therefore be found, and consequently the conditional probability density

$$P(\mathbf{y}_s \mid \mathbf{x}_s) = \prod_{i=0}^{i=s} P(y_s \mid x_s). \tag{26}$$

In a closed system it is necessary to take into account also the vectors

$$\begin{aligned} \mathbf{x}^*_s &= (x^*_0, x^*_1, \ldots, x^*_s), \\ \mathbf{y}_s &= (y_0, y_1, \ldots, y_s), \\ \mathbf{u}_s &= (u_0, u_1, \ldots, u_s), \\ \mathbf{v}_s &= (v_0, v_1, \ldots, v_s), \\ \mathbf{x}_s &= (x_0, x_1, \ldots, x_s). \end{aligned} \tag{27}$$

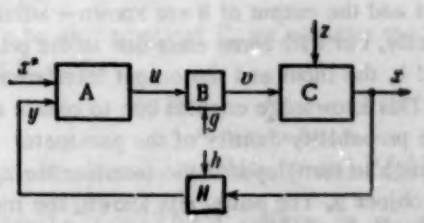

Fig. 3

The determination of the optimum controlling member A is reducible to the determination of its strategy, random in the general case, ensuring the minimizing of the risk R. The function $\Gamma_s(u_s \mid \mathbf{x}_s^*, \mathbf{y}_{s-1}, \mathbf{u}_{s-1})$, is assumed to represent random strategy, that is, the conditional probability density of u_s when the vectors $\mathbf{x}_s^*$, $\mathbf{y}_{s-1}$, and $\mathbf{u}_{s-1}$ remain fixed. Now Γ_s is a function of $\mathbf{x}_s^*$, $\mathbf{y}_{s-1}$, and u_s.

First we shall write down the expression for the conditional partial risk r_s and we shall now understand by it the risk R_s when all the preceding motions of the system A are known, that is, when the vectors $\mathbf{x}_s^*$, $\mathbf{y}_{s-1}$, and $\mathbf{u}_{s-1}$ are fixed. Thus,

$$r_s = M\{W_s \mid \mathbf{x}_s^*, \mathbf{y}_{s-1}, \mathbf{u}_{s-1}\} =$$

$$= \int_{\Omega(x_s, v_s, u_s)} W_s(s, x_s^*, x_s)\, P_s(x_s \mid v_s) \times$$

$$\times P(v_s \mid u_s)\, \Gamma_s(u_s \mid \mathbf{x}_s^*, \mathbf{y}_{s-1}, \mathbf{u}_{s-1})\, d\Omega(x_s, v_s, u_s). \tag{28}$$

In this formula $P_s(x_s \mid v_s)$ is understood to represent the conditional probability density of the output $\underline{x}$ from the object B when its input $\underline{y}$ is known; as shown below, this probability need not be the same for different $\underline{s}$.

If one considers the values of r_s corresponding to different trials of the system, then generally speaking the vectors $\mathbf{u}_{s-1}$ and $\mathbf{y}_{s-1}$, not known beforehand, can for different trials assume different values. Therefore, in computing the average partial risk R_s it is necessary, when averaging r_s, to take into account the joint probability distributions $P(\mathbf{u}_{s-1}, \mathbf{y}_{s-1})$ of the vectors $\mathbf{u}_{s-1}$ and $\mathbf{y}_{s-1}$, which in the general case are not statistically independent of one another. Thus,

$$R_s = M\{r_s\} =$$

$$= \int_{\Omega(x_s, v_s, u_s, y_{s-1})} W_s(s, x_s^*, x_s)\, P_s(x_s \mid v_s)\, P(v_s \mid u_s) \times$$

$$\times \Gamma_s(u_s \mid \mathbf{x}_{s-1}^*, \mathbf{u}_{s-1}, \mathbf{y}_{s-1})\, P(\mathbf{u}_{s-1}, \mathbf{y}_{s-1})$$

$$d\Omega(x_s, v_s, u_s, \mathbf{y}_{s-1}). \tag{29}$$

The values of the quantities u_i and y_i ($i = 0, \ldots, s-1$) are memorized in the controlling member A. Thus the input and the output of B are known — admittedly not exactly, but with some error due to the presence of $\underline{g}$ and $\underline{h}$, the input and the output interference respectively. This knowledge enables one to obtain a more accurate probability density of the parameter vector $\boldsymbol{\mu}$ on which in turn depends the interference z_s acting on the object B. The better $\boldsymbol{\mu}$ is known, the more fully determined is the method of regulating the object. One can derive a Bayesian formula in order to determine the a posteriori probability density of vector $\boldsymbol{\mu}$ in the $\underline{s}$th beat. Consider the probability density† $P(\boldsymbol{\mu}, \mathbf{u}_{s-1}, \mathbf{y}_{s-1})$ of a joint event consisting in a simultaneous occurrence of the vectors $\boldsymbol{\mu}$, $\mathbf{u}_{s-1}$ and $\mathbf{y}_{s-1}$. Let $P(\mathbf{u}_{s-1}, \mathbf{y}_{s-1} \mid \boldsymbol{\mu})$ be the conditional joint probability density of the vectors $\mathbf{u}_{s-1}$ and $\mathbf{y}_{s-1}$ when $\boldsymbol{\mu}$ is kept fixed and $P(\boldsymbol{\mu} \mid \mathbf{u}_{s-1}, \mathbf{y}_{s-1})$ is the conditional probability density of $\boldsymbol{\mu}$ when the vectors $\mathbf{u}_{s-1}$ and $\mathbf{y}_{s-1}$ are fixed. The latter is the required a posteriori probability density of the vector $\boldsymbol{\mu}$. Then, of course,

$$P(\boldsymbol{\mu}, \mathbf{u}_{s-1}, \mathbf{y}_{s-1}) = P(\mathbf{u}_{s-1}, \mathbf{y}_{s-1} \mid \boldsymbol{\mu})\, P(\boldsymbol{\mu}) =$$

$$P(\boldsymbol{\mu} \mid \mathbf{u}_{s-1}, \mathbf{y}_{s-1})\, P(\mathbf{u}_{s-1}, \mathbf{y}_{s-1}). \tag{30}$$

$P(\boldsymbol{\mu})$ denotes the a priori probability density of vector $\boldsymbol{\mu}$. Hence the formula is obtained giving the a posteriori probability density of vector $\boldsymbol{\mu}$:

$$P(\boldsymbol{\mu} \mid \mathbf{u}_{s-1}, \mathbf{y}_{s-1}) = \frac{P(\boldsymbol{\mu})\, P(\mathbf{u}_{s-1}, \mathbf{y}_{s-1} \mid \boldsymbol{\mu})}{P(\mathbf{u}_{s-1}, \mathbf{y}_{s-1})} =$$

$$= \frac{P(\boldsymbol{\mu})\, P(\mathbf{u}_{s-1}, \mathbf{y}_{s-1} \mid \boldsymbol{\mu})}{\int_{\Omega(\mu)} P(\mathbf{u}_{s-1}, \mathbf{y}_{s-1} \mid \boldsymbol{\mu})\, P(\boldsymbol{\mu})\, d\Omega(\boldsymbol{\mu})}. \tag{31}$$

In the latter formula $\Omega(\boldsymbol{\mu})$ denotes the range of variability of vector $\boldsymbol{\mu}$ and $d\Omega(\boldsymbol{\mu})$ its infinitely small element.

In formula (31) a special role is played by the likelihood function $P(\mathbf{u}_{s-1}, \mathbf{y}_{s-1} \mid \boldsymbol{\mu})$. The probability densities of quantities are called likelihood functions when the vector $\boldsymbol{\mu}$, whose values are subject to hypothesis testing, is kept fixed. We obtain the likelihood function for the closed-loop system shown in Fig. 3. Obviously, we have

$$P(\mathbf{u}_{s-1}, \mathbf{y}_{s-1} \mid \boldsymbol{\mu}) = P(u_0, y_0 \mid \boldsymbol{\mu})\, P(u_1, y_1 \mid \boldsymbol{\mu}, u_0, y_0) \times$$
$$\times P(u_2, y_2 \mid \boldsymbol{\mu}, u_1, y_1) \ldots P(u_{s-1}, y_{s-1} \mid \boldsymbol{\mu}, \mathbf{u}_{s-2}, \mathbf{y}_{s-2}). \tag{32}$$

A typical factor on the right-hand side is a probability density

$$P(u_i, y_i \mid \boldsymbol{\mu}, \mathbf{u}_{i-1}, \mathbf{y}_{i-1}) =$$

$$= P(y_i \mid \boldsymbol{\mu}, u_i, \mathbf{u}_{i-1}, \mathbf{y}_{i-1})\, P(u_i \mid \boldsymbol{\mu}, \mathbf{u}_{i-1}, \mathbf{y}_{i-1}) =$$

$$= P(y_i \mid \boldsymbol{\mu}, i, u_i)\, P(u_i \mid \boldsymbol{\mu}, \mathbf{u}_{i-1}, \mathbf{y}_{i-1}) =$$

$$= P(y_i \mid \boldsymbol{\mu}, i, u_i)\, \Gamma_i(u_i \mid \mathbf{u}_{i-1}, \mathbf{y}_{i-1}). \tag{33}$$

Thus $P(y_i \mid \boldsymbol{\mu}, u_i, \mathbf{u}_{i-1}, \mathbf{y}_{i-1})$ depends neither on $\mathbf{u}_{i-1}$ nor on $\mathbf{y}_{i-1}$, but only on $\boldsymbol{\mu}$, on the beat index $\underline{i}$ and on the value of u_i. In addition, $P(u_i \mid \boldsymbol{\mu}, \mathbf{u}_{i-1}, \mathbf{y}_{i-1})$ does not depend on $\boldsymbol{\mu}$ but only on $\mathbf{u}_{i-1}$ and $\mathbf{y}_{i-1}$ and this is precisely the stochastic algorithm Γ_i of the controlling member A.

†In a number of subsequent formulas the dependence of the probability density on $\mathbf{x}_s^*$ is not stated explicitly but it is always implied.

By substituting the expression (33) into (32) we find that

$$P(\mathbf{u}_{s-1}, \mathbf{y}_{s-1} \mid \mu) = \Big[\prod_{i=0}^{s-1} P(y_i \mid \mu, i, u_i)\Big] \Big[\prod_{i=1}^{s-1} \Gamma_i(u_i \mid \mathbf{u}_{i-1}, \mathbf{y}_{i-1})\Big] P_0(u_0). \quad (34)$$

Here $P_0(u_0)$ is the initial probability density of $\underline{u}$ which also should be given.

Now one is able to substitute the likelihood function obtained in (34) into the a posteriori probability density formula (31). We obtain

$$P_s(\mu) = P(\mu \mid \mathbf{u}_{s-1}, \mathbf{y}_{s-1}) = P(\mu) \frac{\Big[\prod_{i=0}^{s-1} P(y_i \mid \mu, i, u_i)\Big] \prod_{i=0}^{s-1} \Gamma_i}{P(\mathbf{u}_{s-1}, \mathbf{y}_{s-1})}. \quad (35)$$

In the above formula the following notation has been introduced:

$$\Gamma_0 = P_0(u_0). \quad (36)$$

Knowing the a posteriori probability density $P_s(\mu)$ one is able to determine more precisely the expression of the probability density $P_s(x_s \mid v_s)$ which appears in the formula (29). From the formulas (3) and (4) we find that

$$x_s = F_0(z_s, v_s) = F(s, \mu, v_s). \quad (37)$$

The quantities $\underline{s}$ and v_s which appear in the function F are parameters. This formula enables one to find the conditional probability density $P_s(x_s \mid v_s)$ when $P_s(\mu)$ is known.

Since

$$\int_{(\Omega v_s)} P_s(x_s \mid v_s) P(v_s \mid u_s) d\Omega(v_s) = P_s(x_s \mid u_s) = \int_{\Omega(\mu)} P(x_s \mid \mu, u_s) P_s(\mu) d\Omega(\mu), \quad (38)$$

the expression (29) giving R_s can be re-written in the following way:

$$R_s = \int_{\Omega(x_s, \mathbf{u}_s, \mathbf{y}_{s-1})} W_s(s, x_s^*, x_s) \Big[\int_{\Omega(v_s)} P_s(x_s \mid v_s) P(v_s \mid u_s) d\Omega(v_s)\Big] \times \Gamma_s(u_s \mid \mathbf{x}_{s-1}^*, \mathbf{u}_{s-1}, \mathbf{y}_{s-1}) P(\mathbf{u}_{s-1}, \mathbf{y}_{s-1}) d\Omega(x_s, \mathbf{u}_s, \mathbf{y}_{s-1}) = \int_{\Omega(x_s, \mu, \mathbf{u}_s, \mathbf{y}_{s-1})} W_s(s, x_s^*, x_s) P(x_s \mid \mu, u_s) P_s(\mu) \Gamma_s(u_s \mid \mathbf{x}_{s-1}^*, \mathbf{u}_{s-1}, \mathbf{y}_{s-1}) \times P(\mathbf{u}_{s-1}, \mathbf{y}_{s-1}) d\Omega(x_s, \mu, \mathbf{u}_s, \mathbf{y}_{s-1}). \quad (39)$$

Substituting the formula (35) for $P_s(\mu)$ and cancelling $P(\mathbf{u}_{s-1}, \mathbf{y}_{s-1})$ we obtain

$$R_s = \int_{\Omega(x_s, \mu, \mathbf{u}_s, \mathbf{y}_{s-1})} W_s(s, x_s^*, x_s) P(x_s \mid \mu, u_s) P(\mu) \times \times \prod_{i=0}^{s-1} P(y_i \mid \mu, i, u_i) \prod_{i=0}^{s} \Gamma_i d\Omega(x_s, \mu, \mathbf{u}_s, \mathbf{y}_{s-1}). \quad (40)$$

The total risk is given by

$$R = \sum_{s=0}^{s=n} R_s = \sum_{s=0}^{s=n} \int_{\Omega(x_s, \mu, \mathbf{u}_s, \mathbf{y}_{s-1})} W_s(s, x_s^*, x_s) P(x_s \mid \mu, u_s) P(\mu) \times \times \prod_{i=0}^{s-1} P(y_i \mid \mu, i, u_i) \prod_{i=0}^{s} \Gamma_i d\Omega(x_s, \mu, \mathbf{u}_s, \mathbf{y}_{s-1}). \quad (41)$$

Let us compare the expressions (16) and (41) of risks in open and closed systems. In the formula (16) only the $\underline{s}$th component R_s was influenced by the function Γ_s; the total risk associated with Γ_s was exclusively an action risk. In the formula (41), however, the function Γ_s influenced not only the term R_s (action risk) but also all the other components R_i where $i > s$. As regards Γ_s, the sum $\sum_{i=s+1}^{n} R_i$ represents the investigation risk. In fact, the selection of Γ_s influences the character of the process in the subsequent beats, as it causes either a better or a worse investigation of the characteristics of the object B; the latter amounts to the determination of the probability density $P_s(\mu)$. Thus the total risk regarded as a function of Γ_s ($0 \leq s \leq n$) represents the sum of the action risk and the investigation risk. As regards Γ_n only a single action risk occurs.

When the object B has memory the selection of Γ_s influences not only R_s but also the terms R_i when $i > s$ even when the additional investigation of the object B has not taken place (see Paper IV in this series). Consequently, in this case the action risk is expressed by a more involved formula, and the interconnection between the action and the investigation risks proves also to be more involved.

4. Determination of Optimum Strategy in Closed Systems

It is required to select the functions Γ_i in the formula (41) such that the risk R be minimum. As Γ_i represents probability densities they must satisfy the condition (17).

To be able to select Γ_n we consider the last component R_n of R:

$$R_n = \int_{\Omega(x_n, \mu, \mathbf{u}_n, \mathbf{y}_{n-1})} W_n(n, x_n^*, x_n) P(x_n \mid \mu, u_n) P(\mu) \times \times \prod_{i=0}^{n-1} P(y_i \mid \mu, i, u_i) \prod_{i=0}^{n-1} \Gamma_i \Gamma_n \, d\Omega(x_n, \mu, \mathbf{u}_n, \mathbf{y}_{n-1}). \quad (42)$$

We assume that $\Gamma_0, \ldots, \Gamma_{n-1}$ are given and only Γ_n is to be selected such that R_n becomes minimum provided a constraint as in (17) is satisfied:

$$\int_{\Omega(u_n)} \Gamma_n(u_n, \mathbf{u}_{n-1}, \mathbf{y}_{n-1})\, d\Omega(u_n) = 1. \quad (43)$$

In order to simplify the expression (42), put

$$\alpha_n = \alpha_n(\mathbf{u}_n, \mathbf{y}_{n-1}) = \int_{\Omega(x_n, \mu)} W_n(n, x_n, x_n^*)\, P(x_n \mid \mu, u_n)\, P(\mu) \prod_{i=0}^{n-1} P(y_i \mid \mu, i, u_i)\, d\Omega(x_n, \mu). \quad (44)$$

Further, put

$$\beta_k = \prod_{i=0}^{k} \Gamma_k; \quad (45)$$

then

$$R_n = \int_{\Omega(u_n, u_{n-1}, y_{n-1})} \alpha_n(u_n, \mathbf{u}_{n-1}, \mathbf{y}_{n-1})\, \beta_{n-1}\, \Gamma_n\, d\Omega(\mathbf{u}_n, \mathbf{y}_{n-1}) = \int_{\Omega(u_{n-1}, y_{n-1})} \beta_{n-1} \varkappa_n(\mathbf{u}_{n-1}, \mathbf{y}_{n-1})\, d\Omega(\mathbf{u}_{n-1}, \mathbf{y}_{n-1}), \quad (46)$$

where

$$\varkappa_n(\mathbf{u}_{n-1}, \mathbf{y}_{n-1}) = \int_{\Omega(u_n)} \alpha_n(u_n, \mathbf{u}_{n-1}, \mathbf{y}_{n-1})\, \Gamma_n(u_n, \mathbf{u}_{n-1}, \mathbf{y}_{n-1})\, d\Omega(u_n). \quad (47)$$

If the Γ_n is selected such that for any set of vectors $\mathbf{u}_{n-1}$ and $\mathbf{y}_{n-1}$ the quantity $\varkappa_n$ remains least, then the integral (46) will also be minimum (bearing in mind that the quantity β_{n-1} is assumed known. By regarding the vectors $\mathbf{u}_{n-1}$ and $\mathbf{y}_{n-1}$ in the formulas (44) and (47) as parameters, one is able to find a value u_n^* such that the function α_n is minimum. We put

$$\gamma_n^* = \alpha_n(u_n^*, \mathbf{u}_{n-1}, \mathbf{y}_{n-1}) = \min_{u_n \in \Omega(u_n)} \alpha_n(u_n, \mathbf{u}_{n-1}, \mathbf{y}_{n-1}). \quad (48)$$

The quantity u_n^*, of course, depends on $\mathbf{u}_{n-1}$ and $\mathbf{y}_{n-1}$:

$$u_n^* = u_n^*(\mathbf{u}_{n-1}, \mathbf{y}_{n-1}). \quad (49)$$

Then the optimum function Γ_n satisfying the condition (43) is

$$\Gamma_n(u_n, \mathbf{u}_{n-1}, \mathbf{y}_{n-1}) = \delta(u_n - u_n^*), \quad (50)$$

because in this case

$$\varkappa_n = \alpha_n(u_n^*, \mathbf{u}_{n-1}, \mathbf{y}_{n-1}) = (\alpha_n)_{\min} = (\varkappa_n)_{\min}. \quad (51)$$

This follows from the considerations similar to those given above when the conditions (19), (20), and (21) were derived.

Now the optimum function Γ_{n-1} will be determined. Consider the sum of the last two terms R_{n-1} and R_n. First of all, we introduce the function

$$\alpha_k = \alpha_k(u_k, \mathbf{u}_{k-1}, \mathbf{y}_{k-1}) = \int_{\Omega(x_k, \mu)} W_k(k, x_k^*, x_k)\, P(x_k \mid \mu, u_k) \times P(\mu) \prod_{i=0}^{k-1} P(y_i \mid \mu, i, u_i)\, d\Omega(x_k, \mu) \quad (0 \leqslant k \leqslant n). \quad (52)$$

There the expression $\prod_{i=0}^{k-1} P(y_i \mid \mu, i, u_i)$ equals unity when $k = 0$.

Now the sum of the last two terms becomes

$$S_{n-1} = R_{n-1} + R_n = \int_{\Omega(u_{n-1}, y_{n-2})} \alpha_{n-1} \beta_{n-1}\, d\Omega(\mathbf{u}_{n-1}, \mathbf{y}_{n-2}) + \int_{\Omega(u_n, y_{n-1})} \alpha_n \beta_n\, d\Omega(\mathbf{u}_n, \mathbf{y}_{n-1}). \quad (53)$$

When $i \leq n-2$, the Γ_i are assumed to be known and Γ_n is always selected in accordance with the formula (50). Then

$$S_{n-1} = \int_{\Omega(u_{n-2}, y_{n-2})} \beta_{n-2} \left\{ \int_{\Omega(u_{n-1})} \Gamma_{n-1} \alpha_{n-1}\, d\Omega(u_{n-1}) + \int_{\Omega(u_{n-1}, y_{n-1})} \Gamma_{n-1} \alpha_n(u_n^*, \mathbf{u}_{n-1}, \mathbf{y}_{n-1})\, d\Omega(u_{n-1}, y_{n-1}) \right\}. \quad (54)$$

This quantity is least when the expression within the braces is least; we write the latter in full as

$$\varkappa_{n-1}(\mathbf{u}_{n-2}, \mathbf{y}_{n-2}) = \int_{\Omega(u_{n-1})} \left\{ \Gamma_{n-1} \alpha_{n-1} + \int_{\Omega(y_{n-1})} \Gamma_{n-1} \alpha_n(u_n^*, \mathbf{u}_{n-1}, \mathbf{y}_{n-1})\, d\Omega(y_{n-1}) \right\} d\Omega(u_{n-1}) = \int_{\Omega(u_{n-1})} \Gamma_{n-1}(u_{n-1}, \mathbf{u}_{n-2}, \mathbf{y}_{n-2}) \times \left\{ \alpha_{n-1} + \int_{\Omega(y_{n-1})} \alpha_n(u_n^*, \mathbf{u}_{n-1}, \mathbf{y}_{n-1})\, d\Omega(y_{n-1}) \right\} d\Omega(u_{n-1}). \quad (55)$$

Now consider the function

$$\gamma_{n-1} = \gamma_{n-1}(\mathbf{u}_{n-1}, \mathbf{y}_{n-2}) = \alpha_{n-1} + \int_{\Omega(y_{n-1})} \alpha_n(u_n^*, \mathbf{u}_{n-1}, \mathbf{y}_{n-1})\, d\Omega(y_{n-1}). \quad (56)$$

We find the value u_{n-1}^* which is the minimum value of this function. This value obviously depends on $\mathbf{u}_{n-2}$ and $\mathbf{y}_{n-2}$:

$$u_{n-1}^* = u_{n-1}^*(\mathbf{u}_{n-2}, \mathbf{y}_{n-2}). \quad (57)$$

Then the most suitable function Γ_{n-1} such that it ensures the minimum of κ_{n-1} and satisfies the condition (17) will be

$$\Gamma_{n-1}(u_{n-1}, u_{n-2}, y_{n-2}) = \delta(u_{n-1} - u^*_{n-1}). \quad (58)$$

By applying analogous arguments one can determine the whole sequence of the functions Γ_i using the following procedure.

We introduce the function

$$\gamma_{n-k} = \alpha_{n-k} + \int_{\Omega(y_{n-k})} \gamma_{n-k+1}(u^*_{n-k+1}, u_{n-k}, y_{n-k})\, d\Omega(y_{n-k}), \quad (59)$$

where $\gamma_n = \alpha_n$. Let the minimum of γ_{n-k} over u_{n-k} be denoted by γ^*_{n-k}:

$$\gamma^*_{n-k} = (\gamma_{n-k})_{u_{n-k}=u^*_{n-k}} = \min_{u_{n-k}\in\Omega(u_{n-k})} \gamma_{n-k}(u_{n-k}; u_{n-k-1}, y_{n-k-1});$$

$$u^*_{n-k} = u^*_{n-k}(u_{n-k-1}; y_{n-k-1}). \quad (60)$$

Then the optimum function Γ^*_{n-k} is given by the formula

$$\Gamma^*_{n-k} = \delta(u_{n-k} - u^*_{n-k}), \quad (61)$$

where δ is the unit impulse function. Then

$$(S_{n-k})_{\min} = \Big(\sum_{i=0}^{i=k} R_{n-i}\Big)_{\min} = \int_{\Omega(u_{n-k-1}, y_{n-k-1})} \beta_{n-k-1}\gamma^*_{n-k}\, d\Omega(u_{n-k-1}, y_{n-k-1}). \quad (62)$$

In this way Γ_i are determined when $i = n, n-1, \ldots, 1$. As far as the determination of $\Gamma_0 = P_0(u_0)$ is concerned, this function may be given beforehand and then no selection is required. If the best Γ_0 can be chosen, the selection takes place in accordance with the procedure shown above. When $k = n-1$ we arrive at the formula

$$(S_1)_{\min} = \int_{\Omega(u_0, y_0)} P_0(u_0)\gamma^*_1(u_0, y_0)\, d\Omega(u_0, y_0). \quad (63)$$

The total risk therefore when all Γ_i ($i = 1, \ldots, n$) are optimal, is expressed by the formula

$$R = R_0 + (S_1)_{\min} = \int_{\Omega(x_0, \mu, u_0)} W_0(0, x^*_0, x_0) P(x_0 | \mu, u_0) \times P(\mu) P_0(u_0)\, d\Omega(x_0, \mu, u_0) + \int_{\Omega(u_0, y_0)} P_0(u_0)\gamma^*_1(u_0, y_0)\, d\Omega(u_0, y_0) =$$

$$= \int_{\Omega(u_0)} P_0(u_0)\Big[\alpha_0(u_0) + \int_{\Omega(y_0)} \gamma^*_1(u_0, y_0)\, d\Omega(y_0)\Big] d\Omega(u_0), \quad (64)$$

where

$$\alpha_0 = \alpha_0(u_0) = \int_{\Omega(x_0, \mu)} W_0(0, x^*_0, x_0) P(x_0 | \mu, u_0) P(\mu)\, d\Omega(x_0, \mu). \quad (65)$$

We put

$$\gamma_0 = \gamma_0(u_0) = \alpha_0(u_0) + \int_{\Omega(y_0)} \gamma^*_1(u_0, y_0)\, d\Omega(y_0). \quad (66)$$

It can be seen from the formula (64) that the quantity R becomes minimum when

$$\Gamma_0 = P_0(u_0) = \Gamma^*_0 = \delta(u_0 - u^*_0), \quad (67)$$

where the value u^*_0 makes the function $\gamma(u_0)$ minimum.

The value u^*_0 is dependent on the a priori probabilities, also generally on the given data, but not on observations which are not available at the initial moment of time.

Thus in the case of a closed system as well, the optimum strategy proves to be not random but a regular one. This conclusion is naturally valid within the bounds of the limitations accepted when formulating this theory.

The determination of sequence of functions γ_{n-k} may prove rather tedious in actual examples if electronic computers are not used. Even so, it has only been possible so far to solve only relatively simple problems in which the memory capacity necessary to memorize the functions is not too great.

The obtained system with the optimum control algorithm Γ^*_i is, generally speaking, a dual control system in which the u_i serve not only as directing but also as investigating operations. In the absence of investigation, the probability density $P_s(\mu)$ would remain equal to $P_0(\mu)$ and the investigation risk would be null.

It may happen that in a particular case of a dual control system the process of investigating the object proceeds in the same way, no matter what the values of the regulating operations within the admissible bandwidth; what is only required is that the regulating operations take place. Such a system (an example is given in the next paper) is called neutral. In a neutral system the investigation risk is independent of the quantity u_i, but $P_s(\mu)$ is not identical with $P_0(\mu)$ but varies with s.

LITERATURE CITED

1. A. A. Fel'dbaum, "Theory of dual control. I," Avtomat. i Telemekh. 21, No. 9 (1960). ‡

‡See English translation.

THE DYNAMICS OF SELF-ADAPTIVE SYSTEMS WITH EXTREMAL CONTINUOUS ADJUSTMENT OF THE COMPENSATING NETWORK IN THE PRESENCE OF RANDOM DISTURBANCES

I. E. Kazakov

Moscow

Translated from Avtomatika i Telemekhanika, Vol. 21, No. 11, pp. 1465-1474, November, 1960
Original article submitted May 28, 1960

The problem is considered of estimating the accuracy of self-adaptive systems with extremal continuous adjustment of the compensating network parameters, where this adjustment is made by using the gradient method, and variable controlling signals, variable object parameters, and random disturbances are considered.

1. Formulation of the Problem

The development and application of self-adaptive systems gives rise to problems in the probability-theoretic analysis of these systems under the influence of random disturbances. The solution of these problems can be used as a basis for the synthesis and design of the systems. The statistical theory of self-adaptive systems is in its initial stage of development. At the present time, known results have been obtained in the theory of discrete (step) systems of extremal control. The mean error of control and the optimal size of the steps have been determined for such systems in the case of random disturbances of particular types. This work has appeared in several papers. The main directions of these investigations are well described in [1-4].

The statistical dynamics of self-adaptive systems with continuous operation have not yet been sufficiently studied. Moreover, the design of such systems is of practical interest because of the simplicity of their construction. From the probability-theoretic investigations devoted to this type of self-adaptive system, we particularly note the works [1, 5, 6], in which the problem we are considering has been formulated in connection with systems of continuous operation. In [7] the dynamics are investigated of systems with continuous operation that use the gradient method. Also, in [8], the analysis is carried out of a particular case of a system of extremal continuous control, operating in the presence of random disturbances.

In the present work, we consider the problem of analyzing the accuracy of a self-adaptive system with continuous extremal adjustment of the compensating network parameters, where adjustment is obtained by the gradient method in relation to the variation of the external controlling signals and the parameters of the controlled object.

An automatic self-adaptive system with extremal adjustment of the compensating network parameters is essentially a system of automatic synthesis of a compensating network with a given structure. Such a system must ensure the adjustment of the compensating network parameters, such that an extremum is maintained in some index of the performance of the control process. The block diagram of such a linear system is shown in Fig. 1. It consists of a main control network and an auxiliary network for the automatic adjustment of the compensating apparatus. The structure of the compensating network is given, and the parameters of this network depend on the adjustment.

The main control network consists of the object of the control together with the control apparatus and the compensating network. The object and the control apparatus have m variable parameters $y_1, \ldots, y_m$ and are characterized by the linear operator $\Phi_R(y_1, \ldots, y_m, p)$, where $p = d/dt$. The compensating device includes n adjustable parameters $x_1, \ldots, x_n$ and can also be characterized by a linear operator $\Phi_k(x_1, \ldots, x_n, p)$. To the control system is fed the useful control signal $Z(t)$ of an arbitrary unknown form, and the random disturbance $X(t)$. The function $Z(t)$ is smooth, and varies slowly in comparison with the processes in the main control circuit.

The equations describing the operation of the main control network shown in Fig. 1 are

$$\begin{aligned} Y &= \Phi_R(y_1, \ldots, y_m, p)\, V, \\ V &= \Phi_k(x_1, \ldots, x_n, p)\,[\Delta + X], \\ \Delta &= Z - Y \end{aligned} \qquad (1)$$

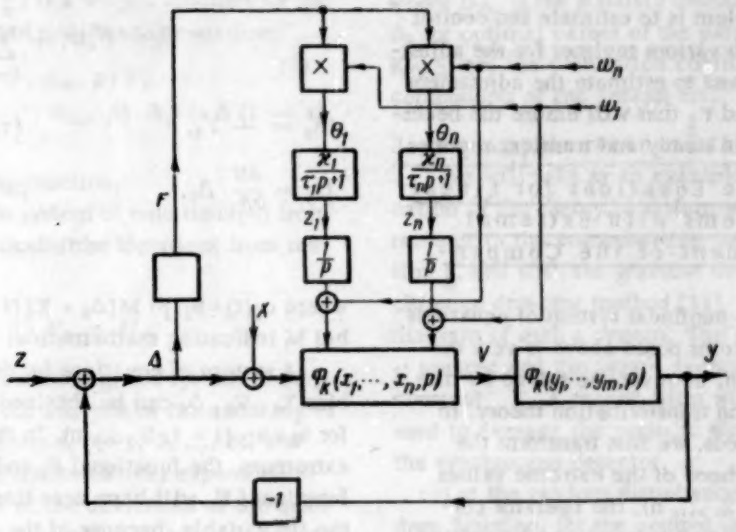

Fig. 1. Block diagram of a self-adaptive continuous system.

The auxiliary networks include a functional device for determining the control performance index F, a device for determining the extremum of the control performance index, and elements that ensure the adjustment of the parameters according to the signals $z_1, \ldots, z_n$. The form of the auxiliary networks for the extremal adjustment depend on the method used in determining the extremum of the control process performance index. This control performance index is a functional of the parameters of the objects of control and the compensating device, and also of the characteristics of the controlling signals and the disturbances.

One of the general methods of obtaining the extremal adjustment is to determine the gradient of the functional in the space of the parameters $x_1, x_2, \ldots, x_n$ and to arrange to have the adjustment of these parameters in the direction of this gradient. The method of estimating the control performance index depends on the type of problem and on the form of the disturbances experienced by the system.

When the controlling signal $Z(t)$ and the parameters of the object $y_1, \ldots, y_m$ vary slowly, and consequently the processes in the device that adjust the compensating network parameters are slow relative to the processes in the main network, and when the random disturbance $X(t)$ is a stationary random function, wide application is found in systems of automatic control of estimating the control process performance by the mean square of the control error. The functional-characterized network for obtaining an estimate of the performance of the control process consists, in this case, of a multiplying block for obtaining the square of the control error $\Delta = Z - Y$ and a device for calculating the mathematical expectation of the square of the error. It is, however, difficult in practice to construct a device that will obtain the mean square error Δ. It is simpler to carry out the averaging operation by using an inertial link with time constant T, which guarantees accurate averaging.

The equations for such a functional-characterized device are

$$U = \Delta^2, \quad (Tp + 1) F = U. \qquad (2)$$

Further auxiliary networks contain synchronous detectors which include multipliers for calculating the product of the signal F and the test signals ($i=1, 2, \ldots, n$) and the subsequent filters and inertial links for averaging the product signals Fw_i. At the output of the synchronous detectors, signals are obtained containing quantities that are proportional to the gradient components of the functional F with respect to the parameters x_i ($i = 1, \ldots, n$). The test signals are also fed directly to the adjustable parameter network. For continuous adjustment of the compensating network parameters, the rates of change of the parameters x_i ($i = 1, 2, \ldots, n$) are proportional to the measured components of the gradient, and the equations of the adjusting network are

$$\theta_i = Fw_i, \qquad (3)$$
$$(\tau_i p + 1)\, z_i = -x_i \theta_i,$$
$$p x_i = z_i + p w_i \qquad (i = 1, 2, \ldots, n),$$

where the quantities τ_i are the time constants of the filters.

The test signals w_i ($i = 1, 2, \ldots, n$) for determining the components of the gradient of F can be both sinusoidal harmonics and random, unrelated signals. When regular test signals are used, their frequency must be chosen sufficiently low, so that the signals will pass through the filter of the functional-characterized network forming the quantity F. If random test signals are used, they must possess a sufficiently low frequency spectrum.

It is obvious that the time constants satisfy the relations $\tau_i > T$ ($i = 1, 2, \ldots, n$). The system of equations (1-3) completely describes the operation of a self-a-

daptive system. The problem is to estimate the control error Δ in the system with various regimes for the adjustment of the parameters, and to estimate the adjustment network parameters κ_i and τ_i that will ensure the necessary accuracy of control in steady and transient regimes.

2. The Approximate Equations for Linear Self-Adaptive Systems with Extremal Continuous Adjustment of the Compensating Networks

The direct use of the nonlinear system of equations (1-3) for solving the problems posed above is very difficult. These problems can, however, be solved by methods from random function transformation theory. In order to apply these methods, we first transform the equations. In the neighborhood of the extreme values of the variables x_{i0} ($i = 1, 2, \ldots, n$), the operator corresponding to the compensating network can be written

$$\Phi_k(x_1, \ldots, x_n, p) = \tag{4}$$

$$= \Phi_k(x_{10}, \ldots, x_{n0}, p) + \sum_{\nu=1}^{n} u_\nu b_\nu(p) + \ldots,$$

where $b_\nu(p) = \left[\frac{\partial \Phi_k(x_i, p)}{\partial x_\nu}\right]_{x_i = x_{i0}}$ $(\nu = 1, 2, \ldots, n)$;

x_{i0} are the values of the variables x_i for which the functional F attains its extremum, and $u_\nu = x_\nu - x_{\nu 0}$ are the variations of the parameters from their extremum values.

We write the variables occurring in the equations (1) and (2) in the form

$$Y = Y_0 + \sum_{i=1}^{n} Y_i, \tag{5}$$

$$V = V_0 + \sum_{i=1}^{n} V_i, \quad \Delta = \Delta_0 + \sum_{i=1}^{n} \Delta_i,$$

$$U = U_0 + \sum_{i=1}^{n} \frac{\partial U}{\partial \Delta} \Delta_i, \quad F = F_0 + \sum_{i=1}^{n} F_i,$$

where the zero subscript indicates values of the variables corresponding to the regime of operation for optimal values of the parameters $x_i = x_{i0}$ ($i = 1, 2, \ldots, n$). The components Y_i, V_i, Δ_i, F_i are the variations of the variables for deviations of the ith parameter x_i from its nominal value. If we use the expressions (4) and (5), and limit ourselves to small quantities of the first order relative to the variations of the parameters and the variables corresponding to these parameters, we obtain the following system of equations for determining the variations in the variables:

$$Y_i = \Phi_R(y_1, \ldots, y_m, p)\, V_i, \tag{6}$$

$$(Tp + 1)\, F_i = U_i,$$

$$V_i = \Phi_k(x_{10}, \ldots, x_{n0}, p)\, \Delta_i + c_i u_i,$$

$$0_i = F_0 w_i + \sum_{k=1}^{n} F_k w_i,$$

$$\Delta_i = -Y_i, \qquad (\tau_i p + 1)\, z_i = -\varkappa_i 0_i,$$

$$U_i = \frac{\partial U}{\partial \Delta_i}\, \Delta_i, \qquad p u_i = z_i + p w_i - p x_{i0}$$

$$(i = 1, 2, \ldots, n),$$

where $c_i(t) = b_i(p)\, M[\Delta_0 + X]$ ($i = 1, 2, \ldots, n$), the symbol M indicating mathematical expectation.

A system of equations for determining the variables Y_0, V_0, Δ_0 can be obtained from the equations (1) for $x_i = x_{i0}$ ($i = 1, 2, \ldots, n$). In the neighborhood of the extremum, the functional F, and consequently, the functional U, will have zero linear terms relative to the ith variable, because of the conditions for an extremum. Therefore in determining the value of $\partial U/\partial \Delta_i$ we must take into account the quadratic term. As a result, the value of $\partial U/\partial \Delta_i$ will be obtained from the equality

$$\frac{\partial U}{\partial \Delta_i} = \sum_{j=1}^{n} \Delta_j \quad (i = 1, 2, \ldots, n). \tag{7}$$

In the general case, the investigation of the accuracy of control and the accuracy of adjustment of the compensating network parameters is therefore reduced to the integration of the system of equations (1) for $x_i = x_{i0}$ and the integration of the system of equations (6) with the conditions (7) and the subsequent calculation of the probability characteristics of the control error Δ. It should be noted that the analysis of these equations does not present any difficulty in principle for arbitrarily rapidly varying parameters, or, therefore, for any operating regime of the system.

In the practically important type of case when the processes in the parameter adjustment network are slow compared with those in the main network, the system of equations (6) can be simplified. In this case, after the main network has been operating for a certain time, the variations $u_i = x_i - x_{i0}$ ($i = 1, 2, \ldots, n$) can be considered as constant parameters. The network equations then take the form

$$(Tp + 1)(\tau_i p + 1)\, z_i = -\varkappa_i w_i^2 \sum_{j=1}^{n} b_{ij} u_j - \varkappa_i \varphi_i,$$

$$p u_i = z_i + p w_i - p x_{i0}, \qquad (i = 1, 2, \ldots, n), \tag{8}$$

where

$$\varphi_i = U_0 w_i + \sum_{k,\, j=1}^{n} b_{kj} [u_k u_j + u_j w_k + u_k w_j + w_k w_j]\, w_i - w_i^2 \sum_{j=1}^{n} b_{ij} u_j$$

$$(i = 1, 2, \ldots, n),$$

$$b_{kj} = a_k a_j \quad (k, j = 1, 2, \ldots, n), \tag{8'}$$

$$a_k = \int_0^\infty g_{\Delta_k}(t, \tau)\, c_k(\tau)\, d\tau \quad (k = 1, 2, \ldots, n).$$

The quantity $g_{\Delta_k}(t, \tau)$ is a weight function for the output Δ_k, where this output satisfies the equations

$$\begin{aligned} Y_i &= \Phi_R(y_1, \ldots, y_m, p)\, V_i, \\ V_i &= \Phi_k(x_{1\theta}, \ldots, x_{n\theta}, p)\, \Delta_i + \delta(t-\tau), \\ \Delta_i &= -Y_i, \end{aligned} \tag{9}$$

where $\delta(t-\tau)$ is the delta function.

In order to obtain the system of equations (8) from the equations (6) we use one of the equations from the system (1) for $x_i = x_{i\theta}$:

$$(Tp+1)\, F_\theta = U_\theta. \tag{10}$$

In the case we are considering, the system of equations (8) can be used for the analysis of the accuracy of adjustment of the parameters x_i ($i = 1, 2, \ldots, n$), and for the calculation of the mathematical expectation m_{u_i} and the mean square of the deviations of the quantities u_i. These accuracy estimates for the adjustment can be applied in the choice of the optimal values of the amplification coefficients κ_i and the time constants τ_i and T, and also for the choice of the test signal amplitudes w_i.

The final calculation of the mathematical expectancy of the control accuracy for a self-adaptive system is made by using the formula

$$m_\Delta = m_{\Delta_\theta} + \sum_{i=1}^{n} a_i m_{u_i}, \tag{11}$$

where m_{Δ_θ} is the mathematical expectation of the control error for the optimal values of the parameters $x_i = x_{i\theta}$, and m_{u_i} is the mathematical expectation of the parameter adjustment errors $u_i = x_i - x_{i\theta}$.

The standard deviation of the control error is calculated from the formula

$$D_\Delta = D_{\Delta_\theta} + 2\sum_{i=1}^{n} a_i K_{\Delta_\theta \Delta_i} + \sum_{i=1}^{n}\sum_{j=1}^{n} a_i a_j K_{\Delta_i \Delta_j}, \tag{12}$$

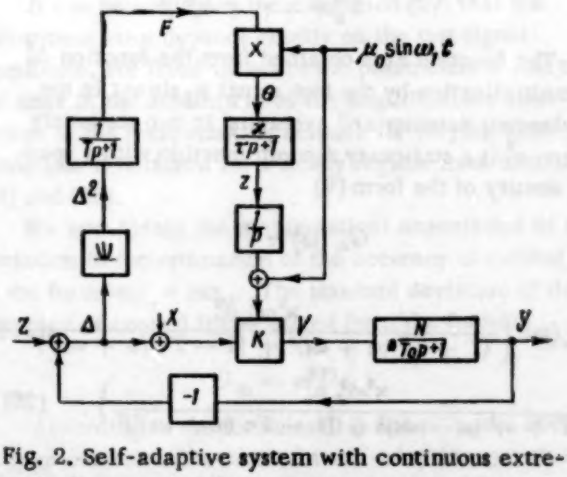

Fig. 2. Self-adaptive system with continuous extremal adjustment of the compensating network amplification coefficient.

where D_{Δ_θ} is the standard deviation of the control error Δ_θ for optimal values of the parameters $x_i = x_{i\theta}$; $K_{\Delta_\theta \Delta_i}$, $K_{\Delta_i \Delta_j}$ are the correlation coefficients of the random components of the control error.

3. An Application of the Theory

We will take as an example to illustrate the application of the theory, a system with one adjustable parameter in the compensating network – its amplification k, and with the gradient determined by the synchronous detector method [11]. Fig. 2 shows a block diagram of such a system. The control error $\Delta = Z - Y$ is squared and the square averaged in a filter with time constant T. A second filter with time constant τ is used to average the periodic signal of the multiplier of the synchronous detector.

Let the random disturbance X be a stationary random function, let the control input $Z = z_0 = \text{const}$, and let the parameters of the object of control N and T_0 vary slowly with respect to time (relative to the processes in the main control network).

On the basis of Fig. 2, the equations of the main control network are

$$(T_0 p + 1)\, Y = Nk\,[\Delta + X], \quad \Delta = Z - Y. \tag{13}$$

If we note that $m_X = 0$, then for the mathematical expectation and the standard deviation of the control error, we have the expressions

$$m_\Delta = \frac{z_0}{1+Nk}, \tag{14}$$

$$\sigma_\Delta^2 = \int_0^\infty \left| \frac{Nk}{T i\omega + 1 + Nk} \right|^2 G_x(\omega)\, d\omega. \tag{15}$$

For $G_X(\omega) = G_0 = \text{const}$, corresponding to a disturbance X in the form of white sound, formula (15) yields the expression

$$\sigma_\Delta^2 = \frac{\pi N^2 G_0 k^2}{2(1+Nk)\, T_0} \tag{16}$$

for the standard deviation.

If we recall that the performance of the control process is measured by the expression $F = m_\Delta^2 + \sigma_\Delta^2$, we find that the extremal value k can be obtained from the condition

$$\frac{d}{dt}\left[m_\Delta^2 + \sigma_\Delta^2\right]_{k=k_0} = 0, \tag{17}$$

where m_Δ and σ_Δ^2 are given by the expressions in (14) and (16).

The equation determining the extremal value k_0 in the given case is

$$\pi N^3 G_0 k_0^3 + \pi N^2 G_0 3k_0^2 + \pi N G_0 2k_0 - 4T_0 z_0 = 0. \tag{18}$$

Equation (18) is best solved graphically, when the functions N(t) and $T_0(t)$ are given. The result yields the optimal value of the amplification factor $k_0(t)$ of the compensating network.

The complete set of equations for the adjustment network in the case we are considering is obtained as the special case of the equations (2) and (3) for one adjustable parameter.

Because of the slowness of the processes in the adjustment network, the approximate equations of the type (8) for the adjusting network are

$$(Tp + 1)(\tau p + 1)z = \tag{19}$$

$$= -\varkappa w^2 a^2 u - \varkappa\varphi, \quad pu = z + pw - pk_0.$$

If we neglect small quantities of the third order, then on the basis of the expression (8') the disturbing function φ satisfies the relation

$$\varphi = U_0 w, \tag{20}$$

where $U_0 = \Delta_0^2$ is the square of the control error for $k=k_0$.

Since we have assumed that the variation of the variables N, T_0, k_0 is slow compared with the processes in the main network, the coefficient a is given by the expression

$$a = -\frac{Nz_0}{(1+Nk_0)^2}\left[1 - \exp\left(-\frac{1+Nk_0}{T_0}t\right)\right].$$

For the analysis of the system of equations (19) and (20) that follows, we must first of all transform the expression (20) by applying the method of statistical linearization to the quadrator [10]. Since the quadrator has an even-symmetric characteristic, we must apply the statistical linearization method in the form [10]

$$U_0 = \Delta_0^2 = f_0 + k_1 \Delta_0^0,$$

where $f_0 = m^2_{\Delta_0} + \sigma^2_{\Delta_0}$ is the mathematical expectation of the function U_0; Δ_0^0 the random component of Δ_0 having a zero mathematical expectation; and $k_1 = 2m_{\Delta_0}$ is the statistical amplification coefficient of this random component.

We now use the system of equations (19), apply the method of statistical linearization [10] to the quadrator to obtain the mathematical expectation of the adjustment error m_u, and obtain the system of linear equations

$$(Tp+1)(\tau p+1)z =$$

$$= -\varkappa w^2 a^2 m_u - \varkappa w\left[m^2_{\Delta_0} + \sigma^2_{\Delta_0}\right], \tag{21}$$

$$pm_u = z + pw - pk_0.$$

Since the time constants T and τ of the filters are such that the variables m_u, m_{Δ_0}, σ_{Δ_0} can be assumed to vary slowly with the processes occurring in the filters, then the system of equations (21) reduces to the following equation for m_u:

$$pm_u + \varkappa b_1 m_u = -pk_0 + pw - \varkappa b_2\left[m^2_{\Delta_0} + \sigma^2_{\Delta_0}\right]. \tag{22}$$

Here

$$b_1 = \int_0^t g_2(t,\tau)\, w^2(\tau) a^2(\tau)\, d\tau,$$

$$b_2 = \int_0^t g_2(t,\tau)\, w(\tau)\, d\tau,$$

where $g_2(t, \tau)$ is a weighting function for the left-hand side of the first equation of the system (21).

The quantities b_1 and b_2 are mean values of the variables a^2w^2 and w, and are obtained by using two filters in the adjustment network. The quantity b_2 is close to zero, while $b_1 \approx$ const. The solution of equation (22) can be used to obtain the function

$$m_u(t) =$$

$$= m_u(0)\, e^{-\varkappa b_1 t} + \int_0^t e^{-\varkappa b_1 (t-\tau)}\left[\dot{w}(\tau) - \dot{k}_0(\tau)\right] d\tau.$$

In particular, for the test signal $w = \mu_0 \sin \omega_1 t$, we obtain

$$m_u = -\frac{\dot{k}_0}{\varkappa b_1} + \frac{\mu_0}{\sqrt{1 + \frac{\varkappa^2 b_1^2}{\omega_1^2}}} \sin \omega_1 t. \tag{23}$$

For finding the random component of the adjustment error u^0 (superscript "0" denotes the centralized random function), we obtain from the system (19) the equation

$$(Tp+1)(\tau p+1)\, z^0 = \tag{24}$$

$$= -\varkappa w^2 a^2 u^0 - \varkappa w 2 m_{\Delta_0} \Delta_0^0, \quad pu^0 = z^0.$$

The system of equations (24) is linear with variable coefficients, and can be solved by using linear-theory methods. However, if we take into consideration what was said about the system of equations (21), the system (24) can also be written as

$$pu^0 + \varkappa b_1 u^0 = \tag{25}$$

$$= -z_1^0, \quad (\tau p+1)(Tp+1)\, z_1^0 = 2\varkappa m_{\Delta_0} w \Delta_0^0.$$

The function Δ_0^0 is a stationary random function with a spectral distribution

$$G_{\Delta_0}(\omega) = \frac{k_0^2 N^2}{T_0^2\omega^2 + (1+k_0N)^2} G_0.$$

The function z_1^0 is obtained from the function Δ_0^0 by multiplication by the test signal $\mu_0 \sin \omega_1 t$ in the synchronous detector and averaging in two stationary filters; z_1^0 is a stationary random function with a spectral density of the form [9]

$$G_{z_1}(\omega) =$$

$$G_{\Delta_0}(\omega)\left\{\frac{\varkappa^2 m^2_{\Delta_0}\mu_0^2}{(T+\tau)^2(\omega+\omega_1)^2 + [1 - T\tau(\omega+\omega_1)^2]^2} + \right.$$

$$\left. + \frac{\varkappa^2 m^2_{\Delta_0}\mu_0^2}{(T+\tau)^2(\omega-\omega_1)^2 + [1 - T\tau(\omega-\omega_1)^2]^2}\right\}. \tag{26}$$

The solution of the first equation of the system (25) can be used to determine the quantity $u^0(t)$ and the standard deviation from the expression

$$D_u(t) = G_0 k_0^2 N^2 \varkappa^2 m_{\Delta_0}^2 \mu_0^2 \int_0^t e^{-\varkappa b_1 t_1} dt_1 \int_0^t e^{-\varkappa b_1 t_2} k_{z_1}(t - t_2 + t_1)\, dt_2, \quad (27)$$

where

$$k_{z_1}(\tau) = \int_0^\infty g_{z_1}(\omega) \cos \omega\tau \, d\omega,$$

$$g_{z_1}(\omega) = \frac{1}{T_0^2\omega^2 + [1 + Nk_0]^2} \left\{ \frac{1}{(T+\tau)^2(\omega+\omega_1)^2 + [1 - T\tau(\omega+\omega_1)^2]^2} + \right.$$

$$\left. + \frac{1}{(T+\tau)^2(\omega-\omega_1)^2 + [1 - T\tau(\omega-\omega_1)^2]^2} \right\}.$$

In a steady state the standard deviation D_u can be obtained by calculating the integral

$$D_u = G_0 k_0^2 N^2 \varkappa^2 m_{\Delta_0}^2 \mu_0^2 \int_0^\infty g_{z_1}(\omega) \frac{1}{\varkappa^2 b_1^2 + \omega^2} d\omega. \quad (28)$$

Moreover, by analyzing the initial second moment of the adjustment error for various values of the parameters κ and τ, we can choose their optimal values to correspond to the minimum of

$$m_{u\max}^2 + D_u = \left(\frac{\mu_0}{\sqrt{1 + \frac{\varkappa^2 b_1^2}{\omega_1^2}}} - \frac{k_0}{\varkappa b_1} \right)^2 + \quad (29)$$

$$+ \frac{G_0 k_0^2 N^2 \varkappa^2 z_0^2 \mu_0^2}{(1 + k_0 N)^2} \int_0^\infty g_{z_1}(\omega) \frac{1}{\varkappa^2 b_1^2 + \omega^2} d\omega.$$

The optimal values of the parameters κ and τ of the adjustment network depend on the level of the spectral density G_0 of the random disturbance, on the size of the useful control signal z_0, and also on the size of the amplification coefficients of the object N and the correlation network k_0.

The parameters of the adjusting network can thus only be chosen to be optimal for definite calculated conditions.

It can be seen from the expression (29) that the adjustment error depends greatly on the test signal amplitude. For fixed values of the parameters κ and τ, the error in the adjustment of the amplification coefficient of the compensating network for varying external conditions is obtained for a steady regime from formulas (23) and (28).

We now obtain the mathematical expectation of the deviation in the estimation of the accuracy of control in the form $m_{\Delta_1} = am_u$. The standard deviation of the accuracy of control is calculated from the formula

$$D_{\Delta_1} = a^2 D_u.$$

According to the formulas (11) and (12), the accuracy of control in the case of a self-adaptive system is calculated from the expressions

$$m_\Delta = m_{\Delta_0} + m_{\Delta_1}, \quad D_\Delta = D_{\Delta_0} + D_{\Delta_1} + 2K_{\Delta_0\Delta_1},$$

where $K_{\Delta_0\Delta_1}$ is the correlation moment for the steady regime, equal to

$$K_{\Delta_0\Delta_1} = \int_0^\infty G_{\Delta_0}(\omega) \left| \frac{\varkappa m_{\Delta_0}\mu_0}{\varkappa b_1 + i\omega} \right.$$

$$\left[\frac{e^{i\omega_1}}{-T\tau(\omega+\omega_1)^2 + (T+\tau)\, i(\omega+\omega_1) + 1} + \right.$$

$$\left. \left. + \frac{e^{-i\omega}}{-T\tau(\omega-\omega_1)^2 + (T+\tau)\, i(\omega-\omega_1) + 1} \right] \right| d\omega,$$

and

$$D_{\Delta_0} = \frac{\pi N G_0 k_0^2}{2(1 + k_0 N) T_0}.$$

LITERATURE CITED

1. Chien Hsüeh-hsien, Technical Cybernetics [Russian translation] (IL, 1956).
2. A. A. Fel'dbaum, The Influence of Random Factors on Processes of Automatic Scanning. The Theory and Application of Discrete Automatic Systems. Transactions of the 1958 conference, edited by Ya. Z. Tsypkin [in Russian] (Izd. AN SSSR, 1960).
3. A. A. Fel'dbaum, "Steady processes in the simplest discrete extremal system in the presence of random disturbances," Avtomat. i Telemekh. 20, No. 8 (1959).*
4. A. A. Fel'dbaum, "The statistical theory of the gradient method of automatic optimization in the case of an object with a quadratic characteristic," Avtomat. i Telemekh. 21, No. 2 (1960).*
5. V. M. Kuntsevich, "The investigation of a system of extremal control in the presence of random disturbances," Izvest. Akad. Nauk SSSR, Otdel. Tekh. Nauk, Énergetika i Avtomatika No. 1 (1960).
6. A. P. Roberts, "Self-optimizing systems for a certain class of randomly varying inputs," Trans. Soc. Instrum. Technology 11, No. 3 (1959).
7. A. A. Krasovskii, "The dynamics of continuous systems of extremal control based on the gradient method," Izvest. Akad. Nauk SSSR, Otdel. Tekh. Nauk, Énergetika i Avtomatika, No. 3 (1959).
8. A. A. Pervozvanskii, "Continuous systems of extremal control in the presence of random disturbances," Avtomat. i Telemekh. 21, No. 7 (1960).*

9. V. S. Pugachev, The Theory of Random Functions and Their Application to Problems of Automatic Control [in Russian](Gostekhizdat, 1958).

10. I. E. Kazakov, "An Approximate Probability Analysis of the Accuracy of Operation of Essentially Nonlinear Systems," Avtomat. i Telemekh. 17, No. 5 (1956).*

11. I. E. Kazakov, The Accuracy of Self-Adaptive Systems with Extremal Continuous Adjustment of the Compensating Network. [in Russian] Zhukovskii Collection of Scientific Works VVIA (1960).

*See English translation.

THE STABILITY OF A CERTAIN NONLINEAR CONTROLLED SYSTEM

Chang Jên-wei

Moscow

Translated from Avtomatika i Telemekhanika, Vol. 21, No. 11,
pp. 1475-1480, November, 1960
Original article submitted May 3, 1960

A method is analyzed for solving the problem of determining the stability of a certain system in which the controlled object has a nonlinear characteristic for large initial perturbations.

1. Statement of the Problem

The stability of a controlled system with a nonlinear actuating mechanism was studied in [1, 2, 3]. In these papers the perturbed movement of the controlled object was described by linear differential equations on the basis of linear object characteristics or by linearization. As we know, the form of the equations for perturbed motion of a controlled system depends on the conditions of the specific problem. We shall study the horizontal flight of a controlled aircraft at a constant velocity. In this case the equations for perturbed motion are of the following form:

$$\begin{gathered} T^2\ddot{\psi} + U\dot{\psi} + K(\beta) + \mu = 0, \\ \dot{\psi} - \dot{\beta} - n\beta = 0, \\ \mu = f(\sigma), \quad \sigma = a\psi + E\dot{\psi} + G^2\ddot{\psi} - \frac{1}{i}\mu. \end{gathered} \tag{1}$$

Here ψ is the yawing angle; β is the slip angle; μ is the deviation angle of the steering wheel; $f(\sigma)$ is the nonlinear characteristic of the servomotor and belongs to functions of class A or A' [2]. The function $K(\beta)$, which characterizes the lateral stability moment, is essentially nonlinear (Figs. 1, 2).

A problem of this type was investigated for the general case of sufficiently small perturbations in a monograph by A. M. Letov [2]. Letov proved the theorem on the stability (in a first approximation) of an automatic control system with an essentially nonlinear actuator. But if we do not limit our analysis to movement near the origin, then it is necessary to take into account the effect of a change in the sign of the function $K(\beta)$. In other words, in that case we cannot linearize the first equation of the system (1).

At present a general method for solving this type of problem does not yet exist. In this paper we study one particular method for analyzing the stability of the system (1) and demonstrate that the known Lyapunov methods can be extended to a control system with a nonlinear object.

2. Investigation of the Stability in the General Case

In order to investigate the stability of the system (1) we make use of the second Lyapunov method. Before formulating the Lyapunov function we shall reduce the original equations of system (1) to dimensionless form. From Fig. 1 it is evident that the nonlinear function $K(\beta)$ can be replaced approximately by the function $k\beta + m\beta^3$, where k and m have opposite signs. Fig. 1 corresponds to $k>0$, $m<0$, and Fig. 2 corresponds to $k<0$, $m>0$.

Introducing the new variables $\eta_1 = \psi$, $\eta_2 = T\frac{d\psi}{dt}$, $\eta_3 = \beta$ and $t = T\tau$, we obtain

$$\begin{aligned} \dot{\eta}_1 &= \eta_2, \\ \dot{\eta}_2 &= a_{21}\eta_1 + a_{22}\eta_2 + a_{23}\eta_3 + m_2\eta_3^3 + n_2\sigma, \\ \dot{\eta}_3 &= \eta_2 + a_{33}\eta_3, \\ \dot{\sigma} &= q_1\eta_1 + q_2\eta_2 + q_3\eta_3 + \bar{q}_2\eta_2\eta_3^2 + \bar{q}_3\eta_3^3 - \gamma\sigma - sf(\sigma), \end{aligned} \tag{2}$$

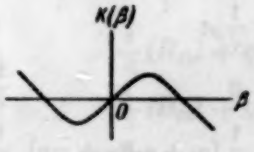

Fig. 1.

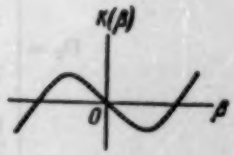

Fig. 2.

where

$$a_{21} = \frac{-alT^2}{T^2 + lG^2}, \quad a_{22} = \frac{-T(U + lE)}{T^2 + lG^2},$$

$$a_{23} = \frac{-kT^2}{T^2 + lG^2}, \quad a_{33} = -nT,$$

$$m_2 = -\frac{mT^2}{T^2 + lG^2},$$

$$n_2 = \frac{lT^2}{T^2 + lG^2}, \quad q_1 = \frac{al(UG^2 - ET^2)}{T(T^2 + lG^2)},$$

$$q_2 = a - \frac{kG^2}{T^2} + \frac{|U + lE|(UG^2 - ET^2)}{T^2(T^2 + lG^2)},$$

$$q_3 = \frac{nkG^2}{T} + \frac{k(UG^2 - ET^2)}{T(T^2 + lG^2)},$$

$$\bar{q}_2 = \frac{-mG^2}{T^2}, \quad \bar{q}_3 = \frac{nmG^2}{T} + \frac{m(UG^2 - ET^2)}{T(T^2 + lG^2)},$$

$$\gamma = \frac{l(UG^2 - ET^2)}{T(T^2 + lG^2)},$$

$$s = \frac{T^2 + lG^2}{lG^2}s, \quad f(\sigma) = h\sigma + \varphi(\sigma), \quad \varphi(\sigma) \geqslant 0.$$

We shall assume that the characteristic equation

$$D(\lambda) = \begin{vmatrix} -\lambda & 1 & 0 \\ a_{21} & a_{22} - \lambda & a_{23} \\ 0 & 1 & a_{33} - \lambda \end{vmatrix} = 0 \qquad (3)$$

has roots restricted to negative real parts. Under these conditions the following inequalities must be satisfied on the basis of the Routh-Hurwitz criterion:

$$a_{22} + a_{33} < 0, \; a_{21}a_{33} > 0, \qquad (4)$$

$$(a_{22} + a_{33})(a_{22}a_{33} - a_{21} - a_{23}) + a_{21}a_{33} < 0.$$

Then, according to the Lyapunov theorem there exists a positive-definite quadratic form $F = \frac{1}{2}\sum_{i,k=1}^{3} B_{ik}\eta_i\eta_k$, whose derivative satisfies the relationship

$$\frac{\partial F}{\partial \eta_1}\eta_2 + \frac{\partial F}{\partial \eta_2}(a_{21}\eta_1 + a_{22}\eta_2 + a_{23}\eta_3) + \qquad (5)$$

$$+ \frac{\partial F}{\partial \eta_3}(\eta_2 + a_{33}\eta_3) = -A(\eta_1^2 + \eta_2^2 + \eta_3^2),$$

where A is a specified positive constant number.

From Eq. (5) we can find the unknown coefficients B_{ik} which are expressed in terms of a_{21}, a_{22}, a_{23}, a_{33}, and A.

We shall study the function

$$V = F(\eta_1, \eta_2, \eta_3) + \frac{1}{2}\sigma^2$$

and shall formulate its total time derivative. In view of (2), we shall have

$$-\dot{V} = -\frac{\partial F}{\partial \eta_1}\eta_2 -$$

$$-\frac{\partial F}{\partial \eta_2}(a_{21}\eta_1 + a_{22}\eta_2 + a_{23}\eta_3 + m_2\eta_3^2 + n_2\sigma) -$$

$$-\frac{\partial F}{\partial \eta_3}(\eta_2 + a_{33}\eta_3) -$$

$$\sigma[q_1\eta_1 + q_2\eta_2 + q_3\eta_3 + \bar{q}_2\eta_2\eta_3^2 + \bar{q}_3\eta_3^2 - \gamma\sigma - sf(\sigma)].$$

Denoting η_3^2 by η and making use of relationship (5), we rewrite $-\dot{V}$ in the following form:

$$-\dot{V} = \frac{1}{2}A\eta_1^2 + \frac{1}{2}A\eta_2^2 + \left(\frac{1}{2}A - m_2B_{23}\right)\eta_3^2 -$$

$$-(m_2B_{12}\eta)\eta_1\eta_3 - (m_2B_{22}\eta)\eta_2\eta_3 + \frac{1}{2}A(\eta_1^2 + \eta_2^2 + \eta_3^2) -$$

$$-(q_1 + n_2B_{12})\sigma\eta_1 - (q_2 + n_2B_{22} + \bar{q}_2\eta)\sigma\eta_3 -$$

$$-(q_3 + n_2B_{23} + \bar{q}_3\eta)\sigma\eta_3 + \gamma\sigma^2 + sh\sigma^2 + s\varphi(\sigma)\sigma.$$

This expression can be treated as the sum of two quadratic forms relative to η_1, η_2, η_3, and σ, whose coefficients depend on η. In order to find the sufficient conditions for stability of the system (2) we formulate the following two determinants:

$$D_1 = \begin{vmatrix} \frac{1}{2}A & 0 & \frac{1}{2}m_2B_{12}\eta \\ 0 & \frac{1}{2}A & \frac{1}{2}m_2B_{23}\eta \\ \frac{1}{2}m_2B_{12}\eta & \frac{1}{2}m_2B_{22}\eta & \frac{1}{2}(A - m_2B_{23}\eta) \end{vmatrix},$$

$$D_2 = \begin{vmatrix} \frac{1}{2}A & 0 & 0 & \frac{1}{2}(q_1 + n_2B_{12}) \\ 0 & \frac{1}{2}A & 0 & \frac{1}{2}(q_2 + n_2B_{22} + \bar{q}_2\eta) \\ 0 & 0 & \frac{1}{2}A & \frac{1}{2}(q_3 + n_2B_{23} + \bar{q}_3\eta) \\ \frac{1}{2}(q_1 + n_2B_{12}) & \frac{1}{2}(q_2 + n_2B_{22} + \bar{q}_2\eta) & \frac{1}{2}(q_1 + n_2B_{23} + \bar{q}_3\eta) & \gamma + sh \end{vmatrix}.$$

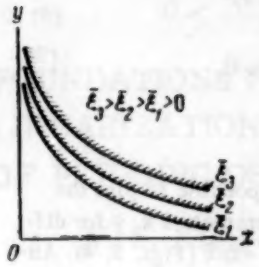

Fig. 3.

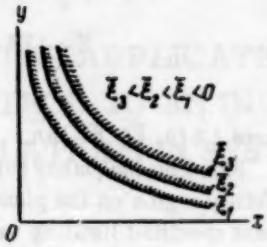

Fig. 4.

Expanding them, we obtain

$$D_1 = A^2 + B_1\eta + C_1\eta^2,$$
$$D_2 = A^2(\gamma + sh) + A_2 + B_2\eta + C_2\eta^2, \tag{6}$$

where the coefficients B_1, C_1, A_2, B_2, C_2 can be found easily.

If the inequalities $D_1>0$, $D_2>0$ had been valid for any value of η, then in accordance with the Silvester criterion the form for $-\dot{V}$ would have been definitely negative in the entire space (η_1, η_2, η_3, σ); therefore the system (2) would have been asymptotically stable as a whole. Since the coefficients of the polynomials (6) may be negative, the inequalities $D_1>0$, $D_2>0$ are satisfied only for a certain finite set of values η.

Basing ourselves on this fact, we use the Lyapunov theorem to state that if the inequalities $D_1>0$, $D_2>0$ are valid for values of η which belong to a certain unbroken continuum $[0, \overline{\eta}]$ containing the origin, then the system (2) will be asymptotically stable for any initial perturbations of η_1, η_2, and σ and for initial perturbations of η_3 such that its absolute values do not exceed $\sqrt{\overline{\eta}}$. The existence of such an $\overline{\eta} > 0$ is guaranteed if $A^2(\gamma + sh) + A_1 > 0$, since in view of the continuity condition it is possible to find a limiting value $\overline{\eta} < \eta^*$ such that over the semi-interval $[0, \eta^*]$ the inequalities $D_1>0$, $D_2>0$ are valid. It is evident that $\eta^* = \min(\eta^{(1)}, \eta^{(2)})$, where $\eta^{(1)}$ and $\eta^{(2)}$ are the first roots of the equations $D_1=0$, $D_2=0$ on the semi-axis $(0, +\infty)$.

3. Investigating the Stability Conditions

We now proceed to a detailed study of the applicability of the inequalities $D_1>0$, $D_2>0$. For simplicity we assume that $n=0$, $G^2=0$, and $f(\sigma)$ belong to the

Fig. 5.

class A' [2]. Then $\eta_1 = \eta_3$ and the system (2) will be written as

$$\dot{\eta}_1 = \eta_2,$$
$$\dot{\eta}_2 = a_{21}\eta_1 + a_{22}\eta_2 + m_2\eta_1^3 + n_2\sigma, \tag{7}$$
$$\dot{\sigma} = q_1\eta_1 + q_2\eta_2 + q\eta_1^3 - \gamma\sigma - sf(\sigma),$$

where

$$a_{21} = -(k + al), \quad a_{22} = \frac{-(U + lE)}{T},$$
$$m_2 = -m, \quad n_2 = l,$$
$$q_1 = \frac{-E}{T}(k + al),$$
$$q_2 = a - \frac{E}{T^2}(U + lE), \quad q = \frac{-Em}{T},$$
$$\gamma = \frac{-El}{T},$$
$$s = \frac{1}{l}, \quad f(\sigma) = h\sigma + \varphi(\sigma), \quad h > 0, \quad \varphi(\sigma) \geqslant 0.$$

In that case the determinants D_1, D_2 are written as

$$D_1 = \begin{vmatrix} \frac{1}{2}A + m_2B_{12}\eta & \frac{1}{2}mB_{22}\eta \\ \frac{1}{2}mB_{22}\eta & \frac{1}{2}A \end{vmatrix},$$

$$D_2 = \begin{vmatrix} \frac{1}{2}A & 0 & \frac{1}{2}(B_{12}l + q_1 + q\eta) \\ 0 & \frac{1}{2}A & \frac{1}{2}(B_{22}l + q_2) \\ \frac{1}{2}(B_{12}l + q_1 + q\eta) & \frac{1}{2}(B_{22}l + q_2) & \frac{h}{l} + \gamma \end{vmatrix},$$

where B_{12}, B_{22} are expressed in terms of A by the following formulas:

$$B_{12}=\frac{A}{k+al}, \quad B_{22}=\frac{T(1+k+al)A}{(k+al)(U+lE)}.$$

Expanding the determinants D_1 and D_2 we obtain

$$D_1=\frac{A}{4}\left[1+\frac{2m}{k+al}\eta-\frac{m^2T^2(1+k+al)^2}{(k+al)^2(U+lE)^2}\eta^2\right],$$

$$D_2=2A^2\left(\frac{h}{l}+\gamma\right)-$$

$$-A\left[\frac{lA}{k+al}-\frac{E(k+al)}{T}-\frac{Em}{T}\eta\right]^2-$$

$$-A\left[\frac{(1+k+al)lTA}{(k+al)(U+lE)}+a-\frac{E}{T^2}(U+lE)\right]^2.$$

We introduce the substitutions

$$k+al=x, \quad \frac{U+lE}{T}=y,$$

$$\frac{hT}{l^2E}-1=z, \quad m\eta=\xi,$$

$$2x^2z=X, \quad \frac{x}{y}(1+x)-y+\frac{aT}{E}=Y$$

and select the as yet undefined constant A in the form

$$A=\frac{(k+al)^2E}{lT}.$$

Making use of these substitutions, we write the sufficient conditions $D_1>0$, $D_2>0$ for stability of the system (7) in the following form:

$$1+2\xi\frac{1}{x}-\frac{\xi^2(1+x)^2}{x^2y^2}>0, \tag{8}$$

$$X-Y^2-\xi^2>0. \tag{9}$$

where $\xi\in[0, \bar{\xi}]$, $\bar{\xi}=m\bar{\eta}$.

Based on inequality (8), it is possible to plot the stability region on the plane of parameters x, y for different specified limiting values $\bar{\xi}=m\bar{\eta}$ (Figs. 3, 4). Analogously, inequality (9) determines the boundaries of the stability region on the X, Y plane for various values of $\bar{\xi}=m\bar{\eta}$ (Fig. 5).

Inequalities (8), (9) must be satisfied simultaneously for different values of $\bar{\xi}=m\bar{\eta}$. In view of continuity and for an appropriate selection of the parameters a, l, E, and h, such a requirement may be satisfied.

In conclusion the author expresses his appreciation to A. M. Letov for a number of valuable suggestions and remarks.

LITERATURE CITED

1. A. I. Lur'e, Certain Nonlinear Problems in Automatic Control Theory [in Russian](Gostekhizdat, 1951).
2. A. M. Letov, Stability of Nonlinear Control Systems [in Russian] (Gostekhizdat, 1955).
3. I. G. Malkin, "On stability theory for controlled systems," Priklad. Mat. i Mekh. No. 1 (1951).

FOUNDATIONS FOR THE APPLICATION OF THE HARMONIC LINEARIZATION METHOD TO AN INVESTIGATION OF PERIODIC OSCILLATIONS IN SYSTEMS WITH LAG*

V. S. Kislyakov

Moscow

Translated from Avtomatika i Telemekhanika Vol. 21, No. 11,
pp. 1481-1489, November, 1960
Original article submitted April 18, 1960

The paper studies the problems of applying the harmonic linearization method (Krylov and Bogolyubov [1, 2]) to an investigation of periodic oscillations in control systems with lag that are described by linear nth order differential equations with a lagging argument.

In [3] a number of specific examples involving the application of the asymptotic methods developed by N. M. Krylov and N. N. Bogolyubov for investigating periodic oscillations in both linear and nonlinear control systems with lag are studied without rigorous mathematical foundations. The essence of the asymptotic methods was reduced to finding the solution for the equation under study in the form of the sum of its particular solutions expanded into formal series in the small parameter ϵ. For the case where a nonlinear equation was investigated the so-called "generating" solution was determined first (i.e., a periodic solution of an ordinary linear differential equation with a lagging argument, which is derived from the nonlinear equation for $\epsilon = 0$). For this purpose it is quite natural to begin with an attempt at applying asymptotic methods (the method of harmonic linearization) in the investigation of periodic oscillations in linear systems with lag. Our present paper is devoted to precisely this subject.

1. Assume that a controlled system with lag is described by ordinary linear differential nth order equations with constant coefficients and a lagging argument:

$$L[y(t)] \equiv y^{(n)}(t) + \sum_{\nu=1}^{n} [a_\nu y^{(n-\nu)}(t) + b_\nu y^{(n-\nu)}(t-\tau_\nu)] = 0, \quad (1)$$

where L is a linear differential operator; a_ν, b_ν are constant real coefficients, and τ_ν are real positive constants which characterize the time lag.

Such an equation was investigated in detail in [4-7] and in other papers. Schmidt [5] studied an equation of the type (1) and demonstrated that if a) the solution y(t) is continuous, together with its first n derivatives, over the entire real axis, and b) for $t \to \pm\infty$ the function y(t) does not increase more rapidly than $c|t|^\alpha$ (α, $c > 0$ are constants), then the nature of the solution for Eq. (1) depends on the existence of real zeros for the transcendental characteristic function defined by the equation

$$l(\omega) = (j\omega)^n + \sum_{\nu=1}^{n} [a_\nu (j\omega)^{n-\nu} + b_\nu (j\omega)^{n-\nu} e^{-j\tau_\nu \omega}]. \quad (2)$$

Schmidt also demonstrated that the function $l(\omega)$ has a finite number of real zeros and proved the following theorem: if $l(\omega)$ contains exactly m real zeros† ($m > 0$), then a) the homogeneous differential equation (1) has m linearly independent particular solutions, and b) any solution y(t) which for $t \to \pm\infty$ does not increase more rapidly than $c|t|^\alpha$ can be written as the sum

$$y(t) = \sum_{k=1}^{m} \alpha_k y_k(t), \quad (3)$$

where α_k are arbitrary constants and $y_k(t)$ are those particular solutions that are contained in any series $y_1(t), y_2(t), \ldots, y_m(t)$ which includes functions of the form $\exp(j\lambda t)$, $t\exp(j\lambda' t)$, $t^2\exp(j\lambda'' t)$, ...; here λ, λ', and λ'' respectively denote all simple, all double, and all triple (etc.) real zeros of the function $l(\omega)$.

2. One of the possible Krylov-Bogolyubov methods, which is called the harmonic linearization method in automatic control theory, can be reduced to the following when applied to nth order equations of the form (1). Equation (1) is replaced by an ordinary linear nth order differential equation of the following form, which has no lag in its argument:

* Paper presented November 19, 1959 at the Seminar on Differential-Difference Equations Held in the Lomonosov Moscow State University.

† We mean $\omega_1, \omega_2, \ldots, \omega_m$.

$$y^{(n)}(t) + \frac{1}{1+c_1}\sum_{\nu=1}^{n} c_{\nu+1} y^{(n-\nu)}(t) = 0, \qquad (4)$$

where c_ν ($\nu = 1, 2, \ldots, n$) are the coefficients to be determined. In order to determine the coefficients c_ν we assume formally that

$$y(t) = A\cos\omega t, \qquad (5)$$

in accordance with the Krylov-Bogolyubov asymptotic methods [2].

Differentiating Eq. (5) n times with respect to t, we obtain

$$\begin{aligned} \dot{y}(t) &= -A\omega\sin\omega t, \\ \ddot{y}(t) &= -A\omega^2\cos\omega t, \\ \dddot{y}(t) &= A\omega^3\sin\omega t, \\ &\ldots\ldots\ldots\ldots \end{aligned} \qquad (6)$$

Substituting the values of y(t) and its n first derivatives from Eq. (5) and (6) into (1) and (4), we set the coefficients of the sines, cosines, and corresponding powers of ω equal to one another. As a result we obtain

$$\begin{aligned} c_1 &= -\frac{b_1}{\omega}\sin\omega\tau_1, \\ c_2 &= a_1 + b_1\cos\omega\tau_1 - \frac{b_2}{\omega}\sin\omega\tau_2, \\ &\ldots\ldots\ldots\ldots\ldots\ldots \\ c_n &= a_{n-1} + b_{n-1}\cos\omega\tau_{n-1} - \frac{b_n}{\omega}\cos\omega\tau_n, \\ c_{n+1} &= a_n + b_n\cos\omega\tau_n. \end{aligned} \qquad (7)$$

Thus the linear differential nth order equation, with periodic solutions of the form (5) that are common to the differential-difference equation (1), will be

$$L^*[y(t)] \equiv \left(1 - \frac{b_1}{\omega}\sin\omega\tau_1\right) y^{(n)}(t) + \sum_{\nu=1}^{n-1}\left(a_\nu + b_\nu\cos\omega\tau_\nu - \frac{b_{\nu+1}}{\omega}\sin\omega\tau_{\nu+1}\right)\times \qquad (8)$$

$$\times\, y^{(n-\nu)}(t) + (a_n + b_n\cos\omega\tau_n)\, y(t) = 0,$$

where L^* is a linear differential operator.

Applying the Euler method [4], consisting of the substitution

$$y(t) = e^{\lambda t}, \qquad (9)$$

to Eq. (1) and (8), we obtain the characteristic equations for (1):

$$F(\lambda) \equiv \lambda^n + \sum_{\nu=1}^{n}\left[a_\nu\lambda^{n-\nu} + b_\nu\lambda^{n-\nu}e^{-\lambda\tau_\nu}\right] = 0 \qquad (10)$$

and (8):

$$F^*(\lambda) \equiv \left(1 - \frac{b_1}{\omega}\sin\omega\tau_1\right)\lambda^n + \sum_{\nu=1}^{n-1}\left[\left(a_\nu + b_\nu\cos\omega\tau_\nu - \frac{b_{\nu+1}}{\omega}\sin\omega\tau_{\nu+1}\right)\lambda^{n-\nu}\right] + a_n + b_n\cos\omega\tau_n = 0, \qquad (11)$$

respectively; here F and F^* are characteristic functions corresponding to the operators L and L^*.

3. We shall prove a number of theorems by means of which we can clarify the possibility of applying the Krylov-Bogolyubov asymptotic methods to an investigation of periodic oscillations in controlled systems with lag. It is assumed that the controlled system can be described by nth order linear differential equations with constant coefficients and a lagging argument.

Theorem 1. Assume the characteristic equations for the linear differential equations (1) and (8) have purely imaginary roots. Then the characteristic functions $F(j\omega)$ and $F^*(j\omega)$ have an equal number of identical real zeros‡ which determine the periodic solutions of Eq. (1) and (8).

Proof. We know that for the existence of periodic solutions of a linear differential equation (even one with a lagging argument [5]) it is necessary and sufficient that its corresponding characteristic equation have purely imaginary roots.

Assuming $\lambda = j\omega$, we obtain

$$F(j\omega) \equiv (j\omega)^n + \sum_{\nu=1}^{n}\left[a_\nu(j\omega)^{n-\nu} + b_\nu(j\omega)^{n-\nu}e^{-j\tau_\nu\omega}\right] = 0, \qquad (12)$$

$$F^*(j\omega) \equiv \left(1 - \frac{b_1}{\omega}\sin\omega\tau_1\right)(j\omega)^n + \sum_{\nu=1}^{n-1}\left[\left(a_\nu + b_\nu\cos\omega\tau_\nu - \frac{b_{\nu+1}}{\omega}\sin\omega\tau_{\nu+1}\right)(j\omega)^{n-\nu}\right] + a_n + b_n\cos\omega\tau_n = 0. \qquad (13)$$

Using the Euler formulas $\exp(-j\omega\tau_n) = \cos\omega\tau_n - j\sin\omega\tau_n$, it is easy to see that Expression (13) can be transformed to

$$F^*(j\omega) \equiv (j\omega)^n + \sum_{\nu=1}^{n}\left[(a_\nu + b_\nu e^{-j\tau_\nu\omega})(j\omega)^{n-\nu}\right] = 0. \qquad (14)$$

‡We mean the roots $\omega_1, \omega_2, \ldots$

From this it follows that for ω equal to the zeros of the characteristic functions we have $F(j\omega) = F^*(j\omega) = l(\omega)$.

Based on the results cited by Schmidt [5], it can be stated that the characteristic functions $F(j\omega)$ and $F^*(j\omega)$ have the same number of identically equal real zeros which determine the periodic solutions of Eq. (1) and (8). Thus we have proved the theorem.

Theorem 2. Assume the periodic solutions of Eq. (1) are determined by the initial functions $\varphi^{(r)}(t)$ ($r = 0, 1, \ldots, 2m-1$) specified over the initial set E_{t_0} consisting of the points on the time segment $t_0 - \tau \leq t \leq t_0$; assume further that for $t = t_0 = 0$ these functions have the value $\varphi^{(r)}(t_0)$. Now assume that the characteristic functions $F(j\omega)$ and $F^*(j\omega)$ have m real zeros. Then the differential equation (8) has periodic solutions of the form $y_k(t) = \beta_{2k-1} \sin \omega_k t + \beta_{2k} \cos \omega_k t$ ($k = 1, 2, \ldots, m$) [where β_{2k-1}, β_{2k} are arbitrary constants, ω_k are the real roots of the characteristic functions $F(j\omega)$ (or $F^*(j\omega)$)] which are common to Eq. (1), provided that the arbitrary constants β_{2k-1}, β_{2k} of the periodic solutions for (8) are identically equal to the arbitrary constants of the periodic solutions for (1).

Proof. In order to determine the arbitrary constants β_{2k-1}, β_{2k} of the periodic solutions for (1) (the quasipolynomial of these constants has m real zeros) it proves sufficient to specify the numerical values of the initial function $\varphi(t)$ and its $(2m-1)$th derivative at the point $t = t_0$.

From the Schmidt Theorem it follows that any solution $y(t)$ of the differential equation (1) (which satisfies the conditions assumed in the theorem) can be written in the form of the sum

$$y(t) = \sum_{k=1}^{m} y_k(t). \qquad (15)$$

In accordance with Theorem 2, $y_k(t) \equiv \bar{y}_k(t)$ ($k = 1, 2, \ldots, m$) where $\bar{y}_k(t)$ are those particular solutions which are determined by the real zeros of the characteristic function $F^*(j\omega)$. Here the arbitrary constants β_{2k-1}, β_{2k} can easily be determined from the solution of algebraic equations which is obtained if Eq. (15) is differentiated $(2m-1)$ times with respect to t, and the resulting expressions are set equal to the numerical values of the initial function $\varphi(t_0)$ and its $(2m-1)$ derivatives for $t = t_0 = 0$. Thus Eq. (8) has periodic solutions

$$y(t) = \beta_{2k-1} \sin \omega_k t + \beta_{2k} \cos \omega_k t \qquad (k = 1, \ldots, m) \qquad (16)$$

that are common to Eq. (1).

Thus the theorem has been proved.

Theorem 3. The sum of the particular solutions for Eq. (1),

$$y(t) = \sum_{k=1}^{m} (\beta_{2k-1} \cos \omega_k t + \beta_{2k} \sin \omega_k t), \qquad (17)$$

(each of these solutions is found using the Krylov-Bogolyubov asymptotic method) satisfies the differential-difference equation (1).

Proof. The statement of the theorem stems from the fact that the particular solutions of (1) that are found using the asymptotic methods coincide exactly with the particular periodic solutions of that equation. The sum of the latter is also a solution of the differential-difference equation on the basis of the Schmidt Theorem cited above. The theorem has been proved.

In 1959 the paper by A. Khalanai [11] was published; this paper provided the foundations of the averaging method as applied to systems of quasilinear differential equations with a lagging argument. It proved the theorem (analogous to the corresponding theorem formulated by N. M. Bogolyubov [12] for systems of differential equations without lag) stating that the error in determining the periodic solution of the averaged system is small compared to error in the periodic solution of the original system of differential equations with a lagging argument. It should be noted that the theorem formulated by A. Khalanai was proved for a system of differential equations with a lagging argument reduced to standard form [2]. However, differential equations with a lagging argument can be reduced to standard form by substitution of variables only for the case where the linear terms in the system do not contain lag. Thus in the general case the problem of reducing a system of differential equations with a lagging argument to standard form should be considered still unsolved. Such reduction is obviously complicated (even when we seek only periodic oscillations) by the fact that the second order differential equation with a lagging argument which describes the periodic oscillatory mode may have two proper frequencies (this is in contrast to an ordinary differential equation and was demonstrated above). This result also follows from [13].

4. We shall study the equality between the periodic solutions for nth order equations of the form (1) with a lagging argument and periodic solutions of ordinary differential equations of the 2m-th order. We shall assume that an ordinary linear equation of the 2m-th order has periodic solutions equal to those of an nth order differential equation with a lagging argument if: a) the characteristic equations corresponding to the differential equations with and without lag in the argument have equal purely imaginary roots; b) the periodic solutions are determined by equal arbitrary constants; c) the original equations are satisfied for any combination of periodic solutions of the form

$$y(t) = \beta_1 \sin \omega_1 t + \beta_2 \cos \omega_1 t + \beta_3 \sin \omega_2 t + \beta_4 \cos \omega_2 t + \cdots + \beta_{2m-1} \sin \omega_m t + \beta_{2m} \cos \omega_m t.$$

We shall prove a number of theorems which can be used to provide the foundation for postulating equality

between the periodic solutions of differential equations with a lagging argument (1) and the periodic solutions of equations without lag.

Theorem 4. If the quasipolynomial $F(j\omega)$ of the linear differential nth order equation (1) has m real roots, then: a) the characteristic equation for the ordinary linear differential equation which has purely imaginary roots equal to those of Eq. (1) is of degree 2m; b) its corresponding differential equation is of order 2m.

Proof. From the general theory of linear differential equations it is known that the maximum number of linearly independent solutions of a linear differential equation is equal to its order. It is also known that if the characteristic equation has 2m purely imaginary roots, then the roots can only be conjugate pairs. Therefore the characteristic equation for a linear differential equation without lag that has purely imaginary roots equal to the characteristic equation for the linear differential equation (1) will have the degree 2m; the differential equation that corresponds to it will have the order 2m. The theorem has been proved.

From Theorem 1 it follows directly that the characteristic quasipolynomial $F(j\omega)$ has a finite number of real roots. Assume that the number of purely imaginary zeros of the quasipolynomial $F(j\omega)$ is equal to m. Then from Theorem 4 it follows that the characteristic equation for a linear differential equation with no lag and periodic solutions identically equal to the solutions of the equation with a lagging argument is of degree 2m. We are confronted with the problem of how to determine the coefficients of this characteristic equation. We know that between the coefficients of the algebraic equation

$$\lambda^{2m} + a_1\lambda^{2m-1} + \ldots + a_{2m} = 0 \qquad (18)$$

and its roots $\lambda_1, \lambda_2, \ldots, \lambda_{2m}$ there is the following relationship:

$$\lambda_1 + \lambda_2 + \ldots + \lambda_{2m} = \sum_{i=1}^{2m} \lambda_i = -a_1,$$

$$\lambda_1\lambda_2 + \lambda_1\lambda_3 + \ldots + \lambda_{2m-1}\lambda_{2m} = \sum_{\substack{i,\,j=1 \\ (i<j)}}^{2m} \lambda_i\lambda_j = a_2,$$

$$\lambda_1\lambda_2\lambda_3 + \lambda_1\lambda_2\lambda_4 + \ldots + \lambda_{2m-2}\lambda_{2m-1}\lambda_{2m} = \sum_{\substack{i,\,j,\,k=1 \\ (i<j<k)}}^{2m} \lambda_i\lambda_j\lambda_k = -a_3, \qquad (19)$$

$$\ldots\ldots\ldots\ldots\ldots\ldots\ldots\ldots\ldots\ldots$$

$$\lambda_1\lambda_2 \ldots \lambda_{2m} = (-1)^{2m}a_{2m}.$$

Thus if we know the purely imaginary roots of the characteristic equation for the linear differential equation (1),

$$\lambda_1 = +j\omega_1, \quad \lambda_2 = -j\omega_1, \ldots,$$

$$\lambda_{2m-1} = +j\omega_m, \quad \lambda_{2m} = -j\omega_m,$$

then it is always possible to determine the coefficients of the characteristic equation in unique fashion; thus it is possible to determine the coefficients of an ordinary linear 2m-th order differential equation in the form

$$y^{(2m)}(t) + a_1y^{(2m-1)}(t) + a_2y^{(2m-2)}(t) + \ldots + a_{2m}y(t) = 0. \qquad (20)$$

Here it is easy to show that the coefficients $a_1, a_3, a_5, \ldots$ for the odd-order derivatives will always be equal to zero.

Theorem 5. Assume the periodic solutions of Eq. (1) are determined by the initial functions $\varphi^{(r)}(t)$ ($r = 0, 1, \ldots, 2m-1$) specified over the initial set E_{t_0}; assume further that for $t = t_0 = 0$ these functions have the values $\varphi^{(r)}(t_0)$, and the periodic solutions of Eq. (20) are determined by the initial conditions for $t = t_0 = 0$, $y_0^{(r)}$ ($r = 0, 1, \ldots, 2m-1$). Now assume the characteristic equations corresponding to the differential equations (1) and (20) have 2m equal purely imaginary roots. Then for $\varphi^{(r)}(t_0) \equiv y_0^{(r)}$ ($r = 0, 1, \ldots, 2m-1$) the differential equations (1) and (20) have equal particular periodic solutions $y_k(t)$, and any solution $y(t)$ can be written in the form of the sum

$$y(t) = \sum_{k=1}^{m} y_k(t),$$

where $y_k(t)$ are those particular solutions which correspond to the purely imaginary roots of the characteristic equations.

Proof. The equality between the particular periodic solutions $y_k(t)$ for Eq. (1) and (20) follows directly from the equality between the purely imaginary roots of the characteristic equations and the equality between the arbitrary constants determined from identical initial conditions. The second postulate in the theorem for Eq. (1) stems from the Schmidt Theorem; for Eq. (20) it stems from the determination of its coefficients. The theorem is proved.

5. As an example that illustrates the theorems proved above, we shall study the equation**

$$\ddot{y}(t) - 2\dot{y}\left(t - \frac{\pi}{2}\right) + 3y(t) = 0, \qquad (21)$$

whose periodic solutions are determined by the initial functions $\varphi^{(r)}(t)$ ($r = 0, 1, 2, 3$) that have the values $\varphi^{(r)}(t_0)$ for $t = t_0 = 0$.

** Equation (21) was presented to the author for solution by A. M. Zverkin in the course of discussing this paper at the Seminar on Differential-Difference Equations in the Lomonosov Moscow State University.

The quasipolynomial corresponding to Eq. (21),

$$E(\lambda) \equiv \lambda^2 - 2\lambda e^{-\frac{\pi}{2}\lambda} + 3 = 0,$$

has purely imaginary roots $\lambda = \pm j$, $\lambda = \pm 3j$ (this can easily be determined by direct substitution); the periodic solution of Eq. (21) corresponding to these roots is written as

$$y(t) = \beta_1 \sin t + \beta_2 \cos t + \beta_3 \sin 3t + \beta_4 \cos 3t.$$

We shall make use of the Krylov-Bogolyubov asymptotic method for determining the periodic solutions of Eq. (21). For this purpose we transform Eq. (21) to the form

$$\left(1 + \frac{2\sin\frac{\pi}{2}\omega}{\omega}\right)\ddot{y}(t) - 2\cos\frac{\pi}{2}\omega\dot{y}(t) + 3y(t) = 0. \quad (22)$$

The corresponding characteristic equation will be

$$F^*(\lambda) \equiv \left(1 + \frac{2\sin\frac{\pi}{2}\omega}{\omega}\right)\lambda^2 - 2\cos\frac{\pi}{2}\omega\lambda + 3 = 0. \quad (23)$$

In order for the differential equation (22) to have periodic solutions it is necessary and sufficient that $\lambda = j\omega$. Substituting $\lambda = j\omega$ into (23) and separating real and imaginary parts, we obtain

$$2\omega\cos\frac{\pi}{2}\omega = 0, \quad -\omega^2\left(1 + \frac{2\sin\frac{\pi}{2}\omega}{\omega}\right) + 3 = 0. \quad (24)$$

From the simultaneous solution of Eq. (24) we find $\omega = 1$; $\omega = 3$. Thus $\lambda = \pm j$, $\lambda = \pm 3j$, and the example does not contradict Theorem 1. The periodic solutions of Eq. (22) corresponding to the particular values of ω are

$$y(t) = \beta_1 \sin t + \beta_2 \cos t, \quad y(t) = \beta_3 \sin 3t + \beta_4 \cos 3t. \quad (25)$$

The arbitrary constants in expression (25) are determined from the solution of the algebraic equations

$$\varphi(t_0) = \beta_2 + \beta_4, \quad \dot{\varphi}(t_0) = \beta_1 + 3\beta_3,$$
$$\ddot{\varphi}(t_0) = -\beta_2 - 9\beta_4, \quad \dddot{\varphi}(t_0) = -\beta_1 - 27\beta_3 \quad (26)$$

and will be equal to

$$\beta_1 = \frac{9\dot{\varphi}(t_0) + \dddot{\varphi}(t_0)}{8}, \quad \beta_2 = \frac{9\varphi(t_0) + \ddot{\varphi}(t_0)}{8},$$
$$\beta_3 = -\frac{\dot{\varphi}(t_0) + \dddot{\varphi}(t_0)}{24}, \quad \beta_4 = -\frac{\varphi(t_0) + \ddot{\varphi}(t_0)}{8}, \quad (27)$$

respectively.

Thus Eq. (21) and (22) have general periodic solutions of the form (25). The results which we have obtained do not contradict Theorem 2. It is easy to see that any solution $y(t)$ that equals the sum of particular periodic solutions $y(t) = \beta_1 \sin t + \beta_2 \cos t + \beta_3 \sin 3t + \beta_4 \cos 3t$ satisfies Eq. (21). The latter does not contradict Theorem 3.

Further, the ordinary linear differential equation whose characteristic equation has the purely imaginary roots $\lambda_{1,2} = \pm j$, $\lambda_{3,4} = \pm 3j$ and whose coefficients are determined from formulas (19) is written as follows:

$$\dddot{y}(t) + 10\ddot{y}(t) + 9y(t) = 0 \quad (28)$$

(the form above can easily be verified). The order of Eq. (28) is $2m = 4$. The latter result does not contradict Theorem 4. Assume the periodic solutions of Eq. (28) are determined by the initial conditions for $t = t_0 = 0$, $y_0^{(r)} \equiv \varphi^{(r)}(t_0)$ $(r = 0, 1, 2, 3)$. Then the general solution of Eq. (28) will be

$$y(t) = \beta_1 \sin t + \beta_2 \cos t + \beta_3 \sin 3t + \beta_4 \cos 3t,$$

in which the arbitrary constants β_1, β_2, β_3, β_4 are determined from the solution of the algebraic equation (26). This result does not contradict Theorem 5.

The author considers it his duty to express his sincere appreciation to all participants of the Seminar on Differential-Difference Equations in the Lomonosov Moscow State University conducted under the supervision of L. É. El'sgol'ts, who took an active part in discussing this paper and helped substantially in the formulation of the paper.

LITERATURE CITED

1. N. M. Krylov and N. N. Bogolyubov, Introduction to Nonlinear Mechanics [in Russian] (Izd. AN Ukr SSR, 1937).
2. N. N. Bogolyubov and Yu. A. Mitropol'skii, Asymptotic Methods in the Theory of Nonlinear Oscillations [in Russian] (Fizmatgiz, 1958).
3. V. S. Kislyakov, "Application of the method of asymptotic Krylov-Bogolyubov approximations to the investigation of systems with lag," Avtomat. i Telemekh. 21, No. 4 (1960).††
4. L. É. El'sgol'ts, Qualitative Methods in Mathematical Analysis [in Russian] (Gostekhizdat, 1955).
5. E. Schmidt, "Uber eine Klasse linearer funktionaler Differentialgleichungen," Math. Ann. 70 (1911).
6. E. Hilb, "Zur Theorie der linearen funktionalen Differentialgleichungen," Math. Ann. 77 (1917).
7. A. F. Leont'ev, "Differential-difference equations," Matematicheskii Sbornik 24 (16), No. 3 (1949).
8. A. D. Myshkis, "General theory of differential equations with a lagging argument," Uspekhi Mat. Nauk 4, No. 5 (1949).

9. A. D. Myshkis, Linear Differential Equations with a Lagging Argument [in Russian] (Gostekhizdat, 1951).
10. V. V. Stepanov, Course in Differential Equations [in Russian] (Gostekhizdat, 1953).
11. A. Khalanai, "Averaging method for systems of differential equations with a lagging argument," Revue de mathematiques pures et appliquees 4, No. 3 (1959).
12. M. A. Krasovskii and S. G. Krein, "On the averaging principle in nonlinear mechanics," Uspekhi Mat. Nauk 10, No. 3 (65) (1955).
13. L. É. El'sgol'ts, "Certain properties of the periodic solutions for linear and quasilinear differential equations with deviating arguments," Vestnik Moskovskovo Universiteta No. 5 (1959).

†† See English translation.

EQUIVALENT TRANSFORMATIONS OF SEQUENTIAL MACHINES

A. Sh. Blokh

Minsk

Translated from Avtomatika i Telemekhanika, Vol. 21, No. 11,
pp. 1490-1496, November, 1960
Original article submitted May 7, 1960

The paper defines certain equivalent transformations of sequential machines and the corresponding structures of the machines.

1. The Structure of a Sequential Machine

We specify the sequential machine A (in abbreviated notation s.m.A) which is defined by the system of functions

$$s = f_1(q), \quad q' = f_2(x, q)$$
$$0 \leqslant s \leqslant m_s, \quad 1 \leqslant x \leqslant m_x, \quad 1 \leqslant q \leqslant m_q). \qquad (\bullet)$$

The values x are called input values; s are called output values; q are called numbers of states (or in abbreviated form x, s, q states). The time is varied in discrete fashion, and the values x, s, q vary only at the discrete instants of time $t_1, t_2, \ldots$. The "prime" denotes the state of the s.m. at the next instant.

By specifying the series of input values $x_1, x_2, \ldots, x_n$ at the instants $t_1, t_2, \ldots, t_n$ and the initial state q_0, we shall obtain the series of output values $s_1, s_2, \ldots, s_n$. The two series $x_1, x_2, \ldots, x_n$ and $s_1, s_2, \ldots, s_n$ are called an experiment of length n. Two experiments are equal if both their input and output series are equal.

For a fixed input value x the equation $q' = f_2(x, q)$ defines a certain transformation of states q (i.e., it defines a certain generalized substitution a_x of the elements q). We shall denote the operator for this substitution by the symbol A_x, and shall write the equation $q' = f_2(x, q)$ as $q' = A_x q$. Such a notation is sometimes more convenient. We depict the substitution a_x graphically as follows: a) we mark m_q points that are numbered $1, 2, \ldots, m_q$; b) the transition from the preceding state q to the next state q' is indicated by an arrow directed from q to q' (Fig. 1).

The graphical representation of the substitution, which indicates the corresponding value of s near q, is called the structure of the substitution. The structures of all substitutions a_x form the structure [1] of s.m.A (Fig. 2). The structure of an s.m. defines it completely.

Discrete (digital) automatic systems are specified in various ways. But for synthesis of such systems we specify them in the form of s.m. (cf., for example, [3]). Depending on the method used for this transition, various s.m. are obtained.

Thus the same digital automatic system can be described by different pairs of functions (•). Thus we are confronted with the problem of choosing the optimum (in a certain sense) s.m. for synthesizing the specified digital automatic system.

2. Equivalent Transformations of Sequential Machines

Two s.m. A and B are called equivalent if for any experiment in machine A it is possible to indicate an equal experiment in machine B and vice versa. The transition from s.m. A to an equivalent s.m. B is called an equivalent transformation of s.m. A to s.m. B; we shall write this transformation as follows; $B = \alpha A$ where α denotes the transformation operator. The simplest operator α is the operator for the enumeration of states when each state q is assigned a different number in such a way that different numbers q correspond to different new numbers. We shall assume that such an enumeration does not alter the structure of the s.m. However, note that a different numbering of states q leads to a different realization; therefore a successful choice of the numbering for q can lead to a structurally simpler automatic system.

Since all equivalent s.m. perform an identical manipulation of the input data we encounter the problem of choosing an s.m. which will satisfy the specified conditions in optimum fashion (in particular, such a condition as the smallest number of different states). In order to achieve such a choice there must be a reserve

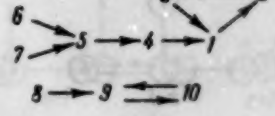

Fig. 1

of definite basic equivalent transformations. Below we shall indicate certain elementary transformations, but they are insufficient for transferring each s.m. into any equivalent s.m. The problem involving the completeness of the set of basic equivalent transformations will be studied in a different paper.

3. Terminology and Notation

The set of states q_i having the property that for a given q_i it is possible to indicate a natural number r_i for which $A_x^{r_i} q_i = q_i$ is defined as the center of the substitution a_x. The sub-sets of the center which are invariant relative to A_x are called kernels of the substitution. If the equation $A_x q = q_1$ does not have a solution, then the element q_1 is called the extreme element of the substitution. The chain $q_0, q_1 = A_x q_0, \ldots, q_\nu = A_x^\nu q_0$ is called a trunk of the substitution a_x with a beginning q_0 (the extreme element) and an end q_ν; the set of trunks with one end q_ν is called a tree with the base q_ν.

Figure 1 shows the graphical representation of the substitution. The elements 1, 2, 3, and 9, 10 form two kernels. The two kernels form a center. The elements 6, 7, 8 are extreme elements.

The two trunks 7, 5 and 6, 5 form a tree. In turn, the tree forms the trunks 7, 5, 4, and 6, 5, 4.

We shall denote an experiment by the letter δ. If we desire to indicate that the experiment δ leads to the state $\underline{q}$, begins with the state $\underline{q}$, or contains $\underline{q}$ in the middle, we write $\delta_{\underline{q}}$, $q\delta$, $\delta_1 \underline{q} \delta_2$, respectively. If the experiment $q_1 \delta q_2$ exists, then q_1 is called the state which precedes q_2, and q_2 is called the state which follows q_1.

4. Identification of Equivalent States

If the experiments $q_1\delta$ and $q_2\delta$ are equal, then q_1, q_2 are called equivalent states relative to the experiment δ. If q_1, q_2 are equivalent for any δ, then q_1 and q_2 are called equivalent states and are denoted by $q_1 \sim q_2$. For the experimenter the states q_1 and q_2 are indistinguishable. It is evident that

1° if $q_i \sim q_j$, then $q_j \sim q_i$;
2° if $q_i \sim q_j$ and $q_j \sim q_v$, then $q_i \sim q_v$;
3° if $q_i \sim q_j$, then for any x we have $A_x q_i \sim A_x q_j$.

Therefore, the set of states can be subdivided into classes $Q_1, Q_2, \ldots, Q_p$ of equivalent states. We shall not study classes consisting of one element. The structure of the s.m. determines those equivalent transformations which can be performed on them. Therefore, we shall study the structure of a s.m. when there are equivalent states. Since the structure of a s.m. is formed by the structures of a substitution, it is sufficient to study the structure of an individual substitution.

Assume $P_1, P_2, \ldots, P_r$ are classes of equivalent states located on a given trunk with a kernel. We shall introduce the set $M = P_1 + P_2 + \ldots + P_r$. Let $q_1 \in M$ denote the element preceding all the remaining elements of M on the specified trunk. If M is contained only in the kernel, then q_1 can be any element in M.

Assume $q_\alpha = A_x^\alpha q_1$ is the first equivalent state following q_1. Then from the property 3° it follows that $A_x q_\alpha \sim A_x q_1$, etc. There the function $s = f_1(q)$ will be a periodic function, beginning with q_1, on the given trunk. Here the number of elements in the kernel is divisible

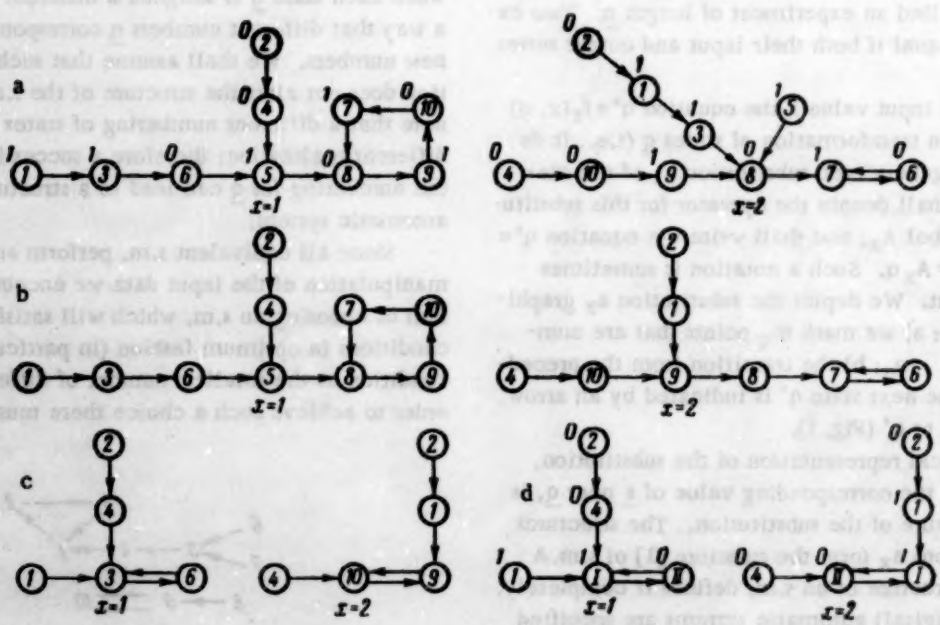

Fig. 2

by the period. If the equivalent states are located on different trunks of the substitution, then $f_1(q)$ acquire equal values over segments of the equivalent states. By identifying equivalent states of s.m.A we obtain (cf. Moore [2]) the s.m.B which is equivalent to the original one. Such a transition consists of the following: in the substitution a_x we retain one of the periods $f_1(q)$ which forms a new kernel; the equivalent portions located on different trunks are joined.

Example (Fig. 2). In machine A we have two classes of equivalent states: $Q_1\{3, 5, 7, 9\}$, $Q_2\{6, 8, 10\}$. The transition from A to B is achieved as follows. In the substitution a_2 we join the equivalent states 3, 5, 9 on different trunks with a common base; we leave the states which are not included in the classes Q_1 and Q_2, and one period later we replace the designations of the elements included in the period with the designation of the corresponding class. In Fig. 2, b, c, d we have shown the stages of the transition. The transition to equivalent machines by identifying equivalent states reduces the number of states. A machine without equivalent states is called a simple machine. In the analysis below we shall study only simple machines.

The indicated structure of an s.m. when equivalent states are present can serve as the necessary identifying feature for detecting equivalent states. But note that if $Q_1, Q_2, \ldots, Q_r$ are classes of equivalent states relative to each substitution, then this does not yet mean that they will be classes of equivalent states. For example (Fig. 3) the states 1, 3 are equivalent with respect to each substitution, but 1 is not equivalent to 3. In order to verify this it is sufficient to study two experiments:

s	1	0	1	0
q	1	2	1	2
x	1	2	2	1

s	1	0	1	1
q	3	4	5	3
x	1	2	2	1

5. Annulment of Regular Sub-Sets

Assume the state q of s.m.A has the following property: for any experiment with the initial state q there is an equal experiment in A. The question arises as to whether this state q can be discarded. But if we discard the state q then the structure of the machine is disrupted since the states preceding q will not have a next state. Therefore the annulment of one state q involves the annulment of all preceding states. We shall formulate this more precisely. The sub-set R of the set of states in s.m.A is called regular if together with $q \in R$ all the preceding q also belong to R, and if for an experiment with its initial state in R there is an equal experiment with its initial state not in R.

Theorem 1. The annulment of regular sub-sets transforms an s.m. into an equivalent one (cf. Appendix).

Example. We shall study machines A (Fig. 4a) and B (Fig. 4b).

It is evident that $A \sim B$. In order to verify this it is sufficient to check state 5. For experiments δ_1 beginning with $x=1$ the state $5 \sim 1$; for experiments δ_2 beginning with $x=2$ the state $5 \sim 4$. The transition from A to B is achieved by discarding the state 5 rather than by identifying equivalent states.

6. Partial Enumeration

As we have already noted, enumeration is an equivalent transformation. We shall now determine the structure required for s.m.A in order to ensure that the enumeration of states over less than all substitutions will be an equivalent transformation.

The states $q_1, q_2, \ldots, q_r$ which are such that from the presence of just experiment δq_1 it follows that there exist r equal experiments δq_ν $(\nu = 1, 2, \ldots, r)$, are called similar states.

Theorem 2. If the states $q_1, q_2, \ldots, q_r$ are similar, then any permutation $q_1, q_2, \ldots, q_r$ in any substitution of s.m.A transforms A to the equivalent s.m.B for which $q_1, q_2, \ldots, q_r$ remain similar (for the proof, cf. Appendix).

Example. We shall study machine A (Fig. 5a). Machine A does not contain equivalent states and regular parts. It would seem that it is impossible to reduce the number of states. Note, however, that the states 1, 3 are similar. Interchanging the positions of states 1, 3 in the substitution a_2, we make the transition to the equiv-

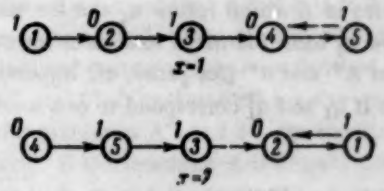

Fig. 3

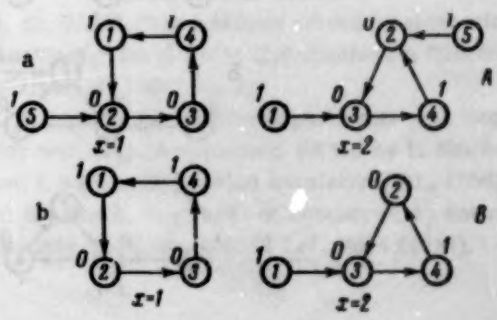

Fig. 4

alent machine B (Fig. 5b). In machine B the state 3 can be discarded. We obtain D ~ A with a smaller number of states (Fig. 5c). As we can see, the simplification was achieved at the expense of the possibility of enumerating the states in one substitution.

The machine is called "simplest" if for each initial state there is an experiment which distinguishes this state from others. If there is just one substitution in the machine for which there are no equivalent states relative to the substitution, then the machine is simplest. For the simplest s.m.A the sufficient condition formulated in Theorem 2 for the equivalence of partial enumeration is also necessary; this flows from Theorem 3 (for proof, cf. Appendix).

Theorem 3. We specify the simplest machines Π_1 and Π_2. Assume $q_1 \to q_2 \to \ldots \to q_r \to q_1$ is one of the cycles for the operator β. If the machines $A = \Pi_1 + \Pi_2$ and $B = \beta\Pi_1 + \Pi_2$ are equivalent, then the elements $q_1, q_2, \ldots, q_r$ are similar.

7. The Search for Equivalent Transformations

The structural properties of s.m. studied above make it possible to find equivalent transformations involving identification and annulment of regular subsets, and partial enumeration. The corollaries of Theorem 4 and its proof cited in the Appendix can facilitate the search for equivalent transformations considerably.

Theorem 4. If in the simple s.m.A there is just one state q_0 such that for any experiment $q_0\delta$ there is an equal experiment $q_0^1\delta$ in the simple s.m.B (where q_0^1 can be different for different experiments $q_0\delta$), then there are identical submachines A^* and B^* in s.m.A and s.m.B.

The theorem is proven in two stages. First we find the states $q_1 \in A$ and $q_1^1 \in B$ which correspond to one another for any experiment δ. Then it is demonstrated that the states in A which follow q_1 and the states in B which follow q_1^1 form identical structures for the two submachines A^* and B^* (for proof, cf. Appendix). Note merely that if q_1 and q_1^1 correspond to one another for any δ, then the state $A_x q_1$ corresponds to the state $B_x q_1^1$ for any δ. Therefore, such corresponding states q_1 and q_1^1 must be sought for in the kernels of the substitutions.

Assume that in s.m.A there is a substitution whose center consists of one kernel. In that case any state in this kernel can be chosen as q_1. All states following q_1 form the submachine A^*. Therefore an investigation of the possibility of applying equivalent transformations to s.m.A must be performed among states which are not included in submachine A^*.

Assume now that s.m.A has no substitutions whose centers consist of one kernel. Without undertaking a more detailed study of the problem, we shall say that it is not possible to accurately indicate which kernel of the substitution a_x contains the state q_1. In that case we formulate the submachines A_ν^* ($\nu = 1, 2, \ldots, r$; $r \le k$) (certain of these submachines may coincide or may be contained in one another) for each of the k kernels of some one substitution a_x.

It is necessary to perform investigations of the possibility of applying equivalent transformations to s.m.A among those states of A which are not included in submachine A_1^*; then we investigate the states of A which are not included in A_2^*, etc.

Let us restate the fact that these conclusions apply to simple s.m. (i.e., to machines without equivalent states).

APPENDIX

Proof of Theorem 1. If the experiment δ begins with $q \in R$, then it does not contain states in R in view of the regularity of R. Therefore, in machine B the same experiment δ corresponds to this experiment. If the experiment δ begins with the state $q_1 \in R$, then according to the condition of the theorem there exists $q_2 \in R$, and $q_2 \sim q_1$ relative to δ. Therefore, in machine B the specified experiment with the initial state q_1 must correspond to an equal experiment with the initial state q_2.

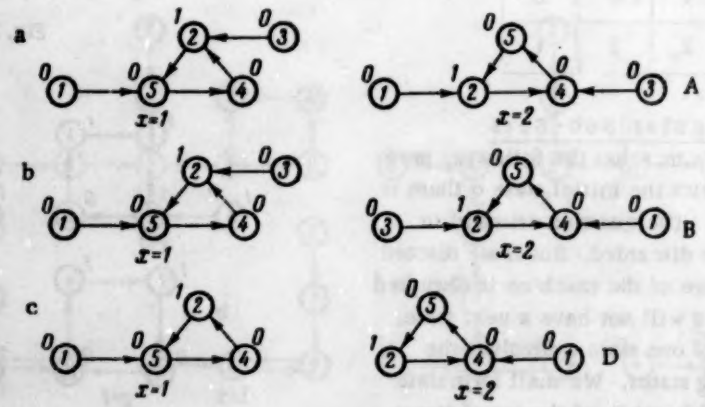

Fig. 5

Proof of Theorem 2. A portion of the substitutions of an s.m. forms the structure of a certain machine Π_1, and the remaining portion of the substitutions forms the structure of another submachine Π_2. We shall represent the original s.m. with the sum of these submachines.

Assume $A = \Pi_1 + \Pi_2$, $B = \beta\Pi_1 + \Pi_2$, where β is the transposition of similar elements q_1, q_2. We shall not only prove that the theorem is satisfied, but we shall also demonstrate that for equal corresponding experiments δ_A and δ_B the last states are identical. For experiments δ_A of length 1 the theorem is obvious, since these δ_A can serve as the experiment δ_B. Assume the theorem and the corollary are valid for experiments of length $l < m$. We shall prove that for this case the theorem is valid for experiments of length m. The experiment δ_A is written in the form $L_1 q_\alpha c_\gamma$.

We shall study two cases.

A. Assume q_α coincides with q_1 or q_2, and q_α separates Π_2 from Π_1; i.e., the next-to-last input value x_α belongs to Π_2, and the last value x_γ belongs to Π_1. In order to be specific we shall assume $q_\alpha = q_1$. We shall formulate the experiment δ_B, which is equal to $L_1 q_1 q_\gamma$, in the following manner. In machine A we take the experiment $\delta_1' q_2$ equal to $\delta_1 q_1$. For machine B we take the experiment $\delta_1'' q_2$ (which is of length $m-1$) to be equal to $\delta_1' q_2$. Continuing it by means of the input value x_γ, we obtain the experiment $\delta_1'' q_2 q_\gamma$ which is equal to $\delta_1 q_1 q_\gamma$.

B. If the conditions for case "A" are not satisfied, then the formulation of δ_B is simplified. On the basis of $\delta_1 q_\alpha$ we formulate an equal $\delta_1'' q_\alpha$ in B and continue it one step to $\delta_1' q_\alpha q_\gamma$ using the input value x_γ. Thus we have proven Theorem 2.

Proof of Theorem 3. We have the arbitrary experiment $\delta_A q_1$. We shall continue it in the machine Π using the experiment δ_1 (i.e., we take the input values of δ_1 from Π_2) which distinguishes the state q_1. For the experiment $\delta_A q_1 \delta_1$ we can indicate an equal experiment $\delta_B q^1 \delta_1$ in the machine B which is equivalent to A. But since L_1 distinguishes the state q_1 in Π_2, we have $q^1 = q_1$.

Thus in B there is an experiment $\delta_B q_1$ equal to $\delta_A q_1$. We shall now continue the experiment $\delta_A q_1$ by means of the experiment δ_2 in the machine Π_1 which distinguishes the state q_1. The experiment $\delta_A q_1 L_2$ has an equal experiment $\delta_B q^1 \delta_2$ in the machine B. But δ_2 distinguishes q_1 in Π_1. Therefore q^1 must be that state which became q_1; i.e., $q^1 = q_r$.

Thus, we have the experiment $\delta_B q_r$ which is equal to $\delta_A q_1$. We shall now take the experiment $\delta_B q_r$. Reasoning analogously, we find that for $\delta_B q_r$ there is an equal experiment $\delta_A q_r$. Therefore, having $\delta_A q_1$, we obtain an equal experiment $\delta_A q_r$. Reasoning analogously with respect to $\delta_A q_r$, we obtain an equal experiment $\delta_A q_{r-1}$, etc. Therefore we immediately have r equal to the experiments

$$\delta_A q_1,\ \delta_A q_2,\ \ldots,\ \delta_A q_r.$$

Proof of Theorem 4. We shall take an arbitrary experiment $q_0\delta_0$ in the machine A. For the machine B there is a set Q of states q_0^1 such that $q_0^1\delta_0$ are equal to $q_0\delta_0$. When the experiment δ_0 is extended the set Q will be decreased; however, due to the condition in the theorem the set will not be vacant. Since the set Q is finite it is possible to find a continuation of $q_0\delta_1$ such that the corresponding set Q_0 will not be diminished for any continuation of it.

Assume the experiment $q_0\delta_1$ ends with the state q_1 and that equal experiments in B end with the state q_i^1 ($i = 1, 2, \ldots, k$). Any experiment $q_1\delta$ in the machine A has k equal experiments $q_1\delta$ in the machine B. In order to verify this it is sufficient to study the experiments $q_1\delta$ and $q_i^1\delta$ as continuations of the experiments $q_0\delta_1$ and $q_0^1\delta_1$. Since the experiments $q_1^1\delta$ are equal, we find that q_i^1 ($i = 1, 2, \ldots, k$) are equivalent states of the machine B; this contradicts the simplicity condition for machine B. Therefore the set Q_0 consists of one element q_0^1. Thus, the state q_1 corresponds not to k states but only to one state q_i^1 for any experiment δ. But if q_1, q_i^1 correspond to one another for any experiment, then the states following them (as parts of equivalent experiments $q_1\delta$ and $q_i^1\delta$) will also correspond to one another. From the simplicity condition for the machines A and B it follows that the correspondence will be mutually single-valued.

Assume that the states following q_1 form the set A^*, and that the states following q_i^1 form the set B^*. We shall show that A^* and B^* are identical sequential machines. Assume $q_2 \in A^*$ and $q_2^1 \in B^*$ correspond. Then from equality of the experiments $q_2\delta q_3$ and $q_2^1\delta q_3^1$ and the simplicity of the machines A and B it follows that q_3 and q_3^1 also correspond. Thus we find that the mutually single-valued correspondence established between the states A^* and B^* is maintained for any experiment. Therefore the machines A^* and B^* are identical.

Corollary. If the machine A is closely coupled and is equivalent to B, then A is identical to a part of B. In fact, for closely coupled machines A^* coincides with A.

LITERATURE CITED

1. A. Sh. Blokh, "On problems solved by sequential machines," Problems in Cybernetics [in Russian] (Fizmatgiz, 1960) No. 3.
2. E. F. Moore, Speculative Experiments with Sequential Machines. Automatons, Edited by E. Shannon and J. McCarthy [Russian translation] (IL, 1956).
3. A. Sh. Blokh, "Synthesis of contact-relay networks," Doklady Akad. Nauk SSSR 117, No. 4 (1957).

THE THEORY OF A MAGNETIC MODULATOR WITH CROSSED FIELDS AND A FUNDAMENTAL FREQUENCY OUTPUT

F. I. Kerbnikov

Moscow

Translated from Avtomatika i Telemekhanika Vol. 21, No. 11, pp. 1497-1502, November, 1960
Original article submitted April 9, 1960

A theory is provided for the operation of a magnetic modulator with crossed fields and a periodically changing inductance of the control winding. The basic conclusions arrived at in the work are confirmed experimentally.

Paper [1] provides the theory and design of a magnetic modulator with mutually perpendicular fields and a fundamental frequency output for an ideal case when under the effect of the current in the excitation winding W_1 (Fig. 1), the inductance of the control winding W_c varies periodically between the values L_{max} and $L_{min} = 0$. In fact, a modulator with a 1000-2000 ferrocart core has a ratio of inductance L_{max} to L_{min} amounting to 4-5 owing to the limited power of the source and nonuniform cross section of the core for the exciting flux, thus leaving some of the core sections unsaturated. Hence, the operation of a magnetic modulator with finite variations of the control winding W_c inductance is of considerable interest.

Let us examine a steady state condition in a control circuit with the signal source connected and a rectangular wave modulating current supplied, for instance, by a magnetic transitron generator through a large resistor.

Let us find the relation between the amplitude of the first harmonic voltage at the output of the modulator and the ratio $L_{max}/L_{min} = m$ for a signal voltage E.

Figure 2a shows the characteristic variations with time of the excitation current i_1; Fig. 2b, those of the inductance L of winding W_c; and Fig. 2c, d, those of i_c flowing through the winding. At instant $t = 0$ the inductance of the control winding rises instantaneously from L_{min} to L_{max}. It is known that with the change in the inductance the value of the flux linkage ψ cannot change immediately (otherwise the control circuit would have an infinitely large emf induced in it [2]). Hence, if we denote by I_{2k} the value of the current in winding W_c of inductance L_{min} before the instantaneous change, the value of current I_{10} at the end of the instantaneous change of the inductance to L_{max} will be represented by

$$\psi(0) = I_{2k}L_{min} = I_{10}L_{max} = \text{const}, \qquad (1)$$

i.e., the current in the control winding will decrease in an inverse proportion to the inductance of the winding:

$$\frac{I_{2k}}{I_{10}} = \frac{L_{max}}{L_{min}} = m. \qquad (2)$$

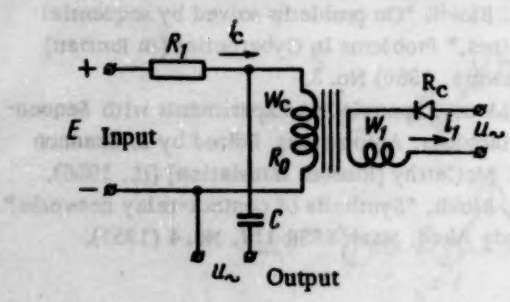

Fig. 1.

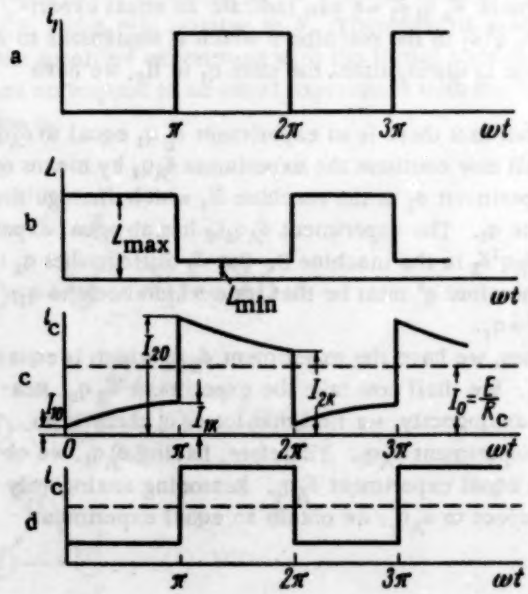

Fig. 2.

After current i_C drops to the value of I_{10} at $t=0$ it will begin to rise exponentially with a time constant of τ:

$$i_{C1} = I_{10} + (I_0 - I_{10})\left(1 - e^{-\frac{t}{\tau}}\right), \quad 0 \leqslant \omega t \leqslant \pi, \tag{3}$$

where

$$\tau = \frac{L_{max}}{R_C}, \quad R_C = R_0 + R_1, \quad L_{max} = \frac{0{,}4\pi W_C^2 \mu_0 S}{l \cdot 10^8}$$

and $I_0 = E/R_C$ is the direct current component in the control circuit at the steady state condition.

At the instant $t = \pi/\omega$ the inductance of the control winding is reduced instantaneously to L_{min}; the control current, which has by then reached the value of I_{1k}, instantaneously rises to I_{20} and then falls exponentially with a time constant of $\tau_1 = \tau/m$:

$$i_{C2} = I_{20} + (I_0 - I_{20})\left[1 - e^{-\frac{m}{\tau}\left(t - \frac{\pi}{\omega}\right)}\right], \quad \pi \leqslant \omega t \leqslant 2\pi. \tag{4}$$

In a steady state at $t = 2\pi/\omega$, the control current $i_C = I_{2k}$.

It is obvious that by similarity with equation (2) it is possible to represent the ratio of currents I_{1k} and I_{20} at the beginning and end of the instantaneous variations of the inductance from L_{max} to L_{min} by

$$\frac{I_{20}}{I_{1k}} = \frac{L_{max}}{L_{min}} = m. \tag{5}$$

By inserting in equations (3) and (4) respectively the values of $t = \pi/\omega$ and $t = 2\pi/\omega$ we obtain for currents I_{1k} and I_{2k} the expressions

$$I_{1k} = I_{10} + (I_0 - I_{10})\left(1 - e^{-\frac{\pi}{\omega\tau}}\right), \tag{6}$$

$$I_{2k} = I_{20} + (I_0 - I_{20})\left(1 - e^{-\frac{\pi m}{\omega\tau}}\right). \tag{7}$$

By solving equations (2), (5), (6), and (7) with respect to I_{10} and I_{20} we obtain

$$I_{10} = I_0 K, \tag{8}$$

$$I_{20} = I_0 K_1, \tag{9}$$

where

$$K = \frac{1 - e^{-\frac{\pi m}{\omega\tau}} + me^{-\frac{\pi m}{\omega\tau}} - me^{-\frac{\pi(m+1)}{\omega\tau}}}{m\left[1 - e^{-\frac{\pi(m+1)}{\omega\tau}}\right]},$$

$$K_1 = \frac{m - me^{-\frac{\pi}{\omega\tau}} + e^{-\frac{\pi}{\omega\tau}} - e^{-\frac{\pi(m+1)}{\omega\tau}}}{1 - e^{-\frac{\pi(m+1)}{\omega\tau}}}.$$

By inserting the values of I_{10} and I_{20} in equations (3) and (4) we have

$$i_{C1} = I_0 - I_0 e^{-\frac{t}{\tau}}(1 - K), \quad 0 \leqslant \omega t \leqslant 2\pi, \tag{10}$$

$$i_{C2} = I_0 - I_0 e^{-\frac{tm}{\tau}}(1 - K_1), \quad \pi \leqslant \omega t \leqslant 2\pi. \tag{11}$$

For a voltage at the output of the modulator with a small internal impedance of the signal source we have

$$u_{H1} = i_{C1} R_1 = I_0 R_1 - I_0 R_1 (1 - K) e^{-\frac{t}{\tau}}, \quad 0 \leqslant \omega t \leqslant \pi, \tag{12}$$

$$u_{H2} = i_{C2} R_1 = I_0 R_1 - I_0 R_1 (1 - K_1) e^{-\frac{tm}{\tau}}, \quad \pi \leqslant \omega t \leqslant 2\pi. \tag{13}$$

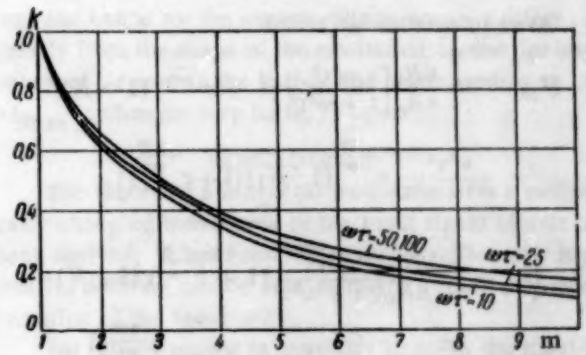

Fig. 3.

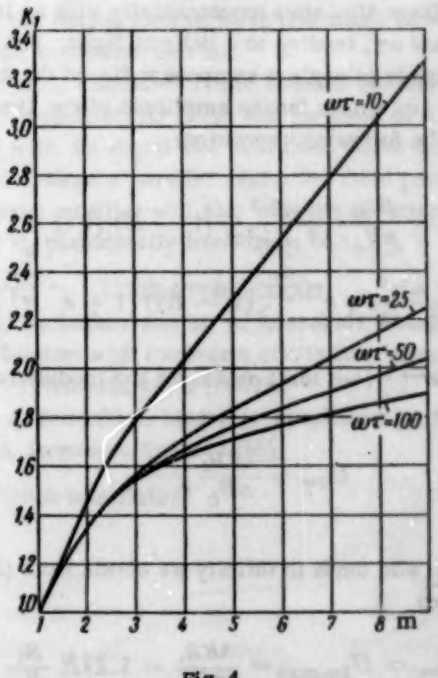

Fig. 4.

Table 1

Core number	D_{ext}, mm	D_{int}, mm	μ_0, gauss/oe	B_s, gauss	H_c, oe	T_k, °C	Cross section for the longitudinal flux, cm^2
1	29.4	17.6	1200	2400	0.1	120	0.68
2	29.4	17.6	2260	2000	0.1	80	0.68

The amplitude of the first harmonic of the output voltage is

$$U_{1m} = \sqrt{U_{1a}^2 + U_{1b}^2},$$

where

$$U_{1a} = \frac{1}{\pi}\int_0^{2\pi} u_n \sin \omega t \, d\omega t,$$

$$U_{1b} = \frac{1}{\pi}\int_0^{2\pi} u_n \cos \omega t \, d\omega t.$$

After integration we obtain

$$U_{1a} = -\frac{ER_1}{\pi R_c}\left[\frac{\omega^2\tau^2}{1+\omega^2\tau^2}\left(1+e^{-\frac{\pi}{\omega\tau}}\right)(1-K) - \right.$$

$$\left. - \frac{\omega^2\tau^2}{m^2+\omega^2\tau^2} e^{-\frac{\pi m}{\omega\tau}}(1-K_1)\left(1+e^{-\frac{\pi m}{\omega\tau}}\right)\right].$$

$$U_{1b} = -\frac{ER_1}{\pi R_c}\left[\frac{\omega\tau}{1+\omega^2\tau^2}\left(1+e^{-\frac{\pi}{\omega\tau}}\right)(1-K) - \right.$$

$$\left. - \frac{\omega\tau}{m^2+\omega^2\tau^2} e^{-\frac{\pi m}{\omega\tau}}(1-K_1)\left(1+e^{-\frac{\pi m}{\omega\tau}}\right)\right].$$

Voltage U_{1m} rises monotonically with an increasing $\underline{m}$ and $\omega\tau$, tending to a definite limit. For $\omega\tau > 10$ it is possible to neglect component U_{1b} of the output voltage and obtain for the amplitude of the first harmonic the following expression:

$$U_{1m} = \frac{ER_1}{\pi R_c}\left[\frac{\omega^2\tau^2}{1+\omega^2\tau^2}(1-K)\left(1+e^{-\frac{\pi}{\omega\tau}}\right) - \right.$$

$$\left. - \frac{\omega^2\tau^2}{m^2+\omega^2\tau^2} e^{-\frac{\pi m}{\omega\tau}}(1-K_1)\left(1+e^{-\frac{\pi m}{\omega\tau}}\right)\right]. \quad (14)$$

If $\omega\tau \to \infty$, we shall obtain for the modulator output voltage,

$$U_{1m} = \frac{4ER_1}{\pi R_c}\frac{m}{m+1}. \quad (15)$$

If $\underline{m}$ also tends to infinity we obtain from (15) the expression

$$U_{1m} = U_{1m\max} = \frac{4ER_1}{\pi R_c} = 1.27E\frac{R_1}{R_c}. \quad (16)$$

Let us note that for $\omega\tau \to \infty$ and $m \to \infty$ the coefficient $K \to 0$ and $K_1 \to 2$. This limiting operating condition of the modulator corresponds to a square wave current in the control winding (Fig. 2d), whose amplitude is twice the direct component $I_0 = E/R_c$ of the current. In fact, the magnetic energy stored in the longitudinal field of the modulator for $L = L_{max}$ is completely dissipated in the load in the following interval, when $L = L_{min}$, thus doubling the load current compared with the direct component of the current in the steady state.

Figures 3 and 4 show the relations of coefficients K and K_1 to $\underline{m}$ for $\omega\tau$ values of 10, 25, 50, and 100. It will be seen that K is relatively independent of $\omega\tau$.

The relation of the first harmonic amplitude to $\underline{m}$, calculated from formula (14) for various values of $\omega\tau$, is shown in Fig. 5. It will be seen that with a decreasing $\underline{m}$ and $\omega\tau$ the amplitude of the first harmonic voltage at the output decreases, but even for $\omega\tau = 25$ and $m = 5$ it remains equal to half its maximum possible value, and it is only 25% below U_{1m} which corresponds to $\omega\tau \to \infty$.

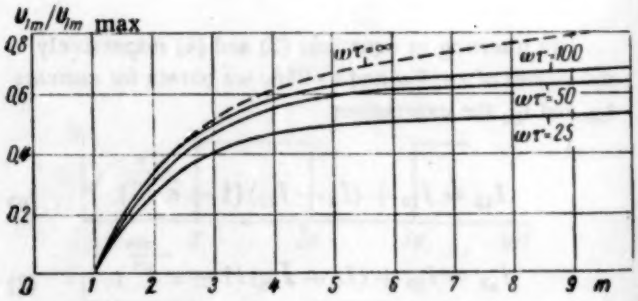

Fig. 5

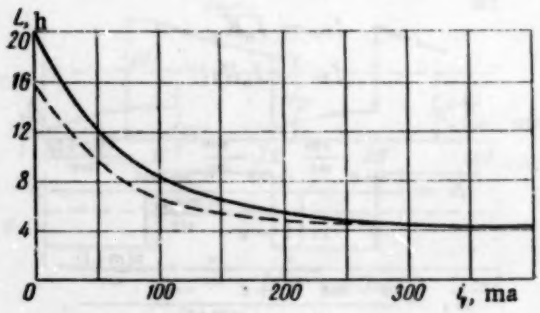

Fig. 6

Table 2.

ωτ	R_c, (ohms)	m = 2 calc.	m = 2 expt.	m = 3 calc.	m = 3 expt.	m = 4 calc.	m = 4 expt.	m = 5 calc.	m = 5 expt.	Note
50	2000	0.4	0.4	0.61	0.6	0.71	0.7			Modulator with core No. 1
100	1000	0.43	0.42	0.63	0.6	0.74	0.72			
60	2000	0.4	0.4	0.61	0.6	0.72	0.7	0.76	0.74	Modulator with core No. 2
120	1000	0.43	0.42	0.63	0.63	0.75	0.74	0.83	0.83	

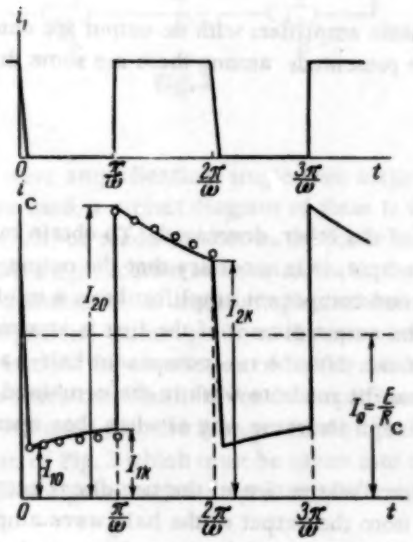

Fig. 7

Tests of several modulators with two different types of cores, whose characteristics are given in Table 1, have fully confirmed the theoretical conclusions obtained above.

Figure 6 shows the experimentally obtained characteristic variations in the inductance of the control winding (W_c = 2800 turns, R_0 = 200) of the modulator with cores No. 1 and No. 2 when the excitation circuit (W_1 = = 200 turns) is fed by a direct current. These characteristics were used for calculating the transfer constants of the modulator when excited with a square-wave current.

Table 2 gives the computed and experimental values of the transfer constant U_{1m}/E for the above modulators at 1000 cps for various values of ωτ and m.

It should be noted that not only the transfer constants but also the curves of the experimental and theoretical current i_c variations in the control winding coincide. For instance, Fig. 7 shows an oscillogram of the excitation current i_1 and the control circuit current i_c for $\omega\tau \approx 50$ and m = 5. The points shown on the curve $i_c = f(t)$ have been calculated from formulas (10) and (11) for the above values of ωτ and m, for which $I_{10} = 0.3I_0$, $I_{20} = 1.7I_0$, $I_{1k} = 0.34I_0$, and $I_{2k} = 1.5I_0$. It will be seen that the shape of the curve for the current in the control winding, and hence for the output voltage, does not differ greatly from the shape of the excitation current for large values of ωτ, and in the half-period corresponding to $L = L_{max}$ it changes very little.

CONCLUSIONS

The theory of a magnetic modulator with a periodically changing inductance in the input signal circuit has been derived. It has been shown that a sufficiently high transfer constant can be obtained with a relatively small variation of the inductance.

For this purpose it is necessary to make the maximum value of ωτ in the input circuit of the modulator sufficiently high ($\omega\tau \geq 25$). Under this condition the shape of the output voltage wave resembles closely that of the excitation current.

The basic conclusions hold both for modulators with mutually perpendicular fields and for those of the same type but with the signal and excitation fields connected in parallel, since a parallel excitation field produced by a half-wave rectifier will also vary the inductance of winding W_c periodically from L_{max} to L_{min}.

LITERATURE CITED

1. F. I. Kerbnikov and M. A. Rozenblat, "Magnetic modulators with transverse excitation," Avtomat. i Telemekh. 19, 9 (1958).*
2. M. A. Rozenblat, Magnetic Amplifiers [in Russian] (Izd. Sovetskoe Radio, 1956).

* See English translation.

REVERSIVE (DUODIRECTIONAL*) MAGNETIC DC AMPLIFIERS OF INCREASED EFFICIENCY

M. A. Boyarchenkov and M. A. Rozenblat

Moscow

Translated from Avtomatika i Telemekhanika, Vol. 21, No. 11, pp. 1503-1513, November, 1960

(Presented at the All-Moscow seminar on contactless magnetic components, March 23, 1960)

Original article submitted April 9, 1960

The conditions for obtaining increased efficiency of reversive magnetic amplifiers with dc output are determined. New circuits for reversive amplifiers satisfying these conditions are presented; among these are some that have increased efficiency without using transformers.

Introduction

The use of dynamoelectric amplifiers in automatic control systems presents numerous difficulties; the most substantial of these difficulties are their lack of dependability in operation, the fact that they are complicated to adjust, their need of periodic maintenance, etc. Therefore, a tendency has lately developed to replace dynamoelectric amplifiers by magnetic amplifiers. The use of magnetic amplifiers makes it possible to create control systems which require almost no adjustment, and which are distinguished by high technical and economic merits. In the creation of such systems, a considerable part is played by the right choice of the magnetic amplifier, by the correct approach to the design of the system, and by the using of advantageous design data.

Any reversive full-wave magnetic amplifier is composed of two, or, in the general case, of several half-cycle (half-wave) amplifiers.

There are two basic principles which may be used in the design of full-wave, two-semicycle amplifiers: the principle of summation of voltages obtained at the outputs of the semicycle amplifiers and the principle of summation of the output currents. A scheme based on the first principle is shown diagrammatically in Fig. 1. In this scheme, separate resistors R_b serve as load resistances for each of the two amplifiers. To obtain a maximum of power in the output when this scheme is used, the total common load resistance R_H must be equal to $\sqrt{2}R_b$. Amplifiers built according to this principle have very low efficiency; therefore, their application is limited to the area of low output power [1].

The diagram of a scheme based on algebraic summation of currents is shown in Fig. 2. When the signal is applied to the control winding, the current in the output of one of the component amplifiers is increased; in the output of the other, decreased. To obtain maximum power output, it is necessary that the output current of the second component amplifier have a minimum value when the output current of the first is at a maximum. To achieve this, the two component half-wave amplifiers must be made to work in the combined full-wave amplifier in the same way as when they operate separately.

Direct subtraction of the two direct currents obtained from the output of the half-wave amplifiers is impossible because of the mutual interaction between the two amplifiers when they are connected with each other as shown. Usually this interaction is decreased by insertion of ballast resistances R_b (shown in Fig. 2 in dotted lines). But these ballast resistances greatly decrease the efficiency. Instead of ballast resistances, control valves can be used in this scheme [2]. In our paper reversive amplifiers are reviewed which do not contain such valves.

Basic Principles for Design of More Efficient Reversive Magnetic Amplifiers

Let us discuss the character of the interaction of the two amplifiers in Fig. 2 in more detail. To present a clearer picture of the conditions, we shall assume that

* In the original Russian and in the author's abstract in English, the term "reversive" is used. Inasmuch as this term is unfamiliar in the USA, it has been replaced in the title by "duodirectional," which is the shortest equivalent term for this concept accepted in authoritative texts of the English-speaking world; see, e.g., Magnetic-Amplifier Circuits by William A. Geyger, 2d edit., McGraw-Hill, New York, 1957, p.77. In the text, however, the word "reversive" has been kept as the shorter of the two terms [Publisher's note].

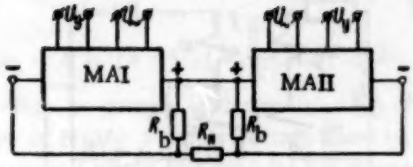

Fig. 1.

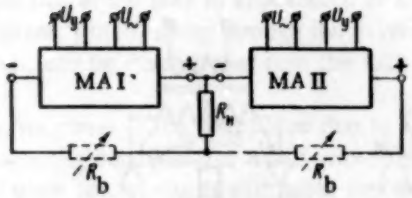

Fig. 2.

for the half-wave amplifications single-core magnetic amplifiers are used; a circuit diagram of these is shown in Fig. 3. As will be made evident in the forthcoming discussion, this amplification scheme serves as the basic element for construction of more complex schemes of magnetic amplifiers. Before going to the examination of the basic circuits for connection of half-wave amplifiers into reversive combinations for dc amplification, let us point out some specific features in the operation of the scheme of Fig. 3 which must be taken into consideration in the design of such reversive amplifiers.

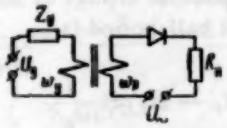

Fig. 3.

Let us assume that the core in the device of Fig. 3 has a rectangular hysteresis loop (Fig. 4). In order to obtain the lowest possible value of the load current in this scheme—$I_{load\,min}$—it is necessary as a rule to have the following condition fulfilled:

$$\int_0^{T/2} u\,dt \leqslant (B_s - B_y)\,w_p S, \qquad (1)$$

where u is the voltage applied during the active (output contributing) half-period to the operational winding w_p; B_y, the value of the magnetic induction in the core at the end of the control half-period (at the start of the active half-period); B_s, the induction at saturation; and T, the period of the supply voltage. In the specific case when $B_y = -B_s$, condition (1) assumes the following form:

$$\int_0^{T/2} u\,dt \leqslant 2w_p S B_s. \qquad (2)$$

When condition (1) is fulfilled, the core either does not reach the saturation state at all, or reaches it only at the end of the active half-period when $\omega t = \pi$. When condition (1) is not fulfilled, then the induction of the core becomes equal to the saturation value B_s at some moment during the active half-period which is determined by the expression

$$\omega t = \alpha = \arccos\left[1 - \frac{\omega (B_s - B_y)}{U_m} w_p S\right] < \pi. \qquad (3)$$

During the time interval when $\alpha \leq \omega t \leq \pi$ there will be a current $i = u/R$ going through the load, where R is the complete resistance of the load circuit. In formula (3) U_m is the amplitude value of the supply voltage, and $\omega = 2\pi f$, its angular frequency. In the half-period scheme of Fig. 3 by itself there is no difficulty whatsoever in fulfilling conditions (1) or (2), and in obtaining a high ratio of high to low load current values. However, when two or more half-wave amplifiers of Fig. 3 are combined into a reversive scheme, condition (1) is usually violated, because of an increase of the left side of the inequality, and/or because of a decrease of the right side.

An increase of the left part of inequality (1) takes place as a result of a redistribution of voltage in the windings of the reversive scheme which are in the active state during a given half-wave period. A decrease of the right side is caused by a redistribution of voltage in the active circuit while it is in the control exercising half-period.

Fig. 4.

Let us illustrate the nature of the voltage redistributions and the consequences thereof by discussing, for example, these phenomena in the most simple full-wave magnetic amplifiers (Fig. 5). Let us examine first the scheme of Fig. 5a, which represents a differential connection of two half-wave amplifiers the active half-periods of which are shifted in phase by a half-period. The instantaneous polarities of the supply voltage for the separate amplifiers are shown in the figure by asterisks. When no signal current is present, the following current relationship is in effect:

$$i_1(t) = -i_2\left(t \pm \frac{T}{2}\right) \qquad (4)$$

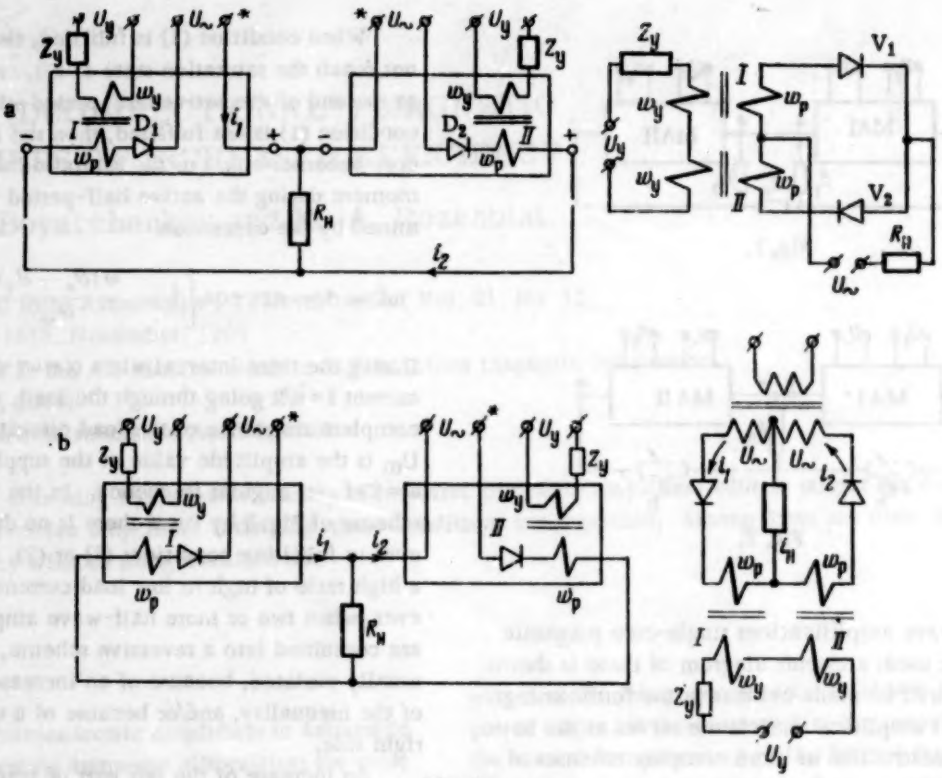

Fig. 5.

and the dc component is absent from the output load. Let us assume now that to the amplifier input a current signal I_y is applied which is of such magnitude and polarity that core II is saturated during the entire active half-period, and the current $i_2 = u/R$ is flowing. In order to obtain the maximum intensity of current in the output from the amplifier, the current i_1 must have the least possible value, that is, the core I must not get saturated before the end of its working half-period. This can be achieved only if, during the control half-period, an induction B_y will be established which will satisfy inequality (1). However, in the scheme of Fig. 5a, this condition cannot be fulfilled. Indeed, if core II, during its active half-period, is saturated, then only a small part of the supply voltage will be applied to rectifier valve V_1 which is equal to

$$u_{rev} = u - i_2 R_н = i_2 (R_0 + R_в), \qquad (5)$$

where R_0 and R_B are the resistances of the winding w_p and of the rectifier valve in the forward direction.

This voltage determines the highest rate of change of the magnetic induction in core I that can possibly be produced by the signal I_y during the control half-period; indeed, when the condition

$$w_p S \frac{dB_I}{dt} \geqslant u_{rev} \qquad (6)$$

is reached, valve V_1 becomes conducting, and the circuit loop formed by the valves and operational (active) w_p, which has a rather low total resistance, practically shortcircuits the control winding w_y of core I, because of the transformer coupling between the windings w_y and w_p of core I.

The largest possible change of induction in core I during the control half-period is

$$\Delta B = B_s - B_y \approx \frac{1}{w_p S} \int_0^{T/2} u_{rev} dt = \frac{U_{av}\left(1 - \dfrac{R_н}{R_н + R_0 + R_в}\right)}{2 f w_p S}, \qquad (7)$$

where U_{av} is the average value of the supply voltage and f—its frequency.

Thus, B_y for core I will differ but little from B_s, and during the next half-period the mean value of current i_1 will differ only very little from the mean value of current i_2, regardless of the magnitude of the signal. Because of this, the maximum value of the constant component of the load current in the scheme of Fig. 5a will be much smaller than for the nonreversive half-wave scheme of Fig. 3 by itself.

Let us now consider the scheme of Fig. 5b. Here, in distinction from scheme 5a, the operational periods for the two cores are not shifted in time, but coincide. Let us assume that the magnitude and the polarity of the signals are such, that at the end of the control half-period we have induction $B_{yI} = -B_s$ in core I, and in core II the induction $B_{yII} = +B_s$. During the entire operational half-period core II is saturated, and to the opera-

tional winding w_p of core I the following voltage is applied:

$$u_2 = u + [u - i_2(R_0 + R_n)] \approx 2u. \qquad (8)$$

Therefore, to comply with condition (1) or (2), for the scheme of Fig. 5b a supply voltage must be chosen which is one-half of the one used for the scheme of Fig. 3. Otherwise, core I also would reach the saturation stage approximately in the middle of its operational half-period, and this would lead to appearance of a considerable i_1 current, which, going through the valves and the w_p windings, can be much larger than the load current i_H.

Thus, we come to the conclusion that in order to keep the working conditions of a half-wave amplifier unaltered when connecting it with other similar amplifiers into a reversive scheme, we must remove the effect of the load voltage upon the operation of the half-wave amplifier which must have a minimum of output current at the time. This effect can be avoided by the use of the well-known bridge scheme (Fig. 6) of subtraction of

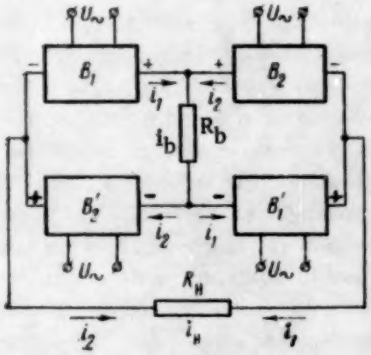

Fig. 6.

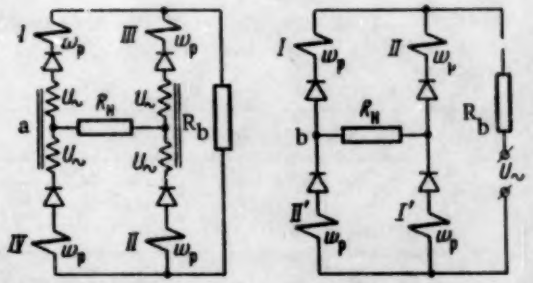

Fig. 7.

the output currents from two half-wave amplifiers. The device is built up from four controlled rectifying amplifier elements. As such, single-core half-wave magnetic amplifiers such as shown in Fig. 3 may be used, or any known combinations of part cycle amplifiers, such as two-half-wave or multiphase amplifiers. Let the assembly be so arranged that the rectified current in the output of elements B_1 and B_1' increases, and the rectified current in the output of elements B_2 and B_2' decreases when the control signal is in action. The presence of ballast resistance R_b which is equal in value to the load resistance R_H prevents redistribution of voltage when the signal is on. Indeed, the voltage drops across R_b and R_H are applied to B_2 and B_2' with opposite polarities. This results in the fact that the operating conditions of elements B_2 and B_2', when included in this combined operation system, remain practically the same as when they are used separately. Therefore, the current in the output of these elements can actually reach minimum values at the proper time, and thus assure maximum output in the load circuit of the assembly. In distinction from the scheme of Fig. 2, the system of Fig. 6 has a much higher efficiency, which reaches 50% in the absence of losses in the windings and in the rectifiers.

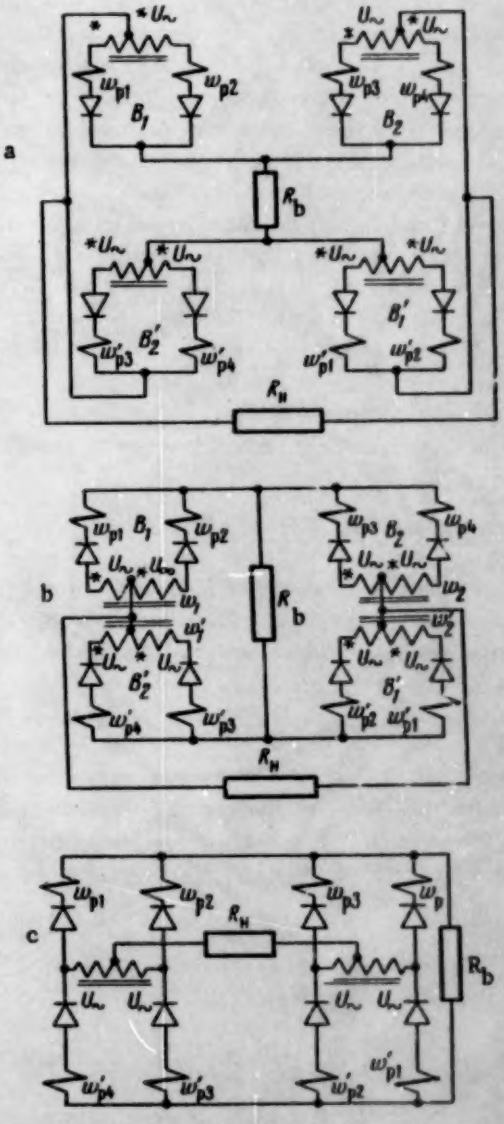

Fig. 8.

If in the system of Fig. 6 each of the four elements B_1, B_1', B_2, and B_2' consists of a single-core amplifier (Fig. 3), then the assembly is the well known bridge scheme of reversive full-wave amplification by means of half-wave components (Fig. 7a). The scheme of Fig. 7a may easily be simplified by using a common source of power supply (Fig. 7b) and employing two amplifiers instead of four; the latter is possible since the cores I and II and the cores III and IV work in identical regimes, and it is therefore possible to have only two cores with two operational windings on each core, and connect the four windings in the bridge scheme (Fig. 7b). This is possible to do in every full-wave scheme built up from any half-wave elements.

When, for instance, the component magnetic amplifiers (controlled rectifying elements) in Fig. 6 consist of twin half-period devices with center tap connections, we have the amplifier scheme of Fig. 8a. And this scheme also can be simplified by the use of common cores for pairs of two operational windings through which the same currents must pass (as e.g., the windings w_{p1} and w_{p1}', and w_{p2} and w_{p2}'), and also by decreasing the number of secondary windings of the supply transformer; the latter is achieved by means of connecting together the points in the circuit which are at equal potentials. For this purpose, the scheme of Fig. 8a is redrawn as shown in Fig. 8b, wherein those ends of the secondary windings which at a given moment are at a positive potential are shown by asterisks. From Fig. 8b it is evident that the two secondary windings w_1 and w_1', and the two secondary windings w_2 and w_2' can be replaced each by a single winding. As a result, the scheme of Fig. 8a is transformed into Fig. 8c.†

Other magnetic amplifiers with reversive or duodirectional operation may be constructed in a similar manner.

Dependence of Efficiency upon Various Factors

We shall examine the basic factors which affect the efficiency of magnetic amplifiers built according to the scheme of Fig. 6. The dc power output in the load is equal to

$$P_н = I_н^2 R_н = (I_{10} - I_{20})^2 R_н, \qquad (9)$$

where I_{10} and I_{20} are the dc components of the output currents from the corresponding half-wave amplifiers. The effective (root-mean-square) values of these currents are respectively $I_1 = k_{f1} I_{10}$, $I_2 = k_{f2} I_{20}$, and $I_{Heff} = k_f I_H$.

Let us assume for the sake of simplicity that $k_{f1} = k_{f2} = k_f$. Then the entire power consumed in the circuit is approximately equal to

$$P_c = (I_1 + I_2)^2 R_b + (I_1 - I_2)^2 R_н + I_1^2 2R + I_2^2 2R, \qquad (10)$$

where R is the resistance of one operational winding together with the valve connected in series with it. From (9) and (10) we find the following expression for the efficiency of the amplifier:

$$\eta = \frac{P_н}{P_c} = \frac{(I_1 - I_2)^2 R_н}{k_f^2 [(I_1 + I_2)^2 R_b + (I_1 - I_2)^2 R_н + (I_1^2 + I_2^2) 2R]}. \qquad (11)$$

We introduce the following denotations: 1) the ratio of the currents in the windings of the two half-wave amplifiers $k = I_1/I_2$, and 2) the ratio of the resistance of one operational winding and the valve associated with it to the load resistance $m = R/R_H$. After introduction of these denotations into (11) and assuming that $R_b = R_H$, we have

$$\eta = \frac{\left(1 - \frac{1}{k}\right)^2}{2k_f^2 (1 + m)\left(1 + \frac{1}{k^2}\right)}. \qquad (12)$$

Values of efficiencies calculated by (12) for various reversive amplifiers built according to the scheme of Fig. 6 are given in Table 1 below. The efficiency data in this table are all computed for the same resistances ratio m = 0.1, but for a number of different current ratios k of the half-wave component amplifiers. The data in Table 1 are arranged in three columns: a) for the case when each arm of the bridge in Fig. 6 contains a single-half-period single-phase magnetic amplifier according to Fig. 7; b) for the case when the bridge arms are made up of twin half-period single-phase amplifiers according to Fig. 8; and c) for the case of three-phase half-period amplifiers according to Figs. 9 and 10 in the bridge arms.

TABLE 1. Efficiency values of reversive magnetic amplifiers with resistive loading and m = 0.1

k	Amplifier in bridge arms		
	Single half-period	Two half-periods single-phase	Two half-periods three-phase
	$k_f = 1.57$	$k_f = 1.11$	$k_f \approx 1.00$
5	0.11	0.23	0.28
10	0.15	0.30	0.36
20	0.17	0.33	0.41
∞	0.19	0.37	0.46

† It should be emphasized that the output leads from the transformers in the schemes of Fig. 8 are connected to center taps of the secondary windings, and that in both halves of the secondary windings on either side of the center taps there are always equal potentials $U_{\sim}$.

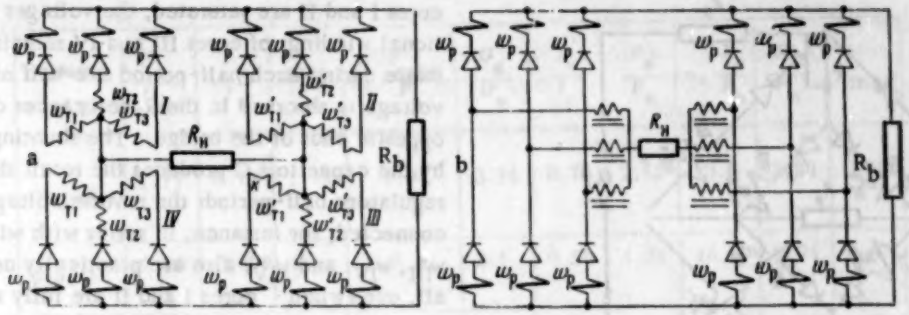

Fig. 9.

The values for k_f given in the table all correspond to the maximum value of the load current and to a currents ratio $k = \infty$.

Reversive schemes of magnetic amplifiers using three-phase elements can be built on the same principles as those described above. In Fig. 9a a scheme of a reversive amplifier is shown which is composed of a three-core magnetic amplifier with internal feedback. Comparing Figs. 9a and 9b, it is evident that by combining each two secondary transformer windings of Fig. 9a designated by the same symbols w_{T1}, w_{T2}, etc., a simplified version of the scheme (Fig. 9b) is obtained. For correct operation of the amplifier, the voltages across the transformer windings w_{T1}, w_{T2}, and w_{T3} must be shifted in phase by 180° with respect to the voltages of the corresponding transformer windings w'_{T1}, w'_{T2}, and w'_{T3}. The entire amplifier is built on six cores. If the three-core amplifier in the scheme of Fig. 9 is replaced by a three-phase bridge magnetic amplifier composed of six cores, the result is the scheme shown in Fig. 10 [3].

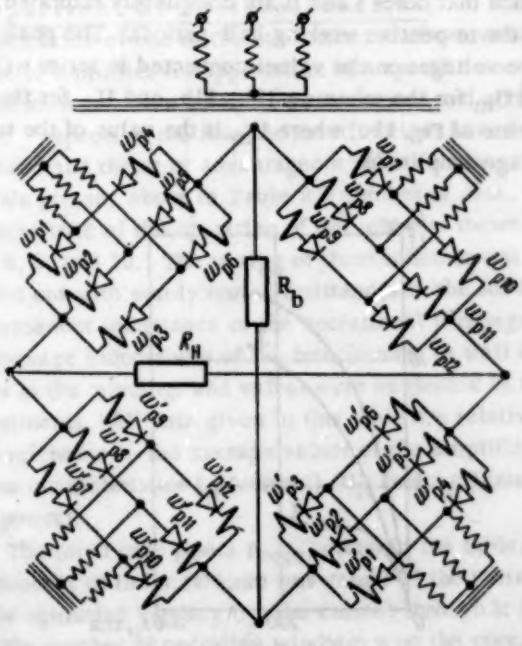

Fig. 10.

Two-half-period Schemes of Reversive Magnetic Amplifiers of High Efficiency Without Transformers

In the schemes of Figs. 8, 9, and 10, a supply transformer with a power rating exceeding 2-3 times the load power (see Table 2) is an inevitable part of the device.

However, utilizing the principles for designing reversive amplifier schemes stated above, it is possible to construct schemes of two-half-period reversive amplifiers without the use of supply transformers. It would appear that such an amplifier could be constructed by combining two single-half-period reversive amplifiers built according to the scheme of Fig. 7b and delivering during alternating half-periods their outputs to a common load. One of the feasible schemes of such a combination of single-half-period amplifiers is shown in Fig. 11a. In this scheme a common ballast resistance $R_0 = R_H$ is connected in series with the power supply. However, this scheme is inoperative, for this addition of resistance R_0 eliminates the redistribution of the supply voltage during the active half-period only in the w_p windings of an unsaturated core after saturation of one of the other cores. However, if one of the cores (for instance, I) is saturated during the entire working half-period, then the reverse supply voltage on the valves connected in series with the operational windings of another core (IV), which is at the time in the control half-period, will be close to zero; and that will be so, specifically, also for the core which, for efficient operation, should have a minimum of current in its windings at that time. As was pointed out above, this lowering of the reverse voltage on the valves leads to a considerable increase of the current through the operational windings in the next active half-period of operation; and thus the current in the output load is considerably lowered.

Better operational characteristics are obtained by a two-half-period reversive scheme suggested by the authors which is shown in Fig. 11b.

As pointed out above, to be sure of high efficiency in any reversive magnetic amplifier, the following two conditions must be fulfilled: 1) saturation of one or several cores during a half-period must not lead to an increase of the voltage applied to the terminals of the

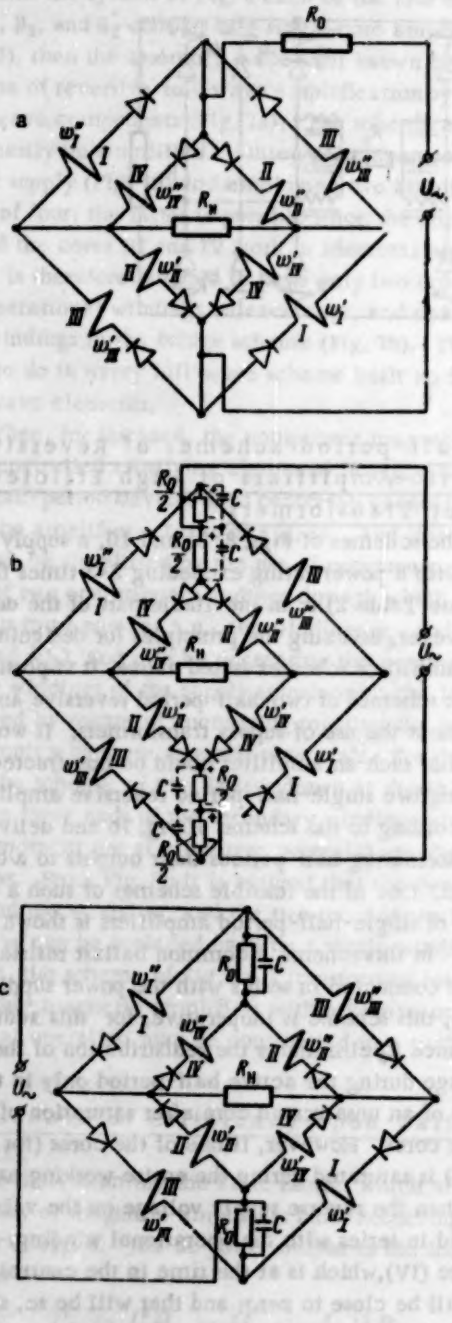

Fig. 11.

operational windings of the unsaturated cores during that half-period; 2) presence of a signal at the input of the amplifier, and, hence, of a voltage in the output load must not lead to a decrease of the reverse voltage on the valves in the regulatory half-period.

Satisfaction of both above conditions is achieved in the scheme of Fig. 11b by adding, prior to the entrance of the supply voltage to each of the two apexes of the two bridges of Fig. 11a, a resistance $R_0/2$ and a capacitance C in parallel with each of these resistors. The value of R_0 is chosen to be equal to one-half of the load resistance $R_н$. As a result of this, when, for instance, cores I and II are saturated, the voltages on the operational windings of cores III and IV remain unaltered, because during each half-period one-half of the supply voltage is absorbed in the R_0 resistances connected at opposite ends of the bridge. The shunting of the resistors by the capacitors C produces the result that during the regulatory half-periods the reverse voltages on the valves, connected, for instance, in series with windings w'_{III}, w''_{III}, w'_{IV}, and w''_{IV}, also are practically not decreased at all, even when cores I and II are fully saturated during the working half-period. The magnitude of capacitance C is not critical; it may be chosen to equal $C \approx (1-2)/(R_0 f)$, where f is the frequency of the supply voltage. Electrolytic condensers may be used for this purpose, since, first, the voltages across the resistors $R_0/2$ are of constant polarity as shown in Fig. 11b, and, second, leakage currents in the condensers have no substantial effect on the operation of the amplifier.

A warning, however, must be given against the choice of condensers of capacitance values so high that the voltage across them during the entire period of the supply voltage will practically be equal to the full amplitude variation of voltage across R_0 at $C = 0$; for, since the voltage across the condensers is subtracted from the supply voltage, with such very high capacitances an output voltage from the amplifier is observed which is somewhat lower than the maximum possible.

In place of the scheme of Fig. 11b, the scheme of Fig. 11c can also be used, which makes it possible to satisfy the above indicated condition with fewer resistors and condensers. This scheme, however, has the drawback that the reverse voltage on the valves may reach higher values than in scheme 11b. Let us assume, for example, that the magnitude and polarity of the signals is such that cores I and II are completely saturated during the respective working half-periods. The peak inverse voltages on the valves connected in series will then be $\frac{1}{2} U_m$ for the scheme of Fig. 11b, and U_m for the scheme of Fig. 11c, where U_m is the value of the supply voltage amplitude.

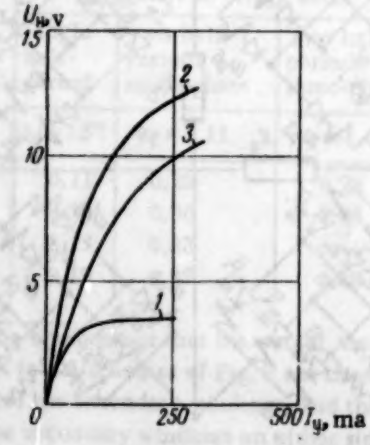

Fig. 12.

TABLE 2

Scheme of:	$\frac{U_p}{U_н}$	$\frac{I_p}{I_н}$	$\frac{P_{core}}{P_н}$	$n_c \frac{P_{core}}{P_н}$	$\frac{U_в}{U_н}$	$\frac{I_в}{I_н}$	$\frac{P_в}{P_н}$	$n_в \frac{P_в}{P_н}$	$\frac{P_{tr}}{P_н}$	η_{max}
Fig. 8	1.11	0.78	1.74	6.94	3.14	0.78	2.45	19.6	2.96	0.406
Fig. 9	0.855	0.59	1	6	2.1	0.59	1.24	14.9	2.74	0.5
Fig. 10	0.37	0.82	0.43	5.15	1.05	0.58	0.61	14.6	2.1	0.5

A consideration of the actual working conditions will decide which of the above schemes is the most advantageous in every specific case.

In Fig. 12, characteristic curves are given for amplifiers constructed according to the scheme of Fig. 11a (curve 1), according to the scheme of 11b with ripple-smoothening condensers (curve 2), and according to the same scheme without ripple-smoothening (curve 3). The differences in characteristics evident in Fig. 12 will become still larger when there is an opposing emf or an inductance in the amplifier output load.

Experimental comparisons of the proposed schemes with all other known schemes of reversive half-period amplifiers with dc output have shown that the proposed schemes not only make it possible to operate without a power transformer, but also have the highest efficiency, which approaches 0.4 when losses in windings and valves are small.

Comparison of Various Schemes

Selection of one or the other scheme of a reversive magnetic amplifier for application in a specific control system must be made after all the technical and economic aspects of the feasible modifications have been discussed and the most advantageous decided upon.

We present above in Table 2 a number of data, characteristic of the operation of our schemes shown in Figs. 8, 9, and 10. The testing of these schemes was carried out with purely ohmic resistances in the loads; the remanent inductance of the operational windings and the leakage inductances of the transformer as well as losses in the windings and valves were neglected in these experiments. All data given in this table are relative—with reference to the average values of the amplifier output characteristics I_H (current), U_H (voltage), and P_H (power).

The rated core power P_{core}, given in the table, is the product of the maximum rms values of the voltage in the operating winding U_p, the current through it I_p, and the number of operating windings n on the core. The rated rectifier power P_B is understood to equal the product of the peak inverse voltage U_B at the valve with the maximum rms value of the current I_B through the valve.

In the above table n_c designates the number of cores, and n_B the number of valves used in the scheme. P_{tr} is the rated power of the transformer.

CONCLUSIONS

On the basis of our investigation the following conclusions can be drawn:

1) For construction of reversive (duodirectional) schemes of magnetic amplifiers with dc output operating with higher efficiencies, it is advantageous to use a scheme based on subtraction of currents of nonreversive amplifiers.

2) To obtain increased efficiency in these schemes the following conditions must be fulfilled:

a) saturation of one or of several cores must not lead to increase of the voltage at the terminals of the working windings of any of the nonsaturated cores during the working half-period;

b) the voltage on the load must not produce a decrease of the inverse (rectifier) valve voltage during the control half-period.

3) Fulfillment of condition 2) can be assured by connection of half-wave amplifiers into the bridge scheme of Fig. 6.

4) To obtain higher efficiency, it is necessary in addition to fulfillment of conditions 2) to assure a high ratio of high to low current in the working windings of the nonreversive amplifiers and small pulsations in the rectified current. Therefore, all other conditions being equal, reversive amplifiers using three-phase current have the highest efficiency.

5) In this paper new schemes for reversive magnetic amplifiers with dc outputs without the use of transformers have been proposed; they satisfy conditions 2) and have high efficiencies.

LITERATURE CITED

1. M. A. Rozenblat, Magnetic Amplifiers [in Russian] (Izd. Sovetskoe Radio, 1960).

2. M. A. Rozenblat and G. V. Subbotina, "Increase of efficiency in reversive magnetic amplifier by means of transistors," Avtomat. i Telemekh. 20, No. 9 (1959);‡

3. S. S. Roizen, "Application of magnetic amplifiers in electric transmissions," Byull. Tyazhpromélektroproekta, No. 3 (1957).

‡ See English translation.

APPLICATION OF TRANSISTORS IN CIRCUITS OF VIBRATIONAL VOLTAGE REGULATORS

A. G. Zdrok

Moscow

Translated from Avtomatika i Telemekhanika, Vol. 21, No. 11
pp. 1514-1524, November, 1960
Original article submitted May 6, 1960

Electrical circuits are reviewed in which transistors and two position vibrators are used for voltage regulation of dc generators. Arrangements are presented which provide increase of the armatures frequency of vibration, as well as schemes using additional transformers or choke coils to secure better performance of the regulator at elevated ambient temperatures. Results of experimental investigations are given.

Vibratory electromagnetic relays and regulators have found wide application in various technical fields [1]; for instance, voltage regulation of modern dc and ac generators of automobiles is carried out exclusively by means of vibrating regulators [2].

A serious shortcoming of vibratory regulators is the presence of a continuously vibrating switching system which all the time breaks and makes contacts to open and close an inductive current-carrying electrical circuit.

It is known that the wearing out of contacts is due to mechanical, chemical, and electrical phenomena. The greatest wear is caused by electrical phenomena occurring when an arc is produced during the breaking of contacts. However, when the current in the circuit of the contacts is lower than 0.05-0.06 amp, and the voltage applied to them is less than the breakdown voltage of the air gap at the contact, then there is practically no erosion taking place when contacts are broken [1]. Such conditions for operation of contacts can be obtained by various schemes using semiconductors.

In the present paper, electrical regulation schemes are reviewed which use transistors and two-position vibrators for control of dc generators.

1. Simplest Circuits for Voltage Regulation

A number of schemes for voltage regulation of dc generators in which transistors and vibratory elements are employed were reviewed in [3]. The vibrators reviewed there consist of nonsymmetrical polarized two-position relays (one of the two contact positions being "predominant").

In actual operations two-position vibrational regulators having one pair of normally closed contacts proved the most dependable; our manufacturing industry has become quite familiar with the production techniques of such regulators. Therefore, it is most advantageous in schemes employing transistors also to use vibrational regulators with one pair of contacts.

One of the feasible schemes for voltage regulation by means of a vibratory device in combination with a transistor is shown in Fig. 1. In this figure, OB is the excitation winding of a generator, and OO and K are the

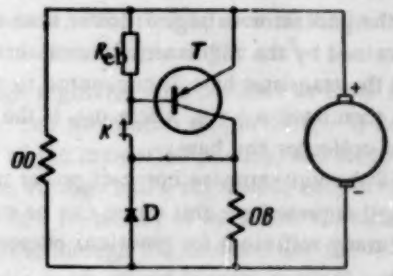

Fig. 1.

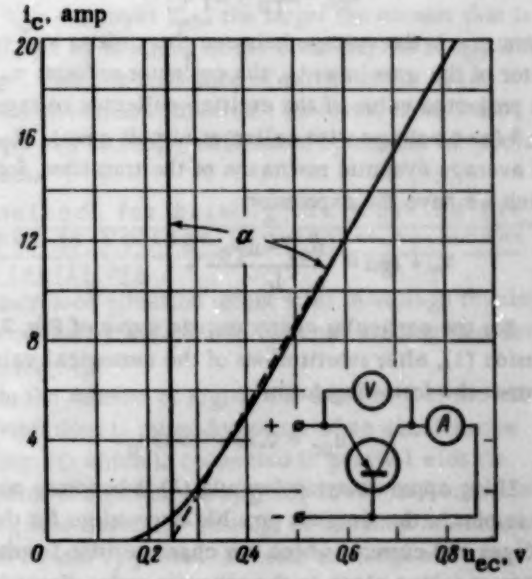

Fig. 2.

energizing coil and the contacts of the vibrator. R_{eb} is a resistance connected as shown between the emitter and base electrodes of transistor T which serves the purpose of decreasing the potential difference between these electrodes when contacts K are broken. Semiconductor diode D serves to eliminate the effect of the self-induction emf in the generator's excitation winding upon the operation of the transistor; see [4] and [5]. The generator excitation winding is in our figure connected in the collector loop of transistor T. However, it may be connected instead in the emitter circuit. The power being broken by the separation of the contacts is the same in both cases; therefore, in general, both of these methods of connection of the excitation winding are of equal value.

However, in single conductor systems it is more advantageous to have the generator excitation winding in the emitter circuit of the transistor: in this case, if the generator minus pole is connected to the housing, it will not be necessary to insulate the transistor housing from the generator housing. In this way the generator housing may be utilized as a thermal sink to carry away the heat from the transistor. Such schemes will be discussed below.

The scheme of Fig. 1 operates in the following manner.

When the generator voltage is lower than the one to be maintained by the regulator, the contacts K are closed, and the transistor base is connected to the collector. We then have $u_{cb}=0$, where u_{cb} is the voltage between the collector and base.

In Fig. 2 the volt-ampere curve of power transistor P 208 at $u_{cb}=0$ is presented; this curve can be expressed with an accuracy sufficient for practical purposes by the formula

$$u_{ec}=u_{T0}+R_T i_c, \tag{1}$$

where u_{ec} is the voltage between the emitter and collector of the transistor; i_c, the collector current; u_{T0}, the projected value of the emitter-collector voltage at $i_c=0$ (e-c voltage with collector circuit open). R_T is the average dynamic resistance of the transistor, for which we have the expression

$$R_T=\operatorname{tg}\alpha=\frac{u_{ec}-u_{T0}}{i_c}.$$

For the particular characteristic curve of Fig. 2, expression (1), after substitutions of the numerical values, assumes the following form:

$$u_{ec}=0.25+0.029\,i_c.$$

Using approximation formula (1) it becomes possible to obtain the simplest possible expressions for the voltages and currents which are characteristic for the processes taking place in the schemes under discussion. For example, when self-excitation takes place in the generator, the voltage generated u_G is balanced by the sum of the voltage drops in the transistor and in the excitation winding; that is, we have

$$u_G=u_{ec}+i_B r_B, \tag{2}$$

where r_B and i_B are respectively the resistance of and the current in the excitation winding.

Considering that $i_B=i_c$ (Fig. 1), and substituting (1) and (2), we obtain the following expression for the generator excitation current:

$$i_B=\frac{u_G-u_{T0}}{r_B+R_T}. \tag{3}$$

When the generator voltage u_G reaches the standard output value, contacts K are opened. Then we have $u_{eb}\approx 0$, since the base is usually connected with the emitter by a resistance R_{eb} of low ohmage. In order to obtain simple relationships, let us assume that the inductances of the excitation winding of the generator and of the vibrator energizing coil are constant, and that the resistance of the transistor in the reverse direction is infinite. Then for our scheme in its present condition the following equation will be valid:

$$L_B\frac{di_B}{dt}+i_B r_B+u_D=0, \tag{4}$$

where u_D is the potential drop across the rectifier diode D, L_B–the inductance of the generator excitation winding.

Since in this state the resistance of the transistor is considerably higher than that of the diode which is now in the forward conductance state, it is possible to consider that as a first approximation the extra current caused by the closing of passage through the transistor is going through the diode loop, and that

$$i_B\approx i_D. \tag{5}$$

Vibrating voltage regulators usually have high ratios of release currents to holding current reaching up to 0.95. By the time the next contact make is due, the current in the diode usually has not had time to go down to zero. Therefore, the volt-ampere curve of the shunting diode may be expressed, with accuracy sufficient for practical purposes, by an experimental formula similar to (1), which is as follows:

$$u_D=u_{D0}+i_D R_D. \tag{6}$$

Solving equation (4) for the generator excitation current i_B, taking into account (1), (5), and (6), we obtain the following formula for the excitation current during the time when the regulator contacts are open:

$$i_B=i_{B0}e^{-\frac{r_B+R_D}{L_B}t}-\frac{u_{D0}}{r_B+R_D}\left(1-e^{-\frac{r_B+R_D}{L_B}t}\right), \tag{7}$$

where i_{B0} is the magnitude of the generator excitation current at the moment of opening of the contacts.

Expression (7) makes it possible in a relatively simple way to obtain an approximate estimate of the average value of the diode current, and to choose the proper type of diode. To do this it is sufficient to substitute into (7) the value of i_D from (5). Also the time interval must be known during which the contacts remain open, and the vibration frequency. Then for the average value of the diode current I_D the following formula is obtained:

$$I_D = \frac{f_c L_B}{r_B + R_D} \left[\left(i_{B0} + \frac{u_{D0}}{r_B + R_D} \right) \left(1 - e^{-\frac{r_B + R_D}{L_B} t_p} \right) - \frac{u_{D0}}{L_B} t_p \right], \quad (8)$$

where f_c is the frequency of vibration of the contacts, and t_p is the time the contacts are open during a cycle.

By the use of a shunting semiconductor diode not only is the proper operation of the transistor under the prevailing conditions of back and forth switching secured, but also the appearance of excessive voltage between the emitter and collector is excluded.

When the contacts are open, the generator voltage u_G and the voltage across the diode are of the same polarity; consequently

$$u_{ec} = u_G + u_D. \quad (9)$$

Solving equations (6), (7), and (9) simultaneously, we obtain an expression for the voltage u_{ec} between the emitter and collector of the transistor at the time when contacts K are open:

$$u_{ec} = u_G + u_{D0} + R_D \left[i_{B0} e^{-\frac{r_B + R_D}{L_B} t} - \frac{u_{D0}}{r_B + R_D} \left(1 - e^{-\frac{r_B + R_D}{L_B}} \right) \right]. \quad (10)$$

The product of R_D with the expression in the brackets can amount to only a few percent of the voltage to be regulated. The same is true for the voltage u_{D0}. Therefore, one may consider that in schemes where the excitation windings are shunted by a semiconductor diode, the voltage between emitter and collector is approximately equal to the voltage of the generator which is being regulated. The larger the resistance of the diode circuit loop, the higher is the emitter to collector voltage.

Formulas (9) and (10) make it possible to estimate the maximum voltage that can be expected on the transistor in this application, and accordingly to choose the proper transistor for it.

When a shunting diode is not present at the moment the contacts are opened, the voltage across the transistor may exceed the regulation voltage of the generator u_G by a factor of several times [3].

It is the resistance R_{eb} connected between the emitter and the base (Fig. 1) which determines the potential

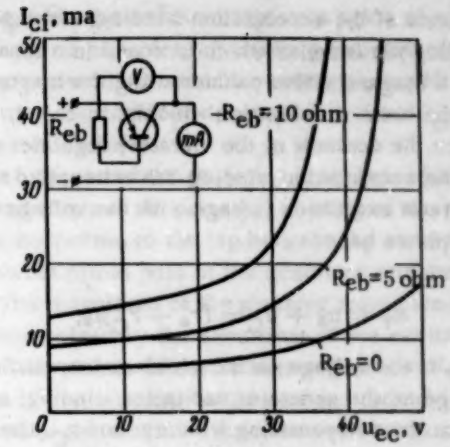

Fig. 3.

difference between the emitter and base when the contacts K are open. Thus, the resistance of the transistor in the nonconducting state is determined by the value of resistance R_{eb}.

In Fig. 3 are presented volt-ampere curves of transistor P208 for various values of resistance R_{eb} to illustrate the effect of the shunting resistance upon the transistor resistance in its nonconducting phase. I_{cl} in Fig. 3 is the initial collector current. The characteristic curves of Fig. 3 were taken at an ambient temperature of 50°C. The measurements were made after a two-hour warmup of the transistor. The surface area of the heat sink, which was made of aluminum, was 750 cm^2.

Voltage regulator schemes such as those shown in Fig. 1 have two substantial shortcomings: 1) Relatively low speed of the regulation process, and large fluctuations in the voltage being regulated, both of these being due to the low frequency of armature vibrations; and 2) the current through the contacts and the resistance of the transistor in its closed (nonconducting) condition are both determined by the magnitude of the shunting resistance R_{eb}; the lower R_{eb}, the larger the current that is interrupted by breaking of the contacts; but if R_{eb} is increased, then the resistance of the transistor in its blocked condition is lowered. However, these shortcomings can be easily eliminated by the use of special schemes.

2. Methods for Raising the Working Frequency in Voltage Regulators by Means of Transistors

Increased vibration frequencies in voltage regulators are obtained by the use of additional windings and resistances (Fig. 4).

In the scheme of Fig. 4a the frequency of the armature vibrations is raised by means of an acceleration winding YO which is connected in parallel with the generator excitation winding OB; in this and in the following schemes the beginnings of windings are indicated in the figures by points. In order to compensate for the lowering of the resultant magnetic force with increasing speed of rotation of the generator armature, caused by

the presence of the acceleration winding, a compensating winding KO is added which is wound in a sense to produce a magnetization counteracting the magnetization by the basic acceleration winding.

When the contacts of the vibratory regulator are closed, the acceleration winding YO has applied to it the generator excitation voltage with the voltage on KO added; thus we have

$$u_y = u_в + u_C = (r_в + r_C) i_в, \qquad (11)$$

where u_Y is the voltage on the acceleration winding; u_B, the voltage on the generator excitation winding; u_C, the voltage on the compensating winding; and r_C, the resistance of the compensating winding.

When contacts K are open, the excitation winding is shortcircuited by the diode; the voltage on the acceleration winding then is equal to the potential drop across the diode. When the contacts are broken, the voltage on winding YO is decreased abruptly by

$$\Delta u_y = (r_в + r_C)\, i_в - u_D. \qquad (12)$$

The change of current through winding YO can be expressed by the following simple formula (neglecting the mutual effects of windings OO and OY):

$$i_y = \frac{(r_в + r_C) i_в}{r_y} e^{-\frac{r_y}{L_y} t} - \frac{u_D}{r_y}\left(1 - e^{-\frac{r_y}{L_y} t}\right), \qquad (13)$$

where r_Y and L_Y are the resistance and inductance of the acceleration winding.

It follows from expression (13) that at the instant

$$t_0 = \frac{L_y}{r_y} \ln\left[1 + \frac{(r_в + r_C) i_в}{u_D}\right] \qquad (14)$$

the current in the acceleration winding changes its direction; when $0 \le t \le t_0$ the resultant magnetizing force is equal to the sum of the magnetizing forces produced by the principal and acceleration windings, and when $t > t_0$ —to their difference.

Consequently, when the contacts are opened, the resulting magnetizing force of the regulator windings is substantially decreased, which leads to a considerable demagnetization of the vibrator core, and this in turn brings about a faster closure of the contacts [remember that the vibrator being of the "normally closed" type, the contact "make" is mostly caused by spring action on the armature opposed to the magnetic action— Translator].

If the "make" of the contacts occurs at time t_p after the preceding break, acceleration winding YO will have at that moment the voltage u_Y applied to it, and the current in this winding will begin to rise; this change will take place according to the following expression:

$$i_y = \frac{(r_в + r_C) i_в}{r_y}\left(1 - e^{-\frac{r_y}{L_y}(t_p + t)}\right) + \frac{u_D}{r_y}\left(e^{-\frac{r_y}{L_y} t} - e^{-\frac{r_y}{L_y}(t_p + t)}\right) \qquad (15)$$

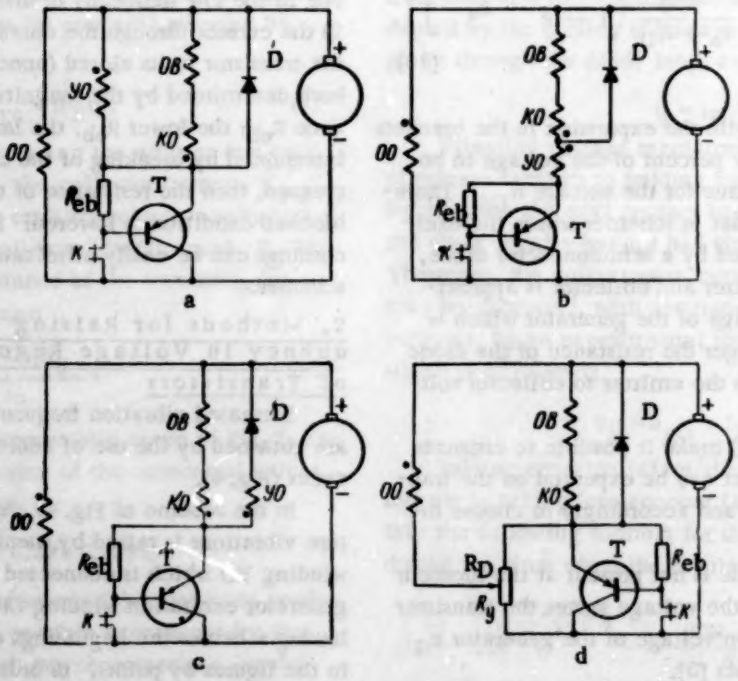

Fig. 4. Scheme of voltage regulation with acceleration of vibration of the regulator armature.

The increasing current in the acceleration winding will speed up the occurrence of the "break" of the vibrator contacts.

In the circuit of Fig. 4b acceleration is achieved by a winding YO connected in series with the emitter of the transistor. When the contacts are closed, the current in this winding is determined by the expression

$$i_y = i_B e^{-\frac{R}{L}t} - \frac{u_{TO}}{R}\left(1 - e^{-\frac{R}{L}t}\right), \qquad (16)$$

where i_B is the excitation current when the contacts are closed,

$R = r_B + R_T + r_Y + r_C$, and $L = L_B + L_Y + L_C$;

here r_Y, r_C, L_Y, and L_C are the resistances and inductances of the acceleration winding and of the compensating winding, connected now in series.

The volt-ampere curve of the transistor in this case is again represented by formula (1).

When the contacts K are opened, the generator excitation current is substantially going only by way of the diode circuit, while the winding YO is practically currentless. Thus, the magnetizing force of the regulator winding is diminished, and thereby conditions for faster closing of the contacts are created.

The frequency of the regulator armature's vibrations can be raised also by connecting an acceleration winding in series with the shunting diode (Fig. 4c). The acceleration winding YO is connected in opposition to the principal regulator winding OO. In the circuit of Fig. 4a the winding YO must be of high resistance, in the circuits of Figs. 4b and 4c—of low resistance.

In Fig. 4d a circuit for voltage regulation of a generator is presented, in which a frequency increase of the vibrator armature is obtained by means of an additional "acceleration resistor" R_Y with another resistor R_D connected in series with it.

The entire resistance $(R_Y + R_D)$ is connected in shunt to the transistor, and the principal winding of the vibrator is now connected to the tap between R_Y and R_O, instead of to the minus pole of the generator armature as before. The magnitude of the shunting resistance $(R_Y + R_D)$ is determined by the excursions of the excitation current in the process of the voltage regulation of the generator. In voltage regulators used in automobiles, the R_Y part of the auxiliary resistance serves not only for purposes of acceleration but also as a heat sink for the principal regulator winding OO.

The voltage applied to the principal vibrator winding when the contacts are closed is almost equal to the generator voltage. The voltage across the shunting resistance $(R_Y + R_D)$ when the contacts are broken is determined by (9) and (10) above. The voltage on the vibrator winding OO is then equal to

$$u_0 = u_{ec}\frac{R_D}{R_y + R_D} - u_D. \qquad (17)$$

Obviously, the smaller R_D, the smaller the voltage on the OO winding at the moment the contacts are broken, and the faster the falling off of the current in it takes place. When $R_D = 0$ the accelerating action of the OO winding in the scheme of Fig. 4d is similar to that of Fig. 4a.

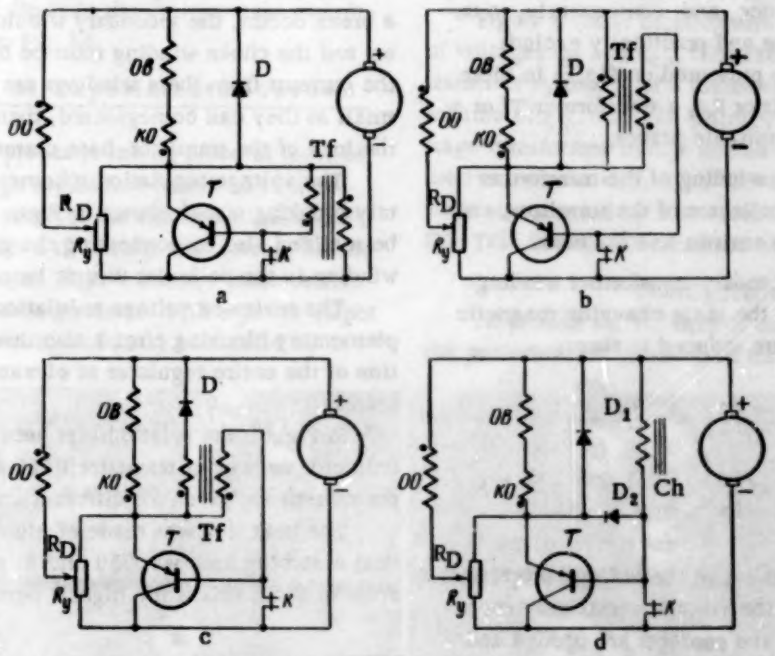

Fig. 5. Scheme of voltage regulation with an additional blocking circuit.

However, these schemes are not altogether equivalent to each other: in the scheme of Fig. 4d closing and opening of the contacts is affected by changes in the magnetizing force of only winding OO, while in the scheme of Fig. 4a both windings OO and YO are having an effect. Also, the magnetizing force produced in the OO winding varies only within relatively small limits in the process of regulation. The latter property is also shared by the schemes of Figs. 4b and 4c.

The scheme using an additional acceleration resistance has, in comparison with the schemes using additional windings for acceleration, also the advantage that less space for accommodation of the windings is needed. This makes it possible to decrease the size of the regulator magnetic system and to save on copper.

An analysis of this kind of scheme for raising the vibration frequency of the regulator armature is given in [2].

In the schemes of Fig. 4 discussed above the generator excitation winding was connected in the emitter circuit of the transistor. However, in all these schemes the excitation winding may be just as well connected in the collector circuit, as was shown in Fig. 1.

3. Voltage Regulation Schemes with an Additional Blocking Circuit

In the voltage regulation schemes of Figs. 1 and 4, the current load on the vibrator contacts is much lower than in the ordinary regulators used at the present time. However, depending upon the magnitude of the R_{eb} resistance, the currents being interrupted by the contacts can still be of considerable magnitude.

Using additional blocking circuits it is possible practically to eliminate the currents depending upon the presence of the R_{eb} resistance, and, consequently, to unload the contacts still more and practically exclude erosion. Such schemes are presented on Fig. 5; in these schemes instead of the resistor R_{eb} a transformer Tf or a choke coil Ch is used in suitable places.

In Fig. 5a the primary winding of the transformer connects the emitter and collector of the transistor, and the secondary winding, the emitter and the base.

If the primary and secondary transformer windings w_1 and w_2 are traversed by the same changing magnetic flux, the following emf's are induced in them:

$$e_1 = -w_1 \frac{d\Phi}{dt}, \qquad e_2 = -w_2 \frac{d\Phi}{dt};$$

from this it follows that

$$\frac{e_1}{e_2} = \frac{w_1}{w_2}.$$

Consequently, if the effect of the voltage drops in the windings is neglected, the voltage variations across the emitter and base when the contacts are opened and closed will be of the same character as those across the emitter and collector. When contacts K are closed the voltage on the primary winding is determined by the transistor volt-ampere curve of Fig. 2; it is equal to the emitter-collector voltage corresponding to the collector voltage $u_c = 0$. When the contacts are open the voltage on the primary transformer winding is determined by formulas (9) and (10). The voltages applied between the emitter and base will be similar in shape. When contacts K are open, the positive pole of the potential, produced by the emf induced in the secondary transformer winding, will be applied to the base, the negative—to the emitter. In this way passage of current through the transistor is reliably blocked. In the scheme of Fig. 5a the primary and secondary transformer windings must be of high ohmage.

The scheme of Fig. 5b works in a similar manner. Here the primary transformer winding is connected in parallel to the generator excitation winding. In Fig. 5c a voltage regulation scheme is shown having a low ohmage primary transformer winding connected in series with the diode. If the variation of the voltage drop across the diode with current is neglected, the shape of the voltage induced in the secondary winding will be the same as that induced in the scheme of Fig. 5a. In the scheme of Fig. 5d, a positive potential on the transistor base relative to the emitter is secured by the use of choke coil Ch connected between the plus pole of the generator and the transistor base.

In order for the induced emf to last longer, the time constant of the choke circuit must be increased. This is easily accomplished by connecting another semiconductor diode D_2 in parallel with the choke. In the scheme of Fig. 5d, the diode D_2 serves also to limit the magnitude of the applied signal.

To decrease the power handled by the contacts when a break occurs, the secondary windings of the transformers and the choke winding must be of high ohmage: if the currents from these windings are made sufficiently small so they can be neglected, then there will be only the load of the transistor base current on the contacts.

The voltage regulation schemes with a supplementary blocking circuit shown in Figs. 5a, 5b, and 5c can be realized also by connecting the generator excitation winding in the collector circuit loop of the transistor.

The reviewed voltage regulation schemes with supplementary blocking circuit also insure dependable operation of the entire regulator at elevated ambient temperatures.

In Fig. 6* the relationships between the emitter-collector voltage of transistor P208 and the collector output current are given for different emitter-base voltages.

The heat sink was made of aluminum, the active heat absorbing area was 750 cm^2 at an ambient temperature of 85°C; this is the highest permissible ambient

*The curves of Fig. 6 are for the same transistor specimen as those of Fig. 3.

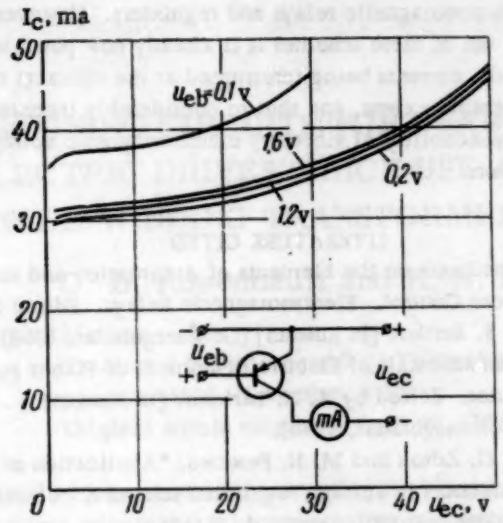

Fig. 6.

temperature when the collector of the transistor is loaded to the maximum rated power output. The voltages between the emitter and base were applied from a source which had a constant output resistance.

With increase of positive potential on the base relative to the emitter, the collector current first decreases. At a potential between 0.2 and 1.2 v the collector current reaches a minimum. With further increase of positive potential on the base, the collector current somewhat increases. Hence, when P208 type transistors are used, the transformer or choke must be so chosen, that positive potentials within the indicated limits are provided on the transistor base when the contacts are open. Base emitter potentials close to those required can be obtained by including in all these schemes an additional germanium or silicon diode in the emitter-base circuit in a manner similar to Fig. 5d.

4. Some Results of Experimental Investigations

To illustrate the processes taking place in some of the schemes for voltage regulation described in this paper and to confirm some of the mathematical relationships given, a number of voltage and current oscillograms are given below in Figs. 7 and 8; these oscillograms were taken on a dc generator with a power output of 1500 w at a rated voltage of 28 v, controlled by a regulator consisting of a vibrator in combination with a transistor. The minimum speed of revolutions of the generator armature at the rated voltage and at full load was 1550 rpm with the generator still cold. A transistor of the P4A type was connected in series with the excitation winding which had a resistance of 8 ohms; a VG-10 valve was in parallel with the excitation winding; the load on the generator consisted of a storage battery which was being charged at a current of 15 amp. To increase the speed of the regulator operation an acceleration resistance $R_Y \approx 0.14\ R_D$ was connected in the circuit.

Figures 7a and 7b represent oscillograms of the generator voltage u_G, of the emitter-collector voltage u_{ec}, of the emitter-base voltage u_{eb}, and of the collector current i_c of the transistor. The potential difference u_{eb} when the transistor is passing current is shown above the zero line, the blocking u_{eb} potential—below the zero line.

These oscillograms illustrate the operation of the scheme shown in Fig. 5a at n = 1500 rpm. The average value of the generator excitation current was 1.43 amp, the generator voltage was 28.2 v. To obtain the blocking voltage u_{eb}, an interstage transformer from a Rodina-47 receiving set was used. The scales of the u_G and u_{ec} voltages on the oscillograms were the same. The u_{eb} voltages are shown on a magnified scale.

The emitter-collector voltage u_{ec} is here approximately equal to the generator voltage u_G; thus relationships (9) and (10) are confirmed. The shape of the u_{eb} voltage variations is approximately the same as that of the u_{ec} variations; the slight differences observed between these two are due to deviations of the vibrator natural frequencies.

The other schemes work in a similar manner.

Figure 8 shows oscillograms of current i_D, and also of voltages u_G and u_{eb}, illustrating the blocking of the transistor by means of a choke coil according to the scheme of Fig. 5d. The primary winding of an interstage transformer from a Rodina-47 receiver-set was used as a choke coil. The emitter-base part of the transistor was shunted by a semiconductor diode of type DG-Ts24 in order to limit the blocking signal.

CONCLUSIONS

At present the industry of our country has mastered the production of germanium transistors for currents up

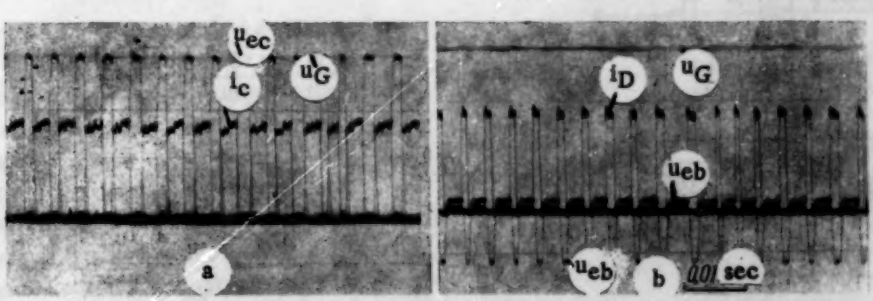

Fig. 7. Oscillograms of voltage and currents illustrating the operation of the circuit of Fig. 5a.

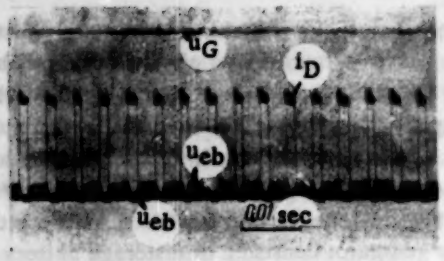

Fig. 8. Oscillograms of u_{eb} and i_D illustrating the operation of the circuit of Fig. 5d.

to 25 amp [6]. By means of the above described schemes it is possible when regulating the voltage of generators with excitation currents to 25 amp to have at the vibrator contacts being broken currents of only 0.3 to 0.8 amp.

The great majority of automobile generators have excitation currents of 1.5–3.0 amp. When vibratory regulators in combination with transistors are used on these generators, the current broken by the vibrator contacts will be from 0.03 to 0.09 amp.

By combined use of vibratory electromagnetic regulators and of transistors it will be possible to avoid erosion of contacts.

The schemes reviewed here by no means exhaust the many feasible combinations of transistors with vibratory electromagnetic relays and regulators. However, by the use of these schemes it is already now possible to lower the currents being interrupted at the contacts to a considerable extent, and thus to considerably increase the dependability of vibratory electromagnetic voltage regulators.

LITERATURE CITED

1. Handbook on the Elements of Automation and Remote Control. Electromagnetic Relays. Edited by B. S. Sotskov [in Russian] (Gosénergoizdat, 1958).
2. Fundamentals of Electric Equipment of Planes and Autos. Edited by A. N. Larionov [in Russian] (Gosénergoizdat, 1955).
3. A. G. Zdrok and M. N. Fesenko, "Application of transistors in voltage regulation schemes," Vestnik Élektropromyshlennosti No. 9 (1958).
4. V. G. Konstantinov, "Transistor amplifier for excitation control of electrical machines," Vestnik Élektropromyshlennosti No. 1 (1959).
5. O. A. Kossov, "Operation of a semiconductor switch with loads of different nature," Élektrichestvo No. 5 (1959).
6. A. V. Krasilov, A. B. Polyanov, and E. S. Saltykova, "A powerful germanium transistor," Élektrichestvo No. 1 (1959).

DESIGNING CIRCUITS FOR STABILIZING COMPOUND ELECTRIC DRIVES WHICH USE A SPECIAL THREE-WINDING TRANSFORMER

O. B. Rosenbauli and R. N. Rodin

Moscow

Translated from Avtomatika i Telemekhanika, Vol. 21, No. 11,
pp. 1525-1535, November, 1960
Original article submitted April 22, 1959

A method is presented for computing the parameters of circuits for stabilizing the speed of compound dc and ac drives using a special three-winding transformer. A graphical method for plotting the circuit characteristics of the drive stabilizer is given; the non-linearity of the magnetization curve of the three-winding transformer core is taken into account.

The methods presented are illustrated by an example in which the parameters and characteristics of a stabilization circuit are given; the circuit controls a dc drive powered from the ac line through a rectifier.

Circuits using a special three-winding transformer for stabilizing the speed of dc and ac motors have found contemporary use [1]. Such circuits have a number of important advantages. In particular, they permit one to realize feedback compensating for perturbations with a single device, to decrease the weight of active materials in the controlling device, to simplify the adjustment of the system, and to decrease the variety and number of circuit elements. The advantages of such circuits permit them to be widely used in a number of dc and ac electric drive systems. The correct choice of the stabilizing circuit parameters is important in designing such systems. At present, problems related to the computation of such stabilizing systems have not been dealt with in periodical literature. This article presents a method for computing the parameters of circuits for stabilizing the speed of dc motors with a choke regulator connected to the ac line through a rectifier, and three-phase motors with a Shenfer rotor; a method for calculating the characteristics of the three-winding transformer used in the speed stabilizer of the drive is also presented.

1. Designing a Three-winding Transformer for a DC Motor Speed Stabilizer

A three-winding transformer is used as the compounding element in the circuit for controlling and stabilizing the speed of a dc motor shown in Fig. 1. It can be seen from this circuit that the load current $I_{\sim}$ flows through the current winding of the transformer; the voltage winding in series with an additional resistance R_d is connected to the supply voltage $U_{\sim}$, and the secondary winding feeds the stabilizing winding of the controlling device through a rectifier. It was shown in [1] that the expression for the current in the secondary circuit of such a transformer, I_2, is

$$I_2 = k(U_{\sim} - k_1 I_{\sim}), \qquad (1)$$

where

$$k = \frac{W_2}{W_u \sqrt{(R_1' + R_2)^2 + \left(\frac{R_2 R_1'}{X_m'}\right)^2}}, \quad k_1 = \frac{W_i R_1}{W_u},$$

if the voltage and current windings are connected opposing.

Here W_i is the number of turns in the current winding of the transformer; W_u the number of turns in the voltage winding; W_2 the number of turns in the secondary winding; R_1' the resistance of the voltage winding referred to the secondary winding; X_m' the inductive reactance of the magnetizing circuit referred to the secondary; and R_2, the resistance of the secondary circuit $R_2 = r_2 + R_L$.

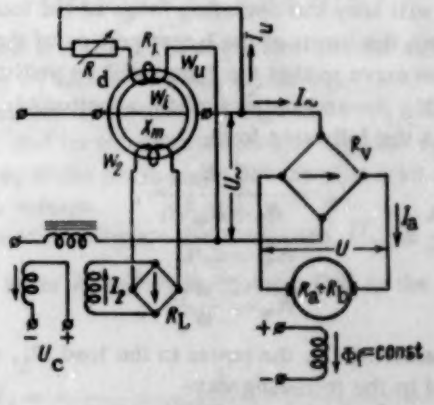

Fig. 1.

The expression for the rotary shaft speed of the motor connected to the supply through a rectifier is

$$n = \frac{U_\sim - I_\sim R_e}{c_n}, \quad (2)$$

where

$$R_e = \frac{k_i}{k_u}(R_r + R_a + R_b), \quad c_n = \frac{c\Phi_f}{k_u}.$$

Here R_r is the rectifier resistance, R_a and R_b are the resistances of the motor armature and brushes, respectively, k_i and k_u are rectifier coefficients for current and voltage, Φ_f is the motor field winding flux, and c is a constant.

Comparing equations (1) and (2), we can conclude that the three-winding transformer is a static speed transducer when the condition

$$\frac{W_i R_1}{W_u} = R_e = \text{const} \quad (2a)$$

is met.

The initial data for designing the compounding transformer are the parameters of the rectifier, motor, and transformer load. It will be assumed that the currents and voltages in the transformer are nearly sinusoidal in all operating modes of the stabilizing system, and that the rectifier resistance and coefficient are constant. Such assumptions are fully justified, since the transformer operates over a linear portion of the core magnetization curve. As was noted in [1], k_u varies over a small range. Therefore, by setting k_u at some value within this range, it can be considered constant with sufficient accuracy. It will be further assumed that the load resistance R_L is significantly greater than the secondary winding resistance, and that the effect of the magnetizing circuit is negligibly small ($X_m \approx \infty$). The assumptions mentioned are justified by the good agreement between the computed and experimentally found transformer parameters. It is recommended that a toroid core made of a high-permeability material (type NP-50, NP-65, etc.) be used for the flux path of the transformers in order to diminish the leakage flux and eddy current losses in the steel.

We will keep the operating range of the transformer within the limits of the linear portion of the magnetization curve so that the signal will be undistorted. Considering the assumptions made, equation (1) can be written in the following form:

$$I_2 = \frac{K_w E_n}{R_2 + K_w^2 R_1}, \quad (3)$$

where

$$E_n = c_n n, \quad (4)$$

$$K_w = \frac{W_2}{W_u}. \quad (5)$$

Considering (3), the power in the load, P_L, can be expressed in the following way:

$$P_L = \frac{K_w^2 E_n^2 R_2}{(R_2 + K_w^2 R_1)^2}. \quad (6)$$

Let us find the condition of maximum power transfer to the load by the transformer. To do this, we will find the greatest maximum of the function $P_L = f(K_w^2, R_2)$:

$$\frac{\partial P_L}{\partial R_2} = (R_2 + K_w^2 R_1)^2 - 2R_2(R_2 + K_w^2 R_1) = 0,$$

whence

$$R_2 = R_1 K_w^2, \quad (7)$$

and

$$\frac{\partial P_L}{\partial (K_w^2)} =$$

$$= (R_2 + K_w^2 R_1)^2 - 2K_w^2 (R_2 + K_w^2 R_1) R_1 = 0,$$

whence

$$K_w^2 = \frac{R_2}{R_1}. \quad (8)$$

It can thus be seen from equations (6) - (8) that the greatest maximum condition for function $P_L = f(K_w^2, R_2)$ is expressed by the equation

$$R_1 = \frac{E_n^2}{4P_L}. \quad (9)$$

It can be shown, by using the initial set of transformer equations given in [1], that the expression for the current in the voltage winding is

$$I_u' = \frac{U_\sim' + I_\sim' R_2}{R_1' + R_2}, \quad (10)$$

in which the apostrophes denote that the corresponding quantities are referred to the secondary winding.

Solving equations (5) and (10) together in terms of I_u, $U_\sim$, $I_\sim$ we get a final equation for the current in the voltage winding:

$$I_u = \frac{U_\sim + I_\sim R_e}{2R_1}. \quad (11)$$

The voltage across the voltage winding of the transformer can be expressed by the following equation:

$$U_v = 4.44 f W_u B_m a b k_{ff} 10^{-8}, \quad (12)$$

where B_m is the effective flux density in the transformer core; a and b are the dimensions of the sides of the core cross section; and k_{ff} is the core fill-factor.

Taking (8) into account, the solution of (12) for the product of the sides of the flux path cross section assumes the form

$$ab = \frac{\sqrt{P_L R_1}\, 10^8}{4.44 f B_m k_{ff} W_u}. \quad (13)$$

Keeping equalities (3) and (8) in mind, the expression for the ampere-turns of the secondary winding can be written in the following manner:

$$I_2 W_2 = \frac{E_n W_i}{2R_e}. \quad (14)$$

If q, Δ, and k_f are the wire cross section, current density, and fill-factor of the flux path window for the various windings, and D_0 is the diameter of this window the joint solution of equation (14) and the window fill equation:

$$\frac{\pi (D_{av} - a)^2}{4} = \quad (15)$$

$$= \frac{q_i W_i 10^{-2}}{k_{fi}} + \frac{q_u W_u 10^{-2}}{k_{fu}} + \frac{q_2 W_2 10^{-2}}{k_{f2}} + \frac{\pi D_0^2}{4}$$

gives the expression for the average diameter of the toroidal flux path:

$$D_{av} = a + \sqrt{\frac{4I_1W_i10^{-2}}{\pi\Delta_i k_{fi}} + \frac{4I_uW_u10^{-2}}{\pi\Delta_u k_{fu}} + \frac{2E_nW_i10^{-2}}{\Delta_2 R_e \pi k_{f_2}} + D_0^2}. \quad (16)$$

Hence the average line length is

$$l_{av} = \pi\left(a + \sqrt{\frac{4I_1W_i10^{-2}}{\pi\Delta_i k_{fi}} + \frac{4I_uW_u10^{-2}}{\pi\Delta_u k_{fu}} + \frac{2E_nW_i10^{-2}}{\Delta_2 R_e \pi k_{f_2}} + D_0^2}\right). \quad (17)$$

The amount of additional resistance in the voltage winding circuit can be found from the equation

$$R_d = R_1 - \frac{\rho l_{vu} W_u}{q_u} 10^{-2}, \quad (18)$$

where

$$l_{vu} = 2a + 2b + 4\lambda_u = 2\left(a + b + 2\frac{q_u W_u 10^{-2}}{l_{av} k_{fu}}\right);$$

λ_u is the thickness of the voltage winding cross section and ρ is the resistivity of the winding wire.

The expression for the resistance of the secondary winding is

$$r_2 = \frac{\rho l_{v_2} W_2}{q_2} 10^{-2}, \quad (19)$$

where

$$l_{v_2} = 2a + 2b + 8\lambda_u + 4\lambda_2 =$$

$$= 2\left(a + b + 4\frac{q_u W_u}{l_{av} k_{fu}} 10^{-2} + 2\frac{q_2 W_2}{l_{av} k_{f_2}} 10^{-2}\right)$$

(λ_2 is the thickness of the secondary winding cross section).

The weight of the copper in the transformer is

$$G_M = \frac{\gamma_M}{\rho}\left[\frac{I_i^2 r_i}{\Delta_i^2} + \frac{I_u^2 R_u}{\Delta_u^2} + \frac{I_2^2 r_2}{\Delta_2^2}\right] \quad (20)$$

(here γ_M is the specific gravity of the copper).

The total weight of the transformer is determined by the sum of the weights of copper and steel:

$$G_{tot} = G_M + V_{st}\gamma_{st}, \quad (21)$$

where γ_{st} is the specific gravity of the core material, and V_{st} is the volume of steel in the core:

$$V_{st} = abl_{av}k_{iff}. \quad (22)$$

This method for designing a transformer is illustrated by an example given at the end of this article.

2. Designing a Three-winding Transformer for Stabilizing the Speed of an AC Motor

Three-winding transformers are used as compounding elements in circuits for stabilizing the speed of a three-phase motor with a Shenfer rotor, and a two-phase motor with a thin-walled rotor, which are shown in Figs. 2a and 2b. These transformers are built like

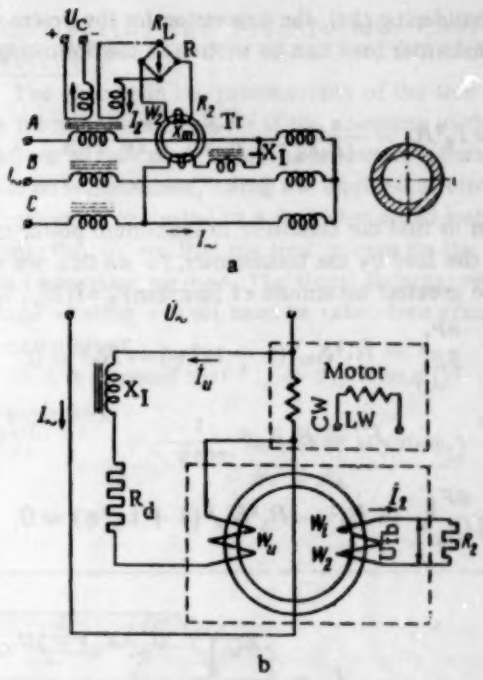

Fig. 2. CW – motor control winding, LW – motor line winding, U_{fb} – feedback voltage.

the transformer shown in the circuit of Fig. 1, except that an additional inductive reactance X_I is connected in the circuit of the voltage windings; X_I is a choke with an air gap.

It has been shown in [1] that if the current and voltage windings are connected opposing, and $X_I' = (R_i' \sin\varphi)/\cos\varphi$, the expression for the current in the secondary circuit is

$$I_2 = k_2 U_\sim - I_\sim k_3. \quad (23)$$

Using the designations mentioned above, we get the following expressions for the coefficients k_2 and k_3 when $X_m = \infty$:

$$k_2 = \frac{K_w}{\sqrt{(R_1K_w^2 + R_2)^2 + X_I^2 K_w^4}},$$

$$k_3 = \frac{\frac{R_1 W_i}{W_u \cos\varphi}}{\sqrt{(R_1K_w^2 + R_2)^2 + X_I^2 K_w^4}}.$$

Here φ is the phase angle between the current in winding W_i and the voltage across W_u.

For the circuit shown in Fig. 2a $\varphi = \varphi_L - 30°$ (see Fig. 3), and for the circuit shown in Fig. 2b $\varphi_L = \varphi$, where φ_L is the phase angle between the load current and the voltage.

We will designate the expression $U_\sim = \frac{I_\sim R_1 W_i}{\cos\varphi W_u}$ by the letter A and write equation (23) in the following form:

$$I_2 = \frac{K_w A}{\sqrt{(R_1K_w^2 + R_2)^2 + R_1^2 K_w^4 \operatorname{tg}^2\varphi}}. \quad (24)$$

Considering (24), the expression for the power in the transformer load can be written in the following form:

$$P_L = I_2^2 R_2 = \frac{K_w^2 A^2 R_2}{(R_1 K_w^2 + R_2)^2 + R_1^2 K_w^4 \operatorname{tg}^2 \varphi}. \quad (25)$$

Let us find the condition of maximum power transfer to the load by the transformer. To do this, we will find the greatest maximum of function $P_L = f(K_w^2, R_2)$:

$$\frac{\partial P_L}{\partial R_2} = R_1^2 K_w^4 (1 + \operatorname{tg}^2 \varphi) - R_2^2 = 0,$$

whence

$$R_2 = R_1 K_w^2 \frac{1}{\cos \varphi}, \quad (25a)$$

and

$$\frac{\partial P_L}{\partial (K_w^2)} = R_2^2 - R_1^2 K_w^4 (1 + \operatorname{tg}^2 \varphi) = 0,$$

whence

$$R_2 = R_1 K_w^2 \frac{1}{\cos \varphi}. \quad (25b)$$

It can thus be seen from equations (25a) and (25b) that the greatest maximum of $P_L = f(K_w^2, R_2)$ is expressed by the equation

$$K_w = \sqrt{\frac{R_2}{R_1} \cos \varphi}. \quad (26)$$

The joint solution of equations (25) and (26) gives the following expression for the resistance of the voltage winding:

$$R_1 = \frac{A^2 \cos \varphi}{2 P_L (1 + \cos \varphi)}. \quad (27)$$

Using the initial set of transformer equations given in [1], it can be shown that the expression for the current in the voltage winding circuit is

$$I_u = \frac{K_w \sqrt{U_\sim^2 K_w^2 + 2U_\sim \frac{W_2}{W_u} I_\sim R_2 \frac{W_1}{W_2} \cos \varphi + I_\sim^2 R_2^2 \left(\frac{W_1}{W_2}\right)^2}}{\sqrt{(R_2 + R_1 K_w)^2 + R_1^2 \operatorname{tg}^2 \varphi K_w^4}}. \quad (28)$$

The voltage across the voltage winding can be found from the following dependence:

$$U_V = 4.44 f W_u B_m ab k_{ff} 10^{-8}. \quad (29)$$

Considering (26), the solution of (29) for the product of the sides of the flux path cross section is

$$ab = \frac{\sqrt{\frac{P_L R_1}{\cos \varphi}} 10^8}{4.44 f B_m k_{ff} W_u}. \quad (30)$$

If $n_{mo} = 0$, then I_2 must also be 0. Consequently, equation (24) can be written thus:

$$U_\sim = c I_\sim, \quad (31)$$

where

$$c = \frac{R_1 W_1}{W_u \cos \varphi}. \quad (32)$$

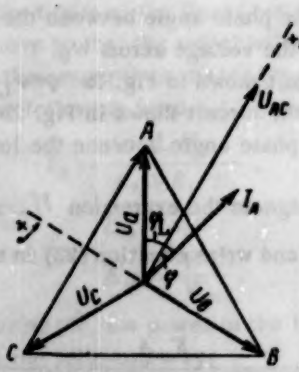

Fig. 3.

Hence, the transformer design consists of the following series of steps:

1. Using equations (27) and (31), we find c and R_1 under starting conditions. The quantity A is determined from conditions when the motor is running steadily at its nominal rpm.

2. We find K_w by using equation (26).

3. Having been given a series of values for W_1, we find the corresponding values of W_u from (32), and knowing K_w, we then find W_2.

4. Using (24) and (28), we find the currents in the secondary and voltage winding circuits.

5. Using (30), we find the transformer flux path cross section for the values of W_u obtained in step 3.

6. Choosing a flux path with a square cross section and expressing the wire cross section in terms of a permissible current and current density, we find the diameter and average line of the flux path from (15).

7. Using (18), we find the value of the additional resistance.

8. We find the copper weight and total weight of the transformer from (20) and (21) for the various values of W_1 assumed in step 3.

9. The last step is to construct a graph of the total transformer weight as a function of the number of turns in the current winding. We then find the number of turns W_1 which gives the minimum total weight, and we take all the parameters computed above which correspond to this W_1.

The graph $G_{tot} = f(W_1)$ is shown in Fig. 4 for a transformer operating as in Fig. 2b, with the following initial data: $I_\sim = 0.25$ amp; $U_\sim = 50$ v; $U_{tr} = 25$ v; $\cos \varphi_L = 0.5$; $P_L = 1$ w; $R_L = 1000$ ohm; $I_2 = 0.033$ amp.

The transformer core material is 50NP.

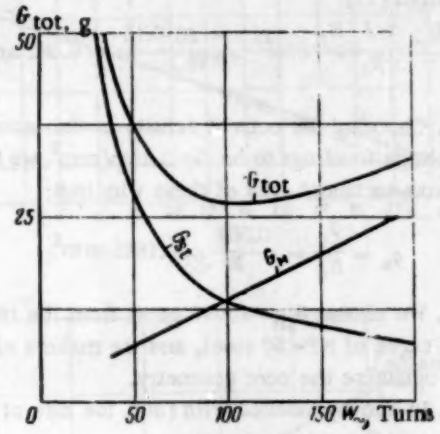

Fig. 4.

3. Computing the Transformer Characteristics

The change in the permeability of the iron in the core must be accounted for if the accuracy of the calculations of the three-winding transformer characteristics is to be increased. Using the equivalent circuit of a transformer operating in a dc motor speed stabilizing circuit (Fig. 5), we find the load current by the equivalent generator method. The linear inductance in the voltage winding circuit must be taken into account in the calculation.

If it is assumed that $\dot{I}_\sim' = I_\sim'(\cos\varphi_L - j\sin\varphi_L)$, the expression

$$\dot{I}_0 = \frac{U_\sim' + I_\sim' R_2(\cos\varphi_L - j\sin\varphi_L)}{R_1' + R_2} \qquad (33)$$

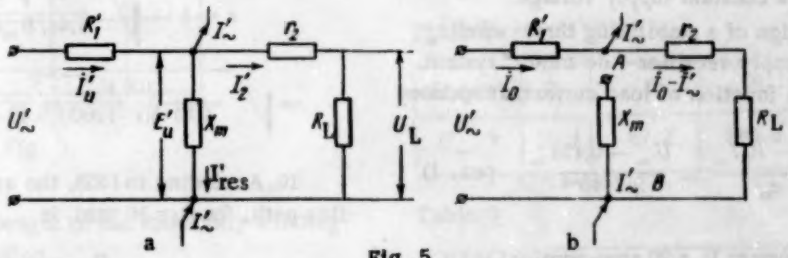

Fig. 5.

is justified for the current $\dot{I}_0$ (see the circuit of Fig. 5b), whence

$$U_{AB} = U_\sim' - \dot{I}_0 R_1' = \qquad (34)$$

$$= U_\sim' - \frac{[U_\sim' + (I_\sim'\cos\varphi_L - jI_\sim'\sin\varphi_L)R_2]R_1'}{R_1' + R_2}.$$

When $\cos\varphi_L = 1$, equation (34) takes the form

$$U_{AB} = U_\sim' - \frac{U_\sim' + I_\sim' R_2}{R_1' + R_2}. \qquad (35)$$

The resistance of the equivalent circuit with respect to terminals AB is equal to

$$R_{AB} = \frac{R_1' R_2}{R_1' + R_2}. \qquad (36)$$

Fig. 6 shows an equivalent diagram of the transformer, consisting of a source U_{AB}, linear resistance R_{AB}, and non-linear reactance X_m connected in series. The current in this circuit is found from the formula

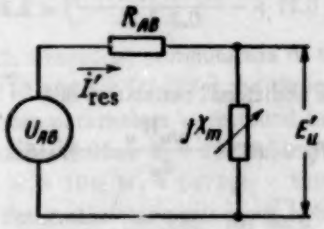

Fig. 6.

$$\dot{I}_{res}' = \frac{\dot{U}_{AB}}{R_{AB} + jX_m}. \qquad (37)$$

If the transformer parameters are known, and a number of values $I_\sim'$ are given, the voltages corresponding to them, U_{AB}, can be found. We will solve equation (37) graphically. Both axes will be given identical voltage scales (Fig. 7). We will plot the voltage E_u – the voltage across the non-linear reactance X_m – along the ordinate, and the voltage across R_{AB} will be plotted along the abscissa. We draw a number of circles with radius U_{AB}, centered at the origin. Each such

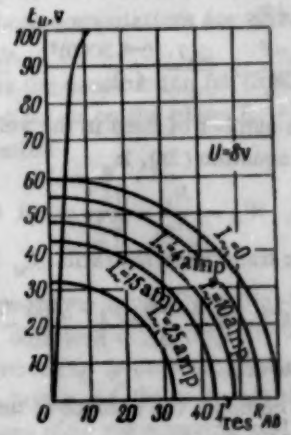

Fig. 7.

circle corresponds to definite values of the voltage $U_\sim$ and current $I_\sim$. If the magnetization curve of the steel core is also plotted on these coordinates, using the equations

$$E_u' = 4.44\, fW_2 B_m S k_{ff}\, 10^{-8}, \qquad (38)$$

$$H_m l_{av} = \sqrt{2}\cdot 0.4\pi I_{res}' W_2, \qquad (39)$$

the points where this curve intersects the circles will be operating points for the transformer. Having a family of curves $E_u' = f(U_{res}' R_{AB})$ for $U_\sim$ = const, and $E_u' = f(I_{res}' R_{AB})$ for $I_\sim$ = const, we find the required dependencies $I_2 = f(U_\sim)$ and $I_2 = f(I_\sim)$. The function $I_2 = f(U_\sim)$ for $I_\sim$ = const is analogous to the function $n = f(U_\sim)$ for a drive with a constant load torque on the motor shaft. The function $I_2 = f(I_\sim)$ for $U_\sim$ = const is analogous to the mechanical characteristic of the drive, $n = f(M)$, for a constant supply voltage.

Example 1. Design of a stabilizing three-winding transformer for a "supply-rectifier – dc motor" system. The drive speed as a function of load current is expressed by the equation

$$n = \frac{U_\sim - R_e I_\sim}{c_n} = \frac{U_\sim - 0.15 I_\sim}{3.7\cdot 10^{-3}}. \qquad (ex.\ 1)$$

The nominal load current $I_\sim$ = 20 amp; nominal shaft speed n = 3000 rpm; transformer power rating P_L = 2 watts (U_2 = 80 v, I_2 = 0.025 amp). Core material is 50 NP.

Considering the size of the load current ($I_\sim$ = 20 amp), it is best, for technical reasons, to make the transformer with a one-turn current winding (W_i = 1). The area occupied by the current winding must be chosen on the basis of an appropriate value of D_0.

1. The supply voltage is found from expression (2), using the nominal values of $I_\sim$ and n:

$$U_\sim = c_n n + I_\sim R_e = 3.7\cdot 10^{-3}\cdot 3000 + 20\cdot 0.15 = 14.1 \text{ v}. \qquad (ex.2)$$

2. The circuit resistance of the voltage winding is found from (9):

$$R_1 = \frac{(c_n n)^2}{4P_L} = \frac{(3.7\cdot 10^{-3}\cdot 3000)^2}{4\cdot 2} = 15.2 \text{ ohms}. \qquad (ex.\ 3)$$

3. The number of turns in the voltage winding, according to equation (2a), is

$$W_u = \frac{R_1}{R_e} = \frac{14.1}{0.15} = 101 \text{ turns}. \qquad (ex.\ 4)$$

4. The transformation ratio K_w equals

$$K_w = \sqrt{\frac{R_L}{R_1}} = \sqrt{\frac{3200}{15.2}} = 14.5 \qquad (ex.\ 5)$$

according to (8).

5. We compute the number of turns in the secondary winding from (5):

$$W_2 = K_w W_u = 14.5\cdot 101 = 1470 \text{ turns}. \qquad (ex.\ 6)$$

6. The current in the voltage winding circuit is found from (11):

$$I_u = \frac{U_\sim + I_\sim R_e}{2R_1} = \frac{14.1 + 20\cdot 0.15}{2\cdot 15.2} = 0.562 \text{ amp}. \qquad (ex.\ 7)$$

7. Choosing the current density in the secondary and voltage windings to be Δ = 3 amp/mm^2, we find the wire cross-sectional area of these windings:

$$q_u = \frac{I_u}{\Delta_u} = \frac{0.562}{3} = 0.1842 \text{ mm}^2. \qquad (ex.\ 8)$$

8. We choose B_m = 12000 gauss from the magnetization curve of NP–50 steel, and we make a = b in order to optimize the core geometry.

9. In correspondence with (30), the side of the toroid flux path cross section is

$$a = b = \sqrt{\frac{10^8\sqrt{P_L R_1}}{4.44 f B_m k_{ff} W_u}} = \sqrt{\frac{10^8\sqrt{2\cdot 15.2}}{4.44\cdot 400\cdot 12000\cdot 0.43\cdot 101}} = 0.77 \text{ cm}. \qquad (ex.\ 9)$$

10. According to (32), the average diameter of the flux path, for D_0 = 10 mm, is

$$D_{av} = a + \sqrt{\frac{4I_u W_u 10^{-2}}{\pi\Delta_u k_{fu}} + \frac{2E_n W_i 10^{-2}}{\pi R_e \Delta_2 k_{f2}} + D_0^2} = 0.77 + \sqrt{\frac{4\cdot 0.562\cdot 101\cdot 10^{-2}}{3.14\cdot 0.3\cdot 3} + \frac{2\cdot 3.7\cdot 10^{-3}\cdot 3000\cdot 10^{-2}}{3.14\cdot 0.15\cdot 0.3\cdot 3} + 1} = 2.3 \text{ cm}. \qquad (ex.\ 10)$$

11. The length of the average toroid line, l_{av}, is found from (33):

$$l_{av} = \pi D_{c_{av}} = 3.14\cdot 2.3 = 7.24 \text{ cm}. \qquad (ex.\ 11)$$

12. The volume of the flux path is

$$V_{st} = a^2 l_{av} k_{ff} = (0.75)^2\cdot 7.24\cdot 0.43 = 1.85 \text{ cm}^3. \qquad (ex.\ 12)$$

13. The average length of a turn in the voltage winding is found from the equation

$$l_{vu} = 4\left(a + \frac{q_u W_u 10^{-2}}{k_{fu} l_{av}}\right) = 4\left(0.77 + \frac{0.1842\cdot 101\cdot 10^{-2}}{0.3\cdot 7.24}\right) = 3.34 \text{ cm}. \qquad (ex.\ 13)$$

14. The additional resistance is

$$R_d = R_1 - \frac{\rho l_{vu} W_u}{q_u} 10^{-2} = 15.2 - \frac{3.34\cdot 101}{57\cdot 0.1842} 10^{-2} = 14.882 \text{ ohms}. \qquad (ex.\ 14)$$

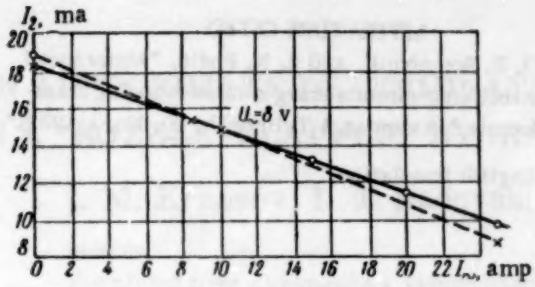

Fig. 8.

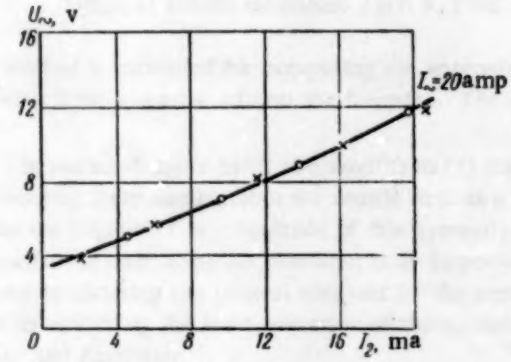

Fig. 9.

15. The average length of the secondary winding is found from the equation

$$l_{v2} = 4\left(a + 2\frac{q_u W_u 10^{-2}}{l_{av}k_{fu}} + \frac{q_2 W_2 10^{-2}}{l_{av}k_{f_2}}\right) = 4$$

$$= \left(0.77 + 2\frac{0.1842\cdot 101\cdot 10^{-2}}{7.24\cdot 0.3} + \frac{0.0081\cdot 1470\cdot 10^{-2}}{7.24\cdot 0.3}\right) = 3.98 \text{ cm}.$$

(ex. 15)

16. The secondary winding resistance equals

$$r_2 = \frac{\rho l_{v2} W_2}{q_2} 10^{-2} = \frac{3.98\cdot 1470}{57\cdot 0.0081} 10^{-2} = 128 \text{ ohms}. \quad \text{(ex. 16)}$$

17. We use the well-known formula

$$G_M = \frac{\gamma_M}{\rho}\left[\frac{I_u^2 R_u}{\Delta_u^2} + \frac{I_2^2 r_2}{\Delta_2^2}\right] =$$

$$= 8.9\cdot 57\left[\frac{(0.562)^2\cdot 0.318}{3^2} + \frac{(0.025)^2\cdot 128}{3^2}\right] = 10.1 \text{ g}$$

(ex. 17)

to find the weight of the copper.

18. The total transformer weight is equal to

$$G_{tr} = G_M + \gamma_{st} V_{st} = 10.1 + 8.2\cdot 1.85 = 25.2 \text{ g}. \quad \text{(ex. 18)}$$

Example 2. Graphical computation of the characteristic $U_\sim = f(I_2)$ and $I_2 = f(I_\sim)$ for the three-winding transformer whose parameters were found in Example 1. The circuit parameters are R_1 = 15.2 ohms; R_2 = 3200 ohms; W_1 = 1; W_u = 101; W_2 = 1470; r_2 = 128 ohms.

1. Let us determine the equivalent values of resistances, currents, and voltages:

$$R_1' = R_1\left(\frac{W_2}{W_u}\right)^2 = 15.2\left(\frac{1470}{101}\right)^2 = 3240 \text{ ohm},$$

$$I_\sim' = I_\sim \frac{W_1}{W_2} = \frac{I_\sim}{1470},$$

$$U_\sim' = U_\sim \frac{W_2}{W_u} = U_\sim \frac{1470}{101}. \quad \text{(ex. 19)}$$

2. Having been given a series of values for $I_\sim$, we will find the equivalent currents. The results are shown in Table 1.

Table 1

$I_\sim$, amp	0	2	4	6	10	15	20	25
$I'_\sim$, ma	0	1.36	2.72	4.07	6.8	10.2	13.6	17

3. Having been given a series of values for $U_\sim$, we find the equivalent voltages. The results are shown in Table 2.

Table 2

$U_\sim$, v	2	6	8	12	16
$U'_\sim$, v	29.1	87.2	116.4	174.5	232.5

Table 3

$I_\sim$, amp	0	4	10	15	25
U_{AB}, v	60.1	55	48.2	43.4	32.1

4. Using equation (36), we find R_{AB}:

$$R_{AB} = \frac{R_1' R_2}{R_1' + R_2} = \frac{3240\cdot 3338}{3240 + 3338} = 1625 \text{ ohm}. \quad \text{(ex. 20)}$$

5. Using equations (38) and (39), we plot the magnetization curve of the 50NP core material on the coordinates E_u' and $I'_{res}R_{AB}$. The curve obtained for the transformer core is shown in Fig. 7.

6. We find the U_{AB} corresponding to the different $I_\sim'$ found in step 2, for each $U_\sim$ assumed in step 3. The results of these computations are given in Table 3 for $U_\sim$ = 8 volts.

Fig. 7 shows the construction for finding the transformer operating points on the plane $E_u' = f(I'_{res}R_{AB})$. Using the expression

$$I_2 = E_u'/R_2. \quad \text{(ex. 21)}$$

where

$$R_2 = R_\sim + r_2. \quad \text{(ex. 22)}$$

we find the dependence $I_2 = f(I_\sim)$ (cf. Fig. 8). The function $I_2 = f(I_\sim)$, observed experimentally with a transformer made according to the design data of Example 1, is shown also in Fig. 8 (circles denote the calculated curve, and crosses show the experimental one). We find the dependence $U_\sim = f(I_2)$ for $I_\sim$ = const from anal-

ogous constructions for other values of U~. Fig. 9 shows $U_{\sim} = f(I_2)$ for $L_{\sim} = 20$ amp. This figure also shows the function $U_{\sim} = f(I_2)$ observed experimentally with the transformer previously mentioned.

The good agreement between the calculated and experimentally observed characteristics shows that the assumptions made above are justified in the design of a three-winding transformer.

LITERATURE CITED

1. O. B. Rosenbauli and R. N. Rodin, "Motor speed stabilizing circuits using a three-winding transformer," Avtomat. i Telemekh. 20, No. 3 (1959).*

* See English translation.

AN APPROXIMATE DETERMINATION OF JET REACTION IN A "NOZZLE-FLAPPER" HYDRAULIC AMPLIFIER

I. M. Krassov, L. I. Radovskii, and B. G. Turbin

Moscow

Translated from Avtomatika i Telemekhanika, Vol. 21, No. 11,
pp. 1536-1538, November, 1960
Original article submitted April 9, 1960

A method is presented for computing the approximate magnitude of the force with which a jet of working fluid, issuing from a nozzle, affects the flapper. The results obtained are compared to experimental data.

In nozzle-flapper hydraulic amplifiers [1] the jet of working fluid issuing from the nozzle acts as a force upon the flapper. The magnitude of this hydro-dynamic force (let us call it the jet reaction) is an important factor in choosing the control element for the amplifier, and in analyzing the joint operation of the control element and amplifier.

In recent years, a number of experimental and theoretical works concerned with the study of the interaction between the jet and flapper have been completed [2-4]. This paper presents a method for calculating approximately the jet reaction; it agrees well with the experimental results given in [4].

One can consider that the jet reaction is composed of three forces:

A. Force N_1, which varies with the mass flow rate of working fluid issuing from the nozzle. This component can be found from the expression

$$N_1 = m(V_c - V_H), \tag{1}$$

where V_c is the projection of the working fluid velocity at the point of exit from the nozzle along an axis perpendicular to the plane of the flapper, V_H is the projection of the working fluid velocity at discharge [over the area of the nozzle end-face of external radius $r_H = d_H/2$ (see figure)] along an axis perpendicular to the plane of the flapper, and m is the mass flow per second issuing from the nozzle.

Setting the velocity of the discharge equal to zero ($V_H = 0$), and assuming that

$$m = Q\rho, \quad V_c = \frac{Q}{F}, \quad F = \frac{\pi d_c^2}{4}, \tag{2}$$

where Q is the volume rate of working fluid discharged through the nozzle, ρ is the density of the working fluid, F is the sectional area of the nozzle end-face, and d_c is the nozzle diameter, we get

$$N_1 = \frac{4\rho Q^2}{\pi d_c^2}. \tag{3}$$

B. The force generated by the pressure of the working fluid on the nozzle end-face area; it equals

$$N_2 = \frac{\pi d_c^2}{4} p_c, \tag{4}$$

where p_c is the working fluid pressure at the nozzle end-face (in atmospheres, gauge).

The pressure p_c is assumed to be identical over the entire area of the nozzle end-face.

C. The force exerted by the working fluid pressure in the gap between the end of the nozzle and the flapper. This third component can be represented in the form

$$N_3 = 2\pi \int_{r_c}^{r_H} p_r r dr, \tag{5}$$

where r is the flow radius of the nozzle end, r_c is the nozzle radius, r_H is the external radius of the nozzle end and p_r is the working fluid pressure in gap between the nozzle end and the flapper, over a radius r.

If we assume that the pressure p_r over the end-face radius varies linearly from p_c to 0, that is,

$$p_r = p_c\left(1 - \frac{r}{r_H}\right), \tag{6}$$

then we get

$$N_3 = \pi p_c \left(\frac{d_H^2 - d_c^2}{4} - \frac{d_H^3 - d_c^3}{6d_H}\right). \tag{7}$$

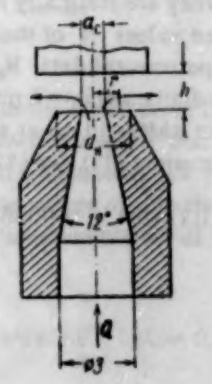

h, mm	p_1, kg/cm²	μ	N, G	N_e, G	[N − N_e], G
0.15	10	0.717	96	95	1
0.20	10	0.667	101	100	1
0.25	10	0.670	109	115	6
0.15	20	0.700	191	190	1
0.20	20	0.647	200	220	20
0.20	30	0.675	303	300	3
0.25	30	0.638	321	320	1
0.15	40	0.637	375	375	—
0.20	40	0.664	400	400	—
0.25	40	0.644	429	420	9

The jet reaction, being the sum of the three components mentioned above, will equal

$$N = \frac{4\rho Q^2}{\pi d_c^2} + \frac{\pi}{6}\left(\frac{d_H^3}{2} + \frac{d_c^3}{d_H}\right) p_c. \quad (8)$$

The formula for volume discharge rate through the nozzle is

$$Q = \mu_c \frac{\pi d_c^2}{4}\sqrt{\frac{2}{\rho}(p_1 - p_c)}, \quad (9)$$

where p_1 is the pressure in the receiver, and μ_c is the inherent discharge rate factor of the nozzle (without the flapper); we find from this that

$$p_c = p_1 - \frac{8\rho Q^2}{\pi^2 d_c^4 \mu_c^2}. \quad (10)$$

In this case,

$$N = \frac{4\rho Q^2}{\pi d_c^2} + \quad (11)$$

$$+ \frac{\pi}{6}\left(\frac{d_H^3}{2} + \frac{d_c^3}{d_H}\right)\left(p_1 - \frac{8\rho Q^2}{\pi^2 d_c^4 \mu_c^2}\right).$$

If the discharge is into the atmosphere, Q can be written in the form

$$Q = \mu \pi d_c h \sqrt{\frac{2}{\rho} p_1}, \quad (12)$$

where μ is the discharge rate factor of the nozzle and flapper combined, and h is the gap between the nozzle and the flapper.

Expressions (11) and (12) enable one to find the jet reaction N, if the parameters d_c, d_H, μ_c, μ, h and p_1 are known. The supply pressure p_0 can be substituted for pressure p_1, since they are statically related.

The calculated values N of the jet reaction were compared with experimental data N_e for a nozzle of the first type with diameters d_c = 1 mm, and d_H=1.35 mm [4], working in AMG-10 oil at a temperature of 50-55°C. Expressions (11) and (12) give

$$N = [8.03(\mu/h)^2 + 0.00865]\, p_1 \quad (13)$$

for a nozzle with these dimensions, and an experimentally determined $\mu_c = 0.9$.

The values of discharge rate factor μ for the nozzle and flapper combination which were used for computing the jet reaction from formula (13) were taken from reference [5]. The calculated results and experimental data are given in the table.

A comparison of the calculated and experimental values of jet reaction given in the table shows satisfactory agreement. Hence the method being considered can be recommended as an approximate determination of the force on a flapper, if the amplifier parameters approximate those given in [4].

CONCLUSIONS

1. Computational formulas are given which permit one to calculate the approximate force on a flapper as liquid flows around it.

2. It is shown that calculated and experimentally found values of the force on a flapper agree.

LITERATURE CITED

1. I. M. Krassov, Hydraulic Amplifiers [in Russian] (Gosénergoizdat, 1959).
2. V. N. Dmitriev and A. G. Shashkov, "The effect of a jet on a flapper in pneumatic and hydraulic controlling apparatus of the 'nozzle - flapper' type," Avtomat. i Telemekh. 17, No. 6 (1956).*
3. E. A. Andreeva, "On computing the static characteristics of a 'nozzle-flapper' element," Pneumatic and Hydraulic Control Systems, Apparatus, and Elements [in Russian] (Izd. AN SSSR, 1959).
4. I. M. Krassov and B. G. Turbin, "Jet effect in a 'nozzle-flapper' hydraulic amplifier," Avtomat. i Telemekh. 20, No. 12 (1959).*
5. I. M. Krassov and B. G. Turbin, "Volume rate factors of a 'nozzle-flapper' hydraulic throttle," The Automation of Industrial Processes [in Russian] (Izd. AN SSSR, 1960) 3rd ed.

*See English translation.

DETERMINING THE EFFECT OF REGULAR SIGNAL DYNAMICS IN THE STATISTICAL LINEARIZATION METHOD

M. I. Gusev

Kalinin

Translated from Avtomatika i Telemekhanika, Vol. 21, No. 11,
pp. 1539-1546, November, 1960
Original article submitted May 19, 1960

The paper studies the effect of the dynamics of a deterministic function on the transfer coefficient for fluctuations when regular and random functions pass simultaneously through a nonlinearity.

1. Statement of the Problem

In analyzing the operational precision of both linear and nonlinear dynamic systems, many engineering computations treat only the first probability moments of random functions. The approximate statistical linearization theory [1, 2] which is based on these engineering requirements has made it possible to perform fruitful investigations of nonlinear systems; these investigations have exposed very interesting system properties which are both harmful and useful from the point of view of engineering practice. According to statistical linearization theory, two functions are considered statistically equivalent if they have identical first and second moments when a specified distribution law governs their arguments. Here, the first or second statistical linearization method is used to determine the transfer coefficients of a nonlinear element: K_0 is the transfer coefficient for the useful signal, and K_1 is the transfer coefficient for fluctuations.

In many engineering problems, the value of the mathematical expectation for the random perturbation varies insignificantly, whereas the useful signal varies relatively rapidly. Therefore, it is natural to consider the dynamics of the useful signal in computing the coefficients K_0 and K_1. In this regard it is of interest to study [3] which provides a method for taking into account the dynamics of the useful signal. Using this method, we derive analytical expressions which make it possible to determine how the transfer coefficient for the fluctuations is affected both by the parameters of the distribution law for the random process and by certain parameters which characterize the dynamics of the regular component.

2. Determining the Transfer Coefficient of a Nonlinear Element for Fluctuations while taking into account the Dynamics of the Regular Signal

We shall assume that the nonlinearity described by the functional relationship $v = f(v_0)$, where v_0 is the input and $\underline{y}$ is the output, is subjected to three components $v_0 = \beta + x + y$, where β is the constant component which contains the practically constant mathematical expectation of the random perturbation; $\underline{x}$ is the random component which has a zero mathematical expectation, and $\underline{y}$ is any regular signal. If K is the equivalent transfer coefficient of the nonlinear element for fluctuations, and $\underline{k}$ is the transfer coefficient for the useful signal, then the instantaneous value of the difference

$$x_d = f(\beta + x + y) - (Kx + ky) \qquad (1)$$

is caused by the neglect of the higher harmonics and a certain constant component λ at the output of the nonlinearity. The instantaneous value of the difference x_d is a function of $\underline{x}$ and $\underline{y}$ whose properties are characterized by the distribution laws $q(x)$ and $p(y)$ respectively. The criterion which we shall choose for selecting the optimal value of the equivalent transfer coefficient will be the minimum mean-square error for the instantaneous difference x_d. Then the problem of finding the equivalent transfer coefficient reduces to finding the minimum for the expression

$$M = \int_{-\infty}^{\infty}\int_{-\infty}^{\infty} x_d^2 q(x)\, p(y)\, dx dy. \qquad (2)$$

With respect to the distribution function $p(y)$ we must note the following. Assume that the useful signal varies according to a sinusoidal law $y = a \sin \xi$, and that each of the possible values of $\underline{y}$ in the limits $-a$ to $+a$ corresponds to an innumerable set of values ξ:

$$\xi_k = \frac{\pi k}{\omega} + \frac{(-1)^k}{\omega} \arcsin \frac{y}{a} \qquad (k = 0, \pm 1, \pm 2 \ldots). \qquad (3)$$

From this we treat ξ in accordance with [4] as a certain random quantity; we find

$$p(y) = \begin{cases} \dfrac{1}{\omega a \sqrt{1-\left(\frac{y}{a}\right)^2}} \sum\limits_{k=-\infty}^{\infty} \omega\left[\dfrac{\pi k}{\omega} + \dfrac{(-1)^k}{\omega} \arcsin \dfrac{y}{a}\right], & |y| < a, \\ 0 & |y| > a. \end{cases} \quad (4)$$

Assume now that the quantity ξ is uniformly distributed over the interval $-\pi \leq \xi \leq +\pi$; then in the infinite sum (4) only two terms corresponding to $k=0$ and $k=1$ will be nonzero. Then $p(y)$ can be written in simpler form:

$$p(y) = \begin{cases} \dfrac{1}{\pi a \sqrt{1-\left(\frac{y}{a}\right)^2}}, & |y| < a, \\ 0, & |y| > a. \end{cases} \quad (5)$$

In this case the distribution function $p(y)$ will characterize the dynamic properties of the regular signal y which is studied jointly with the random process x that is characterized by its distribution function; thus $p(y)$ will, so to speak, itself become random, since the phase of the regular signal is actually distributed uniformly over the interval $-\pi \leq \xi \leq +\pi$ when this signal is treated jointly with the random signal.

Taking the above into account and performing the minimization of expression (2) with respect to K, we obtain the following result after simple computations if we assume that the random signal is distributed normally:

$$K = \frac{1}{\bar{x}^2} \int_{-\infty}^{\infty} \int_{-\infty}^{\infty} xf(\beta + x + y)\, q(x)\, p(y)\, dx dy, \quad (6)$$

where $\bar{x}^2$ is the mean-square value of the input signal x.

For the purposes of further computation we shall modify the expression for K somewhat. Assume that a constant component γ acts at the input of the nonlinear element instead of the random signal x; then the constant component of the output signal is written as

$$g(\gamma) = \int_{-\infty}^{\infty} f(\gamma + \beta + y)\, p(y)\, dy. \quad (7)$$

Now expression (7) shall be treated as a certain fictitious nonlinearity whose input is subjected to the random signal x; then,

$$K_x = \frac{1}{\bar{x}^2} \int_{-\infty}^{\infty} xg(x)\, q(x)\, dx. \quad (8)$$

Substituting Eq. (8) into Eq. (7), we obtain an expression for the equivalent transfer coefficient which coincides with (6). Such a treatment permits us not only to simplify the analytical computations but also experimentally to determine the fictitious nonlinearities by studying the effect of the regular signal on the original nonlinearity. It is convenient to perform the analytical computation of the fictitious nonlinearities and the equivalent transfer coefficients K_x by representing the nonlinearities in terms of "choppers" [5]; the expression for the nonlinearities are shown in Table 1. The results obtained by computing the fictitious nonlinearities and the values of K_x are cited in Table 2. Figure 1 shows the normalized transfer coefficients K_{x_1} and K_{x_3} for fluctuations in the cases of a relay element and an element with "negative overlaps" (cf. third characteristic from top in Table 1) when a constant component, noise and a sinusoidal signal act on these elements. The graph shows the strong effect of the normalized regular signal proper and the constant component normalized to the amplitude of the regular signal; the constant component shifts the value of the transfer coefficient into the negative region for $\eta = 1$ and $\zeta \approx 1{,}2$.

For a relay element with a dead band that is subjected to the same three components the transfer coefficient K_{x_2} also passes into the negative region (Fig. 2). Figure 3 shows the values of the transfer coefficient K_{x_4} for fluctuations in the case of a linear element with a dead band; Fig. 4 shows the transfer coefficient K_{x_5} for fluctuations in the case of a limiter that is subjected to a constant component, a sinusoidal signal, and noise with a Gaussian distribution. From the figures the strong effect of the dynamics of the regular component on the equivalent transfer coefficient is evident.

3. On the Possibility of Generalizing the Effect of the Dynamics of an Arbitrary Signal on the Transfer Coefficient for Fluctuations

In closed-loop control systems the form of the processes can be described with sufficient accuracy by the expression $y = Ce^{-ax} \sin \Omega x$. In order to estimate the effect of a signal having such a form we expand this expression into a Fourier series:

Table 1. Analytical Expression for Inertialess Nonlinearities

Shape of the characteristic	Mathematical expression in terms of "choppers"
	$y = A\frac{\lvert x\rvert}{x}$
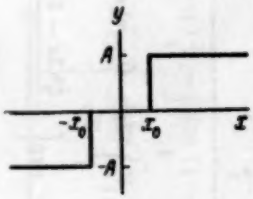	$y = \frac{1}{2}A\left[\frac{\lvert x+x_0\rvert}{x+x_0} + \frac{\lvert x-x_0\rvert}{x-x_0}\right]$
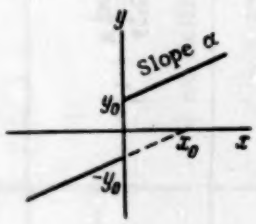	$y = \alpha\left(x + x_0\frac{\lvert x\rvert}{x}\right)$
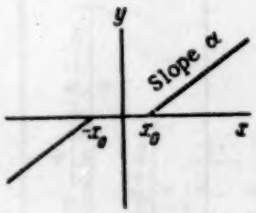	$y = \alpha\left[x - \frac{1}{2}\lvert x+x_0\rvert + \frac{1}{2}\lvert x-x_0\rvert\right]$
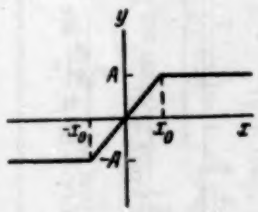	$y = \frac{1}{4}\left\{2\alpha x + \lvert\alpha x + A\rvert - \lvert\alpha x - A\rvert + (2A - \lvert\alpha x + A\rvert - \lvert\alpha x - A\rvert)\frac{\lvert x\rvert}{x}\right\}$

$$y = \frac{a_0}{2} + a_1\cos\omega x + \ldots + a_n\cos n\omega x + b_1\sin\omega x + \ldots + b_n\sin n\omega x,$$

where

$$a_k = \frac{C}{T}\left\{\frac{\Omega - k\omega}{\alpha^2 + (\Omega - k\omega)^2} + \frac{\Omega + k\omega}{\alpha^2 + (\Omega + k\omega)^2} - \right.$$
$$- \frac{e^{-\alpha T}[\alpha\sin(\Omega - k\omega)T + (\Omega - k\omega)\cos(\Omega - k\omega)T]}{\alpha^2 + (\Omega - k\omega)^2} -$$
$$\left. - \frac{e^{-\alpha T}[\alpha\sin(\Omega + k\omega)T + (\Omega + k\omega)\cos(\Omega + k\omega)T]}{\alpha^2 + (\Omega + k\omega)^2}\right\}$$
$$b_k = \frac{C}{T}\left\{\frac{\alpha}{\alpha^2 + (\Omega - k\omega)^2} + \frac{\alpha}{\alpha^2 + (\Omega + k\omega)^2} + \right.$$
$$+ \frac{e^{-\alpha T}[(\Omega - k\omega)\sin(\Omega - k\omega)T - \alpha\cos(\Omega - k\omega)T]}{\alpha^2 + (\Omega - k\omega)^2} +$$
$$\left. + \frac{e^{-\alpha T}[(\Omega + k\omega)\sin(\Omega + k\omega)T - \alpha\cos(\Omega + k\omega)T]}{\alpha^2 + (\Omega + k\omega)^2}\right\}.$$

Table 2. Values of the Effective Nonlinear Characteristic and the Effective Transfer Coefficient

Shape of the characteristic	$g(\gamma)$	K_x
Relay element	$\frac{2A}{\pi}\arcsin\frac{\gamma+\beta}{a}$	$\frac{4\zeta^2\xi}{\sqrt{2\pi^3}}\int_0^1(2x-1-\eta)\arcsin(2x-1)e^{\frac{-\zeta^2(2x-1-\eta)^2}{2}}dx$
Relay element with dead band $V=\frac{x_0}{a}$	$\frac{A}{\pi}\left(\arcsin\frac{\gamma+\beta+x_0}{a}+\arcsin\frac{\gamma-\beta-x_0}{a}\right)$	$\frac{2\zeta^2\xi}{\sqrt{2\pi^3}}\left\{\int_0^1(2x-1-\eta-V)\arcsin(2x-1)\times\right.$ $\times\exp\left[\frac{-\zeta^2(2x-1-\eta-V)^2}{2}\right]dx+\int_0^1(2x-1-\eta+V)\times$ $\left.\times\arcsin(2x-1)\exp\left[\frac{-\zeta^2(2x-1-\eta+V)^2}{2}\right]dx\right\}$
Element with "negative overlaps"	$\alpha(\gamma+\beta)+\frac{2\alpha x_0}{\pi}\arcsin\frac{\gamma+\beta}{a}$	$\alpha\left\{1+\frac{4\zeta^2\xi}{\sqrt{2\pi^3}}V\int_0^1(2x-1-\eta)\arcsin(2x-1)\times\right.$ $\left.\times\exp\left[-\frac{\zeta^2(2x-1-\eta)^2}{2}\right]dx\right\}$

Table 2 (cont'd)

Shape of the characteristic	$g(\gamma)$	K_x
Linear element with dead band $V=\frac{x_0}{a}$	$\alpha(\gamma+\beta)-\frac{\alpha x_0}{\pi}\left(\arcsin\frac{\gamma+\beta+x_0}{2}+\arcsin\frac{\gamma+\beta-x_0}{a}\right)-$ $-\frac{1}{2}\left[\frac{2\alpha(\gamma+\beta)}{\pi}\arcsin\frac{\gamma+\beta+x_0}{a}+\right.$ $\left.+\frac{2\alpha a}{\pi}\sqrt{1-\left(\frac{\gamma+\beta+x_0}{a}\right)^2}\right]+$ $+\frac{1}{2}\left[\frac{2\alpha(\gamma+\beta)}{\pi}\arcsin\frac{\gamma+\beta-x_0}{a}+\right.$ $\left.+\frac{2\alpha a}{\pi}\sqrt{1-\left(\frac{\gamma+\beta-x_0}{a}\right)^2}\right]$	$\alpha\left\{-1-\frac{2\zeta^2}{\sqrt{2\pi^3}}\int_0^1(2x-1-\eta-V)(2x-1)\times\right.$ $\times\arcsin(2x-1)\exp\left[-\frac{\zeta^2}{2}(2x-1-\eta-V)^2\right]dx-$ $-\frac{2\zeta^2}{\sqrt{2\pi^3}}\int_0^1(2x-1)\,(2x-1-\eta+V)\times$ $\times\arcsin(2x-1)\exp\left[\frac{-\zeta^2(2x-1-\eta+V)^2}{2}\right]dx+$ $+\frac{2\zeta^2}{\sqrt{2\pi^3}}\int_0^1\sqrt{1-(2x-1)^2}\left[(2x-1-\eta+V)\times\right.$ $\times\exp\left[-\frac{\zeta^2}{2}(2x-1-\eta+V)^2\right]-(2x-1-\eta-V)\times$ $\left.\left.\times\exp\left[-\frac{\zeta^2}{2}(2x-1-\eta-V)^2\right]\right]dx\right\}$
Limiter $V=\frac{x_0}{a}$	$\alpha(\gamma+\beta)+\frac{\alpha}{2\pi}(\gamma+\beta+x_0)\arcsin\frac{\gamma+\beta+x_0}{a}+$ $+\frac{a\alpha}{2\pi}\sqrt{1-\left(\frac{\gamma+\beta+x_0}{a}\right)^2}-\frac{\alpha}{2\pi}(\gamma+\beta-x_0)\times$ $\times\arcsin\frac{\gamma+\beta-x_0}{a}-\frac{a\alpha}{2\pi}\sqrt{1-\left(\frac{\gamma+\beta-x_0}{a}\right)^2}+$	$\alpha\left\{\frac{1}{2}+\frac{1}{\sqrt{2\pi^3}}\zeta^2\int_0^1(2x-1-\eta-V)\times\right.$ $\times[(2x-1)\arcsin(2x-1)+\sqrt{1-(2x-1)^2}]\times$ $\times\exp\left[-\frac{\zeta^2}{2}(2x-1-\eta-V)^2\right]dx-\frac{1}{\sqrt{2\pi^3}}\zeta^2\int_0^1(2x-1-\eta+V)\times$

Table 2 (cont'd)

Shape of the characteristic	$g(\gamma)$	K_x
	$+\frac{A}{\pi}\arcsin\frac{\gamma+\beta}{a}+\frac{a}{2}\Big[\frac{\gamma+\beta+x_0}{\pi}\arcsin\frac{\gamma+\beta+x_0}{a}-$ $-\frac{\gamma+\beta+x_0}{2}\pi+\frac{a}{\pi}\sqrt{1-\left(\frac{\gamma+\beta+x_0}{a}\right)^2}-$ $-\frac{\gamma+\beta+x_0}{\pi}\arcsin\frac{\gamma+\beta}{a}+\frac{a}{\pi}\sqrt{1-\left(\frac{\gamma+\beta}{a}\right)^2}+$ $+\frac{a}{2\pi}\Big[(\gamma+\beta-x_0)\arcsin\frac{\gamma-\beta}{a}-\frac{\gamma+\beta-x_0}{2}\pi+$ $+a\sqrt{1-\left(\frac{\gamma+\beta}{a}\right)^2}-a\sqrt{1-\left(\frac{\gamma+\beta-x_0}{a}\right)^2}-$ $-(\gamma+\beta-x_0)\arcsin\left(\frac{\gamma+\beta-x_0}{a}\right)\Big]$	$\times\Big[(2x-1)\arcsin(2x-1)+\sqrt{1-(2x-1)^2}\Big]\times$ $\times\exp\Big[-\frac{\zeta^2}{2}(2x-1-\eta+V)^2\Big]dx+\frac{2}{\sqrt{2\pi^3}}\zeta^3V\times$ $\times\int_0^1(2x-1-\eta-V)\Big[(2x-1)\arcsin(2x-1)-\frac{2x-1}{2}\pi+$ $+\sqrt{1-(2x-1)^2}-\sqrt{1-(2x-1-V)^2}-$ $-(2x-1)\arcsin(2x-1-V)\Big]\times$ $\times\exp\Big[-\frac{1}{2}\zeta^2(2x-1-\eta-V)^2\Big]dx+\frac{1}{\sqrt{2\pi^3}}\zeta^3\int_0^1(2x-1-\eta)\times$ $\times\Big\{(2x-1-V)\arcsin(2x-1)-\frac{(2x-1-V)}{2}\pi+$ $+\sqrt{1-(2x-1)^2}-\sqrt{1-(2x-1-V)^2}-$ $-(2x-1-V)\arcsin(2x-1-V)\Big]\times$ $\times\exp\Big[-\frac{1}{2}\zeta^2(2x-1-\eta)^2\Big]dx\Big\}$

Note: For simplicity in performing the computations we have introduced the following substitutions in the table and in the graphs: $\xi=A/a$; $\zeta=a/\sigma$; $\eta=\beta/a$; $V=x_0/a$

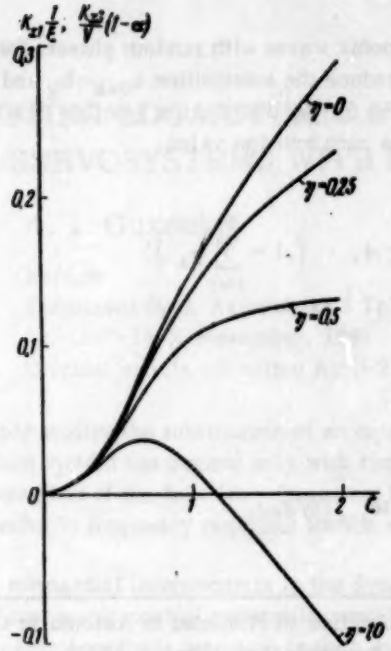

Fig. 1.

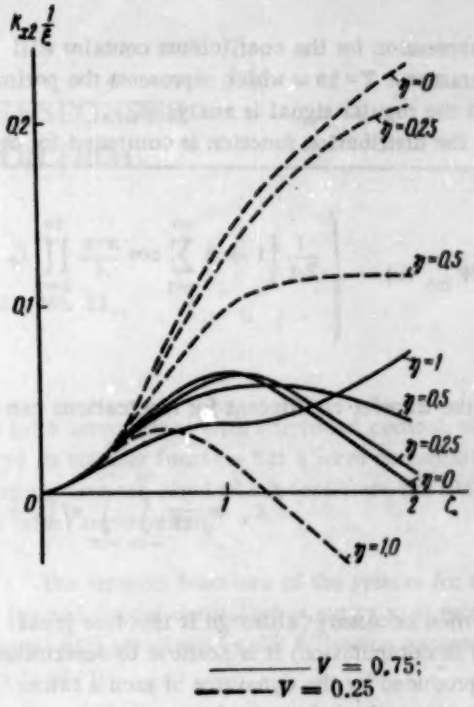

——— $V = 0.75$;
– – – $V = 0.25$

Fig. 2.

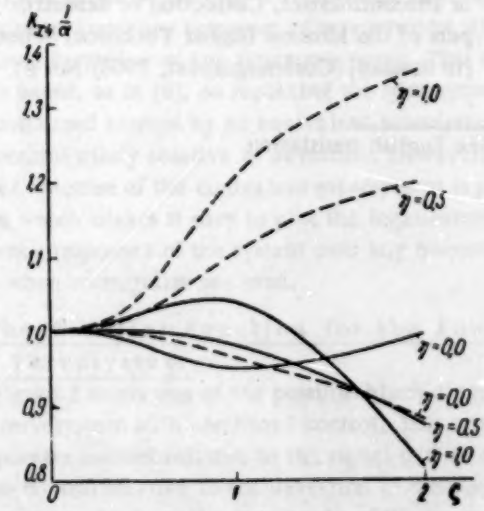

——— $V = 0.25$;
– – – $V = 0.75$

Fig. 3.

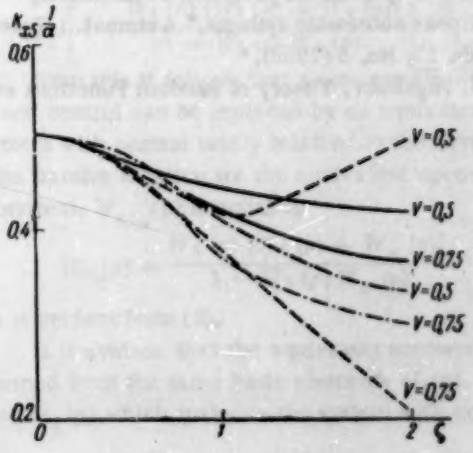

——— $\eta = 1.0$;
– – – $\eta = 0.5$; –·–·– $\eta = 0$

Fig. 4.

The expression for the coefficients contains still another parameter $T = 2\pi\omega$ which represents the period over which the regular signal is analyzed.

In [4] the distribution function is computed for the sum of harmonic waves with random phases. For our case we introduce the substitution $a_{n+k} = b_k$ and obtain the expression for the distribution function of a regular signal with a zero average value:

$$W_{12n}(x) = \begin{cases} \frac{1}{2A}\left[1 + 2\sum_{r=1}^{\infty} \cos\frac{\pi r x}{A} \prod_{k=1}^{2n} I_0\left(\frac{a_k \pi r}{A}\right)\right], & |x| < A, \quad \left(A = \sum_{k=1}^{2n} a_k\right). \\ 0 & |x| > A, \end{cases}$$

Then the transfer coefficient for fluctuations can be written as

$$K_x = \frac{1}{\bar{x}^2} \int_{-\infty}^{\infty} \int_{-\infty}^{\infty} xf\left(x + \frac{a_0}{2} + \beta + y\right) p(x)\, W_{12n}(y)\, dxdy.$$

Thus when necessary (although it involves great difficulties in computation) it is possible to determine the effect produced by the dynamics of such a rather complex signal on the behavior of the transfer coefficients for fluctuations.

In conclusion it is necessary to note the substantial effect produced by the constant signal and the dynamics of the regular signal on the behavior of the transfer coefficient for fluctuations; this underscores the necessity of exercising great care when using statistical linearization methods.

LITERATURE CITED

1. I. E. Kazakov, "Approximate probability analysis of the operational precision of essentially nonlinear automatic systems," Avtomat. i Telemekh. 17, No. 5 (1956).*
2. V. S. Pugachev, Theory of Random Functions and its Application to Problems in Automatic Control [in Russian] (Gostekhizdat, 1957).
3. M. I. Somerville and D. P. Atherton, "Multigain representation for a single-valued nonlinearity with several inputs, and the evaluation of their equivalent gains by cursor method," Proc. IEE, Part C, No. 8 (1958).
4. B. R. Levin, Theory of Random Processes and Its Application in Radio-Engineering [in Russian] (Izd. Sovetskoe Radio, 1957).
5. L. L. Ivanov, On the Solution of a Problem with Functions That Have Discontinuous Derivatives or Discontinuities, Collection of Scientific Papers of the Moscow Higher Technical School [in Russian] (Gosénergoizdat, 1958) No. 87.

* See English translation.

PLOTTING LOGARITHMIC FREQUENCY RESPONSES FOR SERVOSYSTEMS WITH COMBINED CONTROL

A. I. Guzenko

Moscow

Translated from Avtomatika i Telemekhanika, Vol. 21, No. 11,
pp. 1547-1553, November, 1960
Original article submitted April 21, 1960

The paper studies the substitution of an equivalent servosystem for a servosystem with combined control; the equivalent system has control only with respect to deviation, and its transfer function has a form convenient for application of the logarithm frequency response method. Nomograms are cited which facilitate the plotting of logarithmic frequency responses for the elements in the equivalent servosystem.

A substantial improvement in the dynamic properties of automatic control systems is possible when combined control methods are used; in such methods control relative to the basic perturbations acting on the system is combined with control relative to deviation [1-5].

In [6] the possibility of computing servosystems with combined control by the logarithmic frequency response method was demonstrated. This paper developed a convenient method for plotting the logarithmic frequency responses for a servosystem with combined control while taking the perturbation signal into account only in the low-frequency region.

In this paper we develop a method for plotting the logarithmic frequency responses of servosystems with combined control over any frequency range. This method is based, as in [6], on replacing the servosystem with combined control by an equivalent servosystem with control solely relative to deviation. However, the transfer function of the equivalent servosystem is given a form which makes it easy to plot the logarithmic frequency responses of the system over any frequency range when nomograms are used.

1. The Transfer Function for the Equivalent Servosystem

Figure 1 shows one of the possible block diagrams for a servosystem with combined control. This system incorporates control relative to the signal g(t) in addition to control relative to the deviation of the controlled quantity x(t) from the magnitude of the control signal g(t).

To establish the relationship of the quantities $\epsilon(t)$, y(t), and x(t) in the system to the signal g(t), the transforms of the differential equations can be written in the following form:

$$\begin{aligned} \varepsilon(p) &= g(p) - x(p), \\ y(p) &= \varepsilon(p)\, W_1(p) + g(p)\, W_g(p), \\ x(p) &= y(p)\, W_2(p). \end{aligned} \tag{1}$$

The transfer functions of the system for the error $\epsilon(p)$ and for the controlled quantity x(p) relative to the signal g(t) are given by the following expressions on the basis of (1):

$$\begin{aligned} \Phi_{\varepsilon,g}(p) &= \frac{1 - W_2(p)\, W_g(p)}{1 + W_1(p)\, W_2(p)}, \\ \Phi_{x,g}(p) &= \frac{W_2(p)\,[W_1(p) + W_g(p)]}{1 + W_1(p)\, W_2(p)}. \end{aligned} \tag{2}$$

Formulas (2) can be written as

$$\begin{aligned} \Phi_{\varepsilon,g}(p) &= \left[1 + \frac{W_2(p)\,[W_1(p) + W_g(p)]}{1 - W_2(p)\, W_g(p)}\right]^{-1}, \\ \Phi_{x,g}(p) &= \frac{W_2(p)\,[W_1(p) + W_g(p)]}{1 - W_2(p)\, W_g(p)} \times \\ &\times \left[1 + \frac{W_2(p)\,[W_1(p) + W_g(p)]}{1 - W_2(p)\, W_g(p)}\right]^{-1}. \end{aligned} \tag{3}$$

From this it follows that a servosystem with combined control can be replaced by an equivalent servosystem with control solely relative to the deviation. The transfer function for the equivalent open-loop servosystem, $W_{eq}(p)$, is equal to

$$W_{eq}(p) = \frac{W_2(p)\,[W_1(p) + W_g(p)]}{1 - W_2(p)\, W_g(p)}, \tag{4}$$

as is evident from (3).

It is evident that the equivalent servosystem is formed from the same basic elements $W_1(p)$, $W_2(p)$, and $W_g(p)$ which make up the system with combined

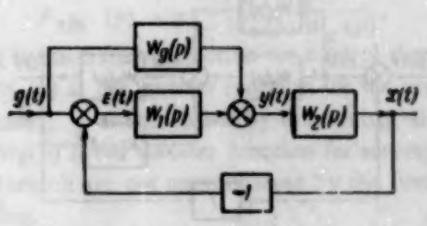

Fig. 1

control. The element $W_g(t)$ in the combined system which performs control relative to the signal forms a direct positive coupling circuit with the element $W_1(p)$, and forms a positive feedback loop with the element $W_2(p)$. Figure 2 shows the block diagram obtained in accordance with (4) for a servosystem with combined control that is equivalent to the block diagram in Fig. 1.

The transfer function of the equivalent servosystem (4) can be written differently:

$$W_{eq}(p) = \frac{W_2(p)\,W_g(p)}{1 - W_2(p)\,W_g(p)}\left[1 + \frac{W_1(p)}{W_g(p)}\right]. \quad (5)$$

This amounts to representing the equivalent servosystem in the form of a serial connection of the element with the transfer function $W_1(p)/W_g(p)$ that is connected by positive direct unity coupling, and the element with the transfer function $W_2(p)\,W_g(p)$ that is connected by unity positive feedback. The block diagram of the equivalent servosystem (5) is shown in Fig. 3.

We denote the transfer function of elements with positive direct unity coupling by $F_{1dir.}(p)$ and the transfer function of elements with unity positive feedback by $F_{1fb}(p)$; i.e., we write

$$F_{1dir.}(p) = 1 + \frac{W_1(p)}{W_g(p)},$$
$$F_{1fb}(p) = \frac{W_2(p)\,W_g(p)}{1 - W_2(p)\,W_g(p)}. \quad (6)$$

Then

$$W_{eq}(p) = F_{1dir}(p)\,F_{1fb}(p). \quad (7)$$

From the above it is evident that the systems in Fig. 1 and Fig. 3 are dynamically equivalent. The subsequent analysis therefore consists of studying the dynamic properties of the system (7). For this purpose it is necessary to plot the frequency response of the system in Fig. 3 for open-loop conditions after first plotting the frequency response of the elements with transfer functions of the form

$$F_{1dir.}(p) = 1 + W(p), \qquad F_{1fb}(p) = \frac{W(p)}{1 - W(p)}. \quad (8)$$

2. Plotting the Logarithmic Frequency Responses for an Element with the Transfer Function $F_{dir.} = W'(p) + W''(p)$

We shall study the more general problem of plotting logarithmic frequency responses for an element with the transfer function

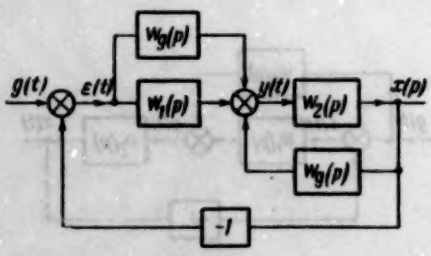

Fig. 2

$$F_{dir.}(p) = W'(p) + W''(p). \quad (9)$$

To do this the amplitude-phase characteristics for elements with transfer functions $W'(p)$ and $W''(p)$ are written as

$$W'(j\omega) = H'(\omega)\,e^{j\theta'(\omega)}, \qquad W''(j\omega) = H''(\omega)\,e^{j\theta''(\omega)}. \quad (10)$$

Therefore

$$W(j\omega) = H(\omega)\,e^{j\theta(\omega)} = H'(\omega)\,e^{j\theta'(\omega)} + H''(\omega)\,e^{j\theta''(\omega)},$$

where $W(j\omega) = F_{dir.}(j\omega)$, or (11)

$$\frac{H(\omega)}{H'(\omega)}\,e^{j[\theta(\omega)-\theta'(\omega)]} = 1 + \frac{H''(\omega)}{H'(\omega)}\cos[\theta''(\omega) - \theta'(\omega)] + j\,\frac{H''(\omega)}{H'(\omega)}\sin[\theta''(\omega) - \theta'(\omega)]. \quad (12)$$

Equation (12) makes it possible to use the known $[H''(\omega) - H'(\omega)]$ db and $[\theta''(\omega) - \theta'(\omega)]^\circ$ to plot the nomograms for the geometric loci of the amplitudes $(H - H')$ db and phases $[\theta(\omega) - \theta'(\omega)]^\circ$; these, in turn, are used to plot the logarithmic amplitude (H, db) and phase (θ°) responses for the element with the transfer function (9).

In [7] we plotted the nomograms for the geometric loci of the values for the amplitude $A(\omega)$ and phase $\varphi(\omega)$ characteristics for a closed-loop system:

$$\Phi(j\omega) = A(\omega)\,e^{j\varphi(\omega)} \quad (13)$$

from the values of the amplitude $H_{ol}(\omega)$ and phase $\theta_{ol}(\omega)$ characteristics of the open-loop system (Fig. 4):

$$W_{ol}(j\omega) = H_{ol}(\omega)\,e^{j\theta_{ol}(\omega)} \quad (14)$$

The relationship between the amplitude-phase responses of the closed-loop $\Phi(j\omega)$ and open-loop $W_{ol}(j\omega)$ systems:

$$\Phi(j\omega) = \frac{W_{ol}(j\omega)}{1 + W_{ol}(j\omega)} \quad (15)$$

can be written as

$$\frac{1}{A(\omega)}\,e^{j\varphi(\omega)} = 1 + \frac{1}{H_{ol}(\omega)}\cos\theta_{ol}(\omega) - j\,\frac{1}{H_{ol}(\omega)}\sin\theta_{ol}(\omega) \quad (16)$$

on the basis of (13) and (14).

Comparing Eq. (12) with Eq. (16), we find that for the condition

$$[H(\omega) - H'(\omega)]\,\text{db} = -A(\omega)\,\text{db},$$
$$\pm[\theta(\omega) - \theta'(\omega)]^\circ = \mp\varphi(\omega)^\circ,$$
$$[H''(\omega) - H'(\omega)]\,\text{db} = -(H_{ol})\,\text{db}, \quad (17)$$
$$\pm[\theta''(\omega) - \theta'(\omega)]^\circ = \mp\theta_{ol}(\omega)^\circ$$

the nomograms plotted for determining the values of the amplitude and phase responses of the closed-loop

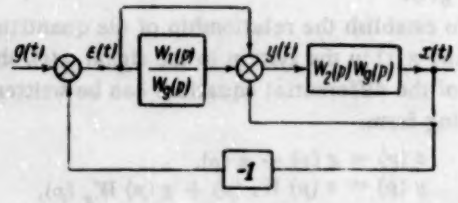

Fig. 3

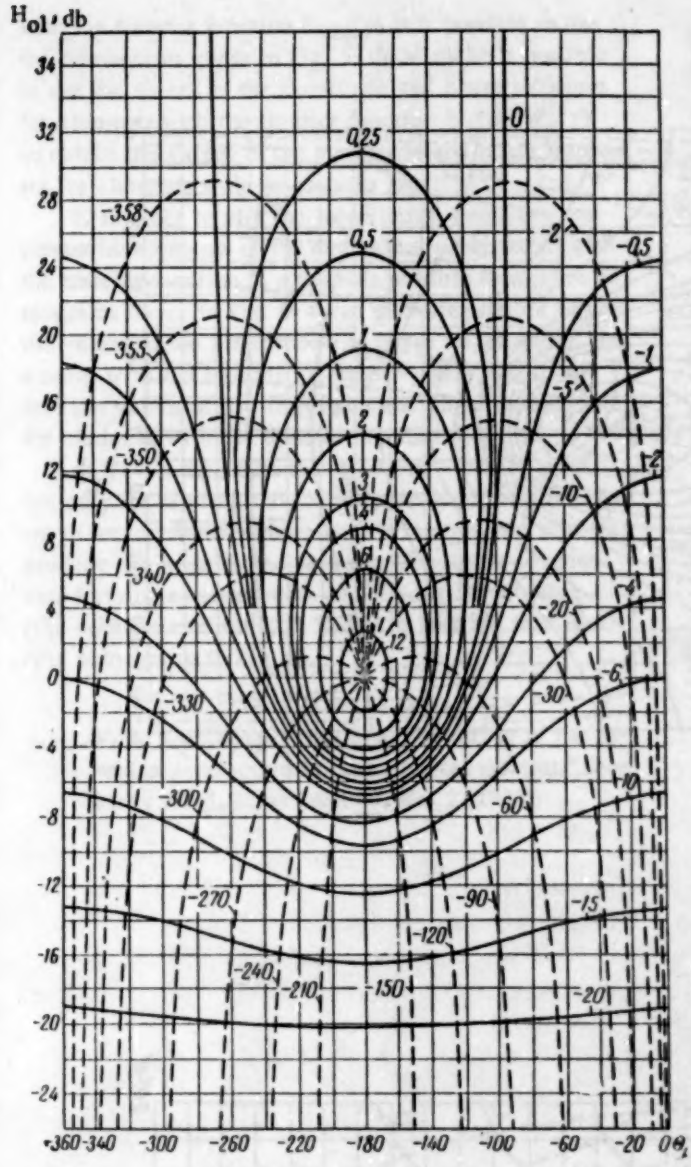

Fig. 4

system from the values of the amplitude and phase responses of the open-loop system can be used for determining the amplitude difference (H'' – H') db and the phase difference $(\theta - \theta')^\circ$.

Figure 5 shows the nomograms for the geometric loci used to determine the difference between the values of the amplitude (H – H') db and phase $(\theta - \theta')^\circ$ characteristics for the elements with the amplitude-phase responses W(jω) and W'(jω) from the difference between the values of the amplitude (H'' – H') db and phase $(\theta'' - \theta')^\circ$ characteristics for the elements with the amplitude-phase responses W''(jω) and W'(jω); this is done on the basis of the nomogram in Fig. 4 and conditions (17). If, as is the case in the example under study, W'(jω) = 1 (i.e., H'(ω) = 0 db and $\theta'(\omega) = 0^\circ$), then Eq. (17) is written as

$$\begin{aligned} H(\omega) &= -A(\omega), \qquad \pm\theta(\omega) = \mp\varphi(\omega), \\ H''(\omega) &= -H_{ol}(\omega), \quad \pm\theta''(\omega) = \mp\theta_{ol}(\omega); \end{aligned} \tag{18}$$

i.e., the nomogram shown in Fig. 5 makes it possible immediately to determine the amplitude-frequency and phase-frequency responses for the system element that is connected by direct positive unity coupling.

3. Plotting the Logarithmic Frequency Responses for an Element with the Transfer Function $F_{1fb}(p) = W(p)/[1-W(p)]$

Assuming $F_{1fb}(j\omega) = B(\omega)e^{j\beta(\omega)}$,

$$W(j\omega) = H(j\omega)\, e^{j\theta(\omega)}, \tag{19}$$

and the amplitude-phase response of the element with the transfer function $F_{1fb}(p) = W(p)/[1+W(p)]$ is

$$\frac{1}{B(\omega)}\, e^{j\beta(\omega)} = -1 + \frac{1}{H(\omega)}\cos\theta(\omega) - j\,\frac{1}{H(\omega)}\sin\theta(\omega). \tag{20}$$

Equation (20) makes it possible to plot the nomograms for the geometric loci of the amplitude (B, db) and phase (β°) from known H, db, and θ°; then it is possible to plot the logarithmic amplitude and phase responses for the element with the transfer function $F_{1fb}(p) = W(p)/[1+W(p)]$.

Comparing Eq. (16) and Eq. (20), we verify the fact that for the conditions

$$\begin{aligned} B(\omega) &= A(\omega), \qquad \beta^\circ = (180 + \varphi)^\circ \\ H(\omega) &= H_{ol}(\omega), \quad \theta^\circ = (180 + \theta_{ol})^\circ \end{aligned} \tag{21}$$

the nomograms plotted from Eq. (16) and (20) are identical.

On the basis of the nomogram in Fig. 4 and conditions (21) Figure 6 shows the nomograms for the geometric loci of the values for the amplitude (B, db) and phase (β°) responses of the element with the amplitude-phase response $F_{1fb}(j\omega)$ as a function of the values for the amplitude (H, db) and phase (θ°) responses of the element with the amplitude-phase response W(jω).

Conclusions

1. In order to plot the logarithmic frequency responses of a servosystem with combined control that is achieved by introducing coupling relative to the control signal (Fig. 1), the block diagram of the equivalent servosystem with control only with respect to deviation must be represented as shown in Fig. 3. In that case the transfer function of the equivalent open-loop servosystem is $W_{eq}(p) = F_{1dir.}(p)\, F_{1fb}(p)$,

where $F_{1dir.}(p) = 1 + \dfrac{W_1(p)}{W_g(p)}$,

$$F_{1fb}(p) = \frac{W_2(p)\, W_g(p)}{1 - W_2(p)\, W_g(p)}.$$

$W_g(p)$ is the transfer function for control signal coupling; $W_1(p)$ is the transfer function for the servosystem elements encompassed by the control-signal coupling; $W_2(p)$ is the transfer function for servosystem elements which are not encompassed by the control-signal coupling.

2. In order to plot the logarithmic frequency responses for the elements of an equivalent servosystem

H, db
0
178
175
170
160
150
120
90
60
30
15
10
6
4
2
1
0,5
0,25
-0,25
-1
-2
-4
-6
-10
-15
-20
-30
-60
-90
-120
-150
-160
-170
-175
-178
36
32
28
24
20
16
12
8
4
0
-4
-8
-12
-16
-20
-24
160°
120
80
40
0
-40
-80
-120
-160

Fig. 6

H''-H', db
0°-0'
20
15
10
6
4
2
1
0,5
0,25
0
-0,25
-0,5
-1
-2
-2,5
-3
-5
-10
-15
-20
-30
-60
-90
-120
-150
-200
-240
-270
-300
-330
-340
-350
-355
-358
24
20
16
12
8
4
0
-4
-8
-12
-16
-20
-24
-28
-32
-36
-60
-100
-140
-180
-220
-260
-300
-360

Fig. 5

with the transfer function $F_{1dir}(p)$ it is possible to use the nomograms given in Fig. 5; these make it possible to use the values of the amplitude and phase responses for elements with the transfer function $W_1(p)/W_g(p)$ to obtain the values of the amplitude and phase responses for elements with the transfer function $F_{1dir}(p)$.

3. In order to plot the logarithmic frequency responses for elements of the equivalent servosystem with the transfer function $F_{1fb}(p)$ it is possible to use the nomograms shown in Fig. 6; these make it possible to use the values of the amplitude and phase responses for elements with the transfer function $W_2(p)W_g(p)$ to obtain the values of the amplitude and phase responses for elements with the transfer function $F_{1fb}(p)$.

4. The nomograms in Figs. 5 and 6 can be used not only for plotting the logarithmic frequency responses of servosystems with combined control, but also for plotting the logarithmic frequency responses of elements forming a circuit with direct positive coupling (the nomograms in Fig. 5) and with positive feedback (the nomograms in Fig. 6).

LITERATURE CITED

1. V. S. Kulebakin, "On the applicability of the invariance principle in real physical systems," Doklady Akad. Nauk SSSR 60, No. 2 (1948).
2. G. M. Ulanov, "Automatic control systems and servosystems which operate on open-loop and closed-loop cycles; the invariance principle," Doklady Akad. Nauk SSSR 96, No. 5 (1954).
3. V. S. Kulebakin, On Basic Problems and Methods in Improving the Performance of Automatic Control Systems, Transactions of the Second All-Union Conference on Automatic Control Theory [in Russian] (Izd. AN SSSR, 1953).
4. B. N. Petrov and G. M. Ulanov, Problems in the Theory of Combined Control, Scientific-Engineering Problems of Automatic Electric Drives [in Russian] (Izd. AN SSSR, 1957).
5. A. G. Ivakhnenko, "On methods for eliminating the steady-state error component in automatic control systems," Doklady Akad. Nauk SSSR 77, No. 6 (1952).
6. V. A. Besekerskii and S. M. Fedorov, Design of Combined-Control Servosystems Using the Method of Logarithmic Frequency Responses, Scientific-Engineering Information on Instrumentation [in Russian] (1957) No. 4.
7. G. Chestnat and R. Maier, Design and Computation of Servosystems and Control Systems [in Russian] (Gosénergoizdat, 1959) Part I.

ON SYNTHESIZING CONTROL PROGRAMS IN SYSTEMS THAT INCLUDE A DIGITAL COMPUTER

P. F. Klubnikin

Moscow

Translated from Avtomatika i Telemekhanika, Vol. 21, No. 11, pp. 1554-1559, November, 1960
Original article submitted May 23, 1960

The paper studies the use of the specified transfer function of the closed-loop system to synthesize the control program of a digital machine which operates in the closed-loop of an automatic control system.

At present automatic control systems which include a digital machine (DM) are widely used in industry. Such systems have a number of advantages over conventional systems [1]; in particular, they make it possible to design control systems with new properties, such as the selection of the optimum mode of operation, the ability to operate in self-adaptive fashion, etc. Moreover, systems including DM have a number of features which require special synthesis methods.

By treating DM as a special kind of pulse element it is possible to use the Ya. Z. Tsypkin theory of pulse systems [2] in order to compute systems that include DM. However, the problems of synthesizing a control program while taking into account the realization of that program in the DM have as yet been treated only cursorily in literature.

Experience in applying DM to automatic control systems shows that in realizing the control program the program volume (in the sense of the number of arithmetic operations and "memory" cells in the machine) is of great significance. This fact must certainly be taken into account for synthesis.

Another important problem in synthesizing the control program is the program stability. Notwithstanding the fact that the stability requirement for the control program in a DM operating in the closed loop of a system has not been considered mandatory by certain authors, experiment shows that an unstable control program is inadequate.

This paper studies the problem of synthesizing the control program for specified performance of the closed-loop system while taking into account the program realization features indicated above.

Synthesis of the Control Program

We shall study the synthesis of the control program for a system whose block diagram is shown in Fig. 1. The devices for conversion of analog quantities to digital quantities and vice versa are referred to the controlled object in the closed loop.

Assume the object is characterized by the transfer function (in the sense of a Laplace transform)

$$W_{\text{H}}(p) = \frac{N(p)}{M(p)},$$

where N(p) and M(p) are polynomials, M(p) = 0 may have one zero root*, and the degree of N(p) is lower than the degree of M(p).

Assuming that the DM computes the control signal during a time T = const (T is the time required for computation cycle) and assuming that a mandatory condition is the presence of a converter at the output of the DM fixing the output quantity of the DM over the time required for the cycle, we obtain

$$W_{\text{H}}^{*}(p) = \sum_{\nu=1}^{k} C_{\nu} \frac{e^{-Tp}}{e^{-Tp_{\nu}} - e^{-Tp}}, \qquad (1)$$

where

$$C_{\nu} = \frac{N(Tp_{\nu})(1 - e^{Tp_{\nu}})}{M'(Tp_{\nu})\,Tp_{\nu}}, \qquad M'(p) = \frac{d}{dp}M(p).$$

In accordance with [3] we use the substitution $e^{-Tp} = z$ and write the transformation (1) as

$$W_{\text{H}}^{*}(z) = \frac{a_k z^k + a_{k-1} z^{k-1} + \ldots + a_1 z}{b_k z^k + b_{k-1} z^{k-1} + \ldots + b_1 z + b_0}, \qquad (2)$$

where a_j and b_j are coefficients that depend on C_ν and $d_\nu = e^{-Tp_\nu}$.

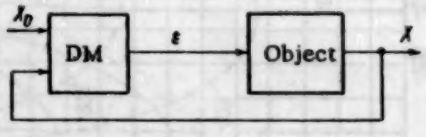

Fig. 1

* This is the case which is most often encountered in practice.

Note that (in contrast to the well-known z transform tables) expression (2) takes into account the fixing of the DM output (i.e., it takes into account the term $(1-e^{-Tp})/p$); therefore the use of (2) simplifies the computations which are required for synthesis of the control program.

Note that the zeros and poles of the rational fraction $\frac{1}{z} W^*_H(z)$ are located outside of the unit circle on the z plane, provided only that the zeros and poles of the transfer function $W_H(p)$ for the object belong to the left half-plane of the plane p. This fact, as we shall see below, facilitates synthesis of a stable control program for specified performance of the closed-loop system.

As we know [3], the control program of the DM can be represented by the transfer function

$$W_M = (z) \frac{A_n z^n + A_{n-1} z^{n-1} + \ldots + A_1 z + A_0}{B_n z^n + B_{n-1} z^{n-1} + \ldots + B_1 z + B_0}, \quad (3)$$

where A_k and B_k are the coefficients to be selected in the synthesis of the control program.

The synthesis of a stable control program (3) is performed for a specified transfer function $W_{sp.}(z)$ of the closed-loop system; this transfer function is selected on the basis of the requirements imposed on the system and the nature of the specified input X_0 (its rate of change, the presence of random noise). It may be written as

$$W_{sp.}(z) = \Gamma_1 z + \Gamma_2 z^2 + \Gamma_3 z^3 + \ldots + \Gamma_m z^m \quad (4)$$

or

$$W_{sp.}(z) = \frac{g_1 z + g_2 z^2 + g_3 z^3 + \ldots + g_l z^l}{g_0 + g_1 z + g_2 z^2 + \ldots + g_{l+m} z^{l+m}}. \quad (5)$$

Note that in the first case (4) the system has a so-called infinite degree of stability and a finite transient response time equal to Tm. It is evident that the condition for first order astatism in the system will be

$$\Gamma_1 + \Gamma_2 + \Gamma_3 + \ldots \Gamma_m = 1. \quad (6)$$

For higher order astatism it is necessary that (4) contain $(1-z)$ to the appropriate power as a multiplier.

In the second case, for which $W_{sp.}(z)$ is written in the form (5), it is necessary that the roots of the denominator in (5) have a modulus greater than unity in order to assure stability of the closed-loop system.

In the analysis we shall assume that the transfer function of the closed-loop system is specified in the form (4) or (5).

By analogy with [4] we subdivide the control program into a series of elements each of which is defined by its transfer function (Fig. 2). However, in contrast to [4], we choose the transfer functions of the elements $D_1(z)$ and $D_3(z)$ in the form

$$D_1(z) = W_3(z), \; D_3(z) = \frac{W_{sp}(z)}{W_H(z)}. \quad (7)$$

Then it follows from a study of the block diagram in Fig. 2 that the transfer function for the closed-loop system is equal to the specified transfer function; i.e., we obtain

$$X^* = W_{sp}(z) X_0^*.$$

The transfer function $D_2(z)$ may be taken in simplest form, and its coefficients are chosen from the conditions of proper stability and stability for the closed loop of the system (Fig. 2). In other words, the transfer function is chosen so that the roots of the equation

$$1 + D_2(z) W_H(z) = 0$$

will have a modulus exceeding unity. For example, sometimes choosing $D_2(z)$ in the form

$$D_2(z) = \frac{a_{11} z + a_{10}}{b_{11} z + b_{10}}, \quad (8)$$

where $\left| \frac{b_{10}}{b_{11}} \right| > 1$, makes it possible to satisfy these conditions.

The resulting control program (Fig. 2) is stable; to verify this it is sufficient to demonstrate the stability of the program corresponding to the element $D_3(z)$. This is very simple to do; in fact, substituting expression (2) into (7), we obtain

$$D_3(z) = \frac{(\Gamma_1 + \Gamma_2 z + \Gamma_3 z^2 + \ldots + \Gamma_m z^{m-1})(b_k z^k + b_{k-1} z^{k-1} + \ldots + b_1 z + b_0)}{a_k z^{k-1} + a_{k-1} z^{k-2} + \ldots + a_2 z + a_1},$$

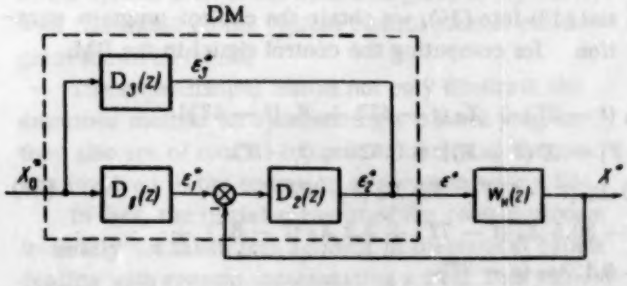

Fig. 2

The stability derives from the fact that the zeros in the denominator coincide with the zeros of $W_H(z)/z$ and lie outside the unit circle. It is evident that the stable control program for the system in Fig. 2 can be written as

$$\varepsilon_1^* = D_1(z) X_0^*, \quad \varepsilon_{cl}^* = D_3(z) X_0^*, \quad (9)$$

$$\varepsilon_2^* = D_2(z)(\varepsilon_1^* - X^*), \quad \varepsilon^* = \varepsilon_2^* + \varepsilon_{cl}^*.$$

The transfer function of the control program (3) will then consist of two transfer functions:

$$\varepsilon^* = W_{1M}(z) X_0^* - D_2(z) X^*,$$

where

$$W_{1M}(z) = D_1(z) D_2(z) + D_3(z).$$

Taking (2), (4), (7), and (8) into account, we write the control program (9) in the form of the difference equations

$$\begin{aligned}
\varepsilon_1(t) &= \Gamma_1 X_0(t-T) + \Gamma_2 X_0(t-2T) + \ldots + \Gamma m X_0(t-mT),\\
\varepsilon_2(t) &= \frac{a_{10}}{b_{10}}[\varepsilon_1(t) - X(t)] + \frac{a_{11}}{b_{10}}[\varepsilon_1(t-T) - X(t-T)] - \frac{b_{11}}{b_{10}}\varepsilon_2(t-T),\\
\varepsilon_3(t) &= C_0 X_0(t) + C_1 X_0(t-T) + C_2 X_0(t-2T) + \ldots + C_i X_0[t-(m+k-1)T] -\\
&\quad - \frac{a_2}{a_1}\varepsilon_3(t-T) - \frac{a_2}{a_1}\varepsilon_3(t-2T) - \ldots - \frac{a_k}{a_1}\varepsilon_3[t-(k-1)T],\\
\varepsilon(t) &= \varepsilon_2(t) + \varepsilon_3(t).
\end{aligned} \tag{10}$$

Here the values of the quantities in each current computation cycle are represented in terms of a function of the argument (t), and the values of the quantities in the preceding nth cycle are given in terms of functions of the argument (t − nT):

$$C_0 = \frac{1}{a_1}\Gamma_1 b_0,$$

$$C_1 = \frac{1}{a_1}(\Gamma_1 b_1 + \Gamma_2 b_0),$$

$$C_2 = \frac{1}{a_1}(\Gamma_1 b_2 + \Gamma_2 b_1 + \Gamma_3 b_0),$$

. . . . . .

$$C_i = \frac{1}{a_1}\Gamma_m b_k.$$

It is obvious that it is not difficult to formulate the program for computing the control signal in the DM using Eq. (10); under these conditions the program volume is small.

Experimental Results

In order to illustrate the above we shall study an example of synthesizing the control program for the DM of a system (Fig. 1) for the case where the object has the transfer function:

$$W_M(p) = \frac{k(T_1 p + 1)}{p(T_2 p + 1)(T_3^2 p^2 + 2\xi T_3 p + 1)}, \tag{11}$$

where

$k = 0.0091$; $T_1 = 1.085$ sec, $T_2 = 2\xi T_3 = 0.05$;

$T_3^2 = 0.0205$ sec^2.

Then for a computing-cycle time T = 0.1 sec we use (1) and (11) to obtain

$$\begin{aligned}
W_H(z) &= \frac{a_4 z^4 + a_3 z^3 + a_2 z^2 + a_1 z}{(1-z)(e^{-\frac{T}{T_3}} - z)(z^2 + k_1 z + k_0)} =\\
&= \frac{a_4 z^4 + a_3 z^3 + a_2 z^2 + a_1 z}{b_4 z^4 + b_3 z^3 + b_2 z^2 + b_1 z + b_0},
\end{aligned} \tag{12}$$

where $a_1 = 0.0625$; $a_2 = -0.045$; $a_3 = 0.00571$; $a_4 = 0.00771$; $b_0 = 9.9$; $b_1 = -24.75$; $b_2 = 24.39$; $b_3 = -10.54$; $b_4 = 1$; $k_0 = 1.277$; $k_1 = -1.747$.

We shall choose the transfer function for the closed-loop system as

$$W_{sp}(z) = \Gamma_1 z + \Gamma_2 z^2 + \Gamma_3 z^3 + \Gamma_4 z^4 + \Gamma_5 z^5, \tag{13}$$

where

$$\Gamma_1 = \Gamma_2 = \Gamma_3 = \Gamma_4 = \Gamma_5 = 0.2. \tag{14}$$

A check of the stability for the closed loop of the system (Fig. 2) shows that the transfer function $D_2(z)$ can be written as the fraction (8). Here the roots of the equation

$$1 + D_2(z) W_H(z) = 0 \tag{15}$$

have a modulus greater than unity for $a_{10} = 1$; $a_{11} = e^{-T/T_2} = 7.8$; $b_{10} = 0.123$; $b_{11} = -0.053$.

Substituting the values of the coefficients in (12) and (13) into (10), we obtain the control-program equation for computing the control signal in the DM:

$$\begin{aligned}
\varepsilon_1(t) &= 0.2[X_0(t-T) + X_0(t-2T) + X_0(t-3T) + X_0(t-4T) + X_0(t-5T)],\\
\varepsilon_2(t) &= 8.13[\varepsilon_1(t) - X(t)] + 63.5[\varepsilon_1(t-T) - X(t-T)] + 0.42\ \varepsilon_2(t-T),\\
\varepsilon_3(t) &= 31.7 X_0(t) - 47.5 X_0(t-T) + 30.5 X_0(t-2T) - 3.2 X_0(t-3T) -\\
&\quad -31.7 X_0(t-5T) + 47.5 X_0(t-6T) - 30.5 X_0(t-7T) + 3.2 X_0(t-8T) +\\
&\quad + 0.72\varepsilon_3(t-T) - 0.091\varepsilon_3(t-2T) - 0.123\varepsilon_3(t-3T),\\
\varepsilon(t) &= \varepsilon_2(t) + \varepsilon_3(t).
\end{aligned} \tag{16}$$

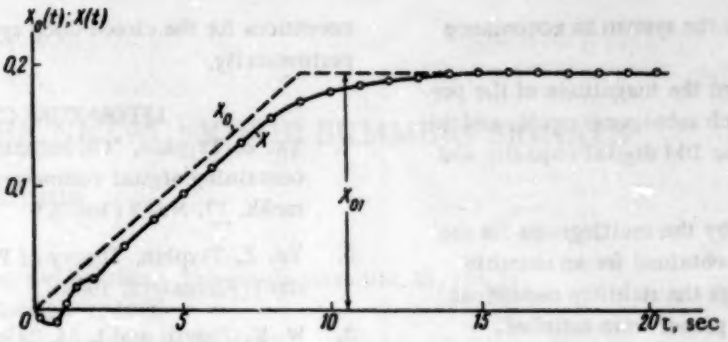

Fig. 3

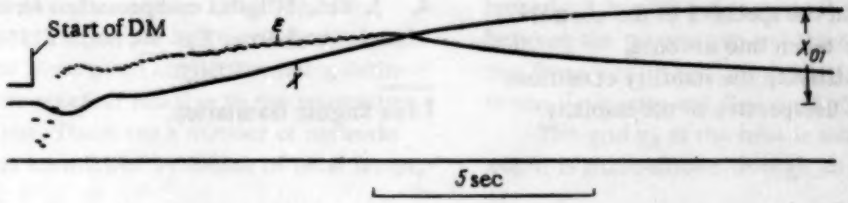

Fig. 4

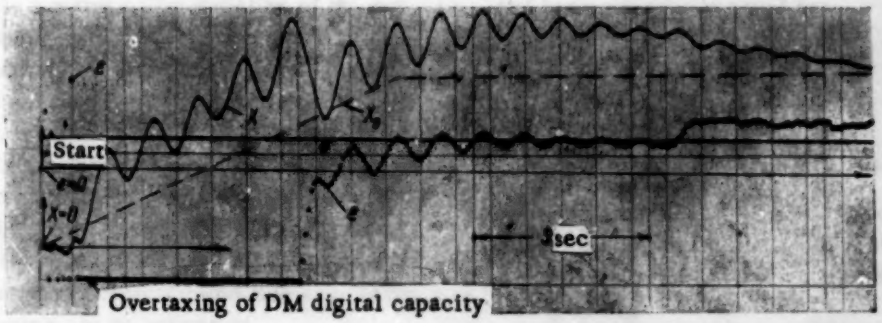

Fig. 5

Figure 3 shows the graph for the control process in the closed-loop system. The control signals were computed from Eq. (16). In performing the experiment we used a specialized high-speed DM which performed the computations during a time equal to a portion of the cycle T = 0.1 sec. We ensured a constant cycle by using a special control network.

From the graph in Fig. 3 it is evident that in accordance with (15) the system has first order astatism and has a velocity gain of approximately 4 sec^{-1}. The segment in Fig. 3 corresponding to the initial operation of the system after it has been energized is especially well illustrated on the typical control process oscillogram shown in Fig. 4.

The experimental results not only illustrate the described method for synthesizing a control program; they also are of special interest in clarifying the specifics involved in the operation of a system with a DM.

In fact, the initial segment of the control process is usually not taken into account in theoretical papers dealing with systems incorporating a DM. This was evidently the reason for previous underestimation of the stability conditions for the control program.

The indicated segment is not a transient response in the general sense of automatic control theory; it arises due to an absence of information in the "memory" of the machine concerning the values of the input and the output quantities over the preceding cycles $X_0(t-hT)$, $X_1(t-hT)$, ... (where h = 1, 2, ..., n), etc., during the initial period of operation for the system. (Incidentally, experiment shows that the process corresponding to the initial segment may also occur when information is lost in the machine due to random failures.) As a result, the input of the object will be subjected to a perturbation (Fig. 3) whose form is determined by the "transfer function of the control program" [in the general case (5)] or by the difference equations (12).

If the control program is stable, then the magnitude of the indicated perturbation decreases; after n cycles, where n is the number of preceding cycles which are used in the program (in our case eight, Fig. 4), it becomes equal to zero. After that the conventional

transient response begins in the system in accordance with (6).

For an unstable program the magnitude of the perturbation increases with each subsequent cycle, and this leads to an overtaxing of the DM digital capacity and cessation of operation.

The above is verified by the oscillograms for the control process (cf. Fig. 5) obtained for an unstable control program even though the stability conditions for the closed-loop system proper were satisfied.

Conclusions

We have analyzed a simple method for synthesizing a control program for specified performance of a closed-loop system when the specifics of the control-program realization are taken into account.

The necessity of satisfying the stability conditions for the control program irrespective of the stability conditions for the closed-loop system was verified experimentally.

LITERATURE CITED

1. Ya. Z. Tsypkin, "On automatic control systems containing digital computers," Avtomat. i Telemekh. 17, No. 8 (1956).†
2. Ya. Z. Tsypkin, Theory of Pulse Systems [in Russian] (Fizmatgiz, 1958).
3. W. K. Zinvill and I. M. Salzer, "Analysis of control systems involving digital computers," Proc. IRE No. 7 (1953).
4. J. Tou, "Digital compensation for control and simulation," Proc. IRE 45, No. 9 (1957).

†See English translation.

A VACUUM-TUBE NETWORK FOR SUMMING SIGNALS

V. D. Vershinin

Moscow

Translated from Avtomatika i Telemekhanika, Vol. 21, No. 11,
pp. 1560-62, November, 1960
Original article submitted May 24, 1960

In servodrives two channels are often used for transmitting signals. The coarse and fine control signals are summed at the input of an amplifier after a definite matching of the receiver relative to the transmitter has been carried out. There are a number of networks for performing this summation by means of neon lamps, transformers, etc.

Figure 1 suggests a simpler and more reliable network for summing such signals.

The principle governing the operation of the network is the following: a bias voltage corresponding to the operating point on the transfer characteristic is applied to one grid of a dual triode, and a negative bias voltage with a magnitude equal to or greater than the cutoff voltage for the tube is applied to the other grid.

We shall derive the expression for the summed ac component of plate voltage as a function of the mismatch angle of the receiver relative to the transmitter.

The receiver produces modulated fine and coarse control signals which can be written as

$$U_c = U_m \sin\theta \sin\omega t,$$
$$U_f = U_m \sin k\theta \sin\omega t,$$

where U_c, U_f are the coarse and fine signals produced by the detectors; U_m is the amplitude of the voltage tapped off from the detectors; θ is the mismatch angle between the transmitter and the receiver; ω is the carrier frequency in sec^{-1}; k is the transfer number between the coarse and fine control detectors.

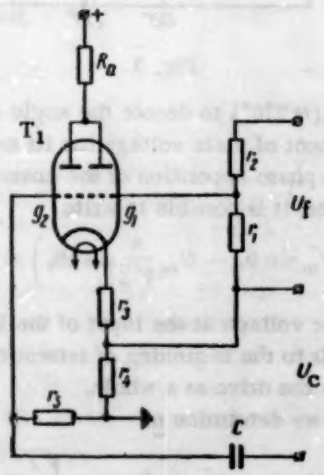

Fig. 1

The grid g_2 of the tube is subjected to a voltage which is phase-shifted through an angle

$$\varphi = \text{arc tg}\frac{x_c}{r_3 + r_{i2} + r_4}$$

and has a magnitude equal to

$$U'_c = U_m m \sin\theta \sin(\omega t - \varphi) - U_{bias2}, \quad (1)$$

where

$$m = \frac{r_4 + r_3}{\sqrt{(r_{i2} + r_3 + r_4)^2 + x_c^2}},$$

r_{i2} is the internal resistance of the coarse-control detector; $U_{bias\ 2}$ is the bias voltage at the second grid and is determined by the voltage drop across the resistors r_3 and r_4.

The first grid g_1 is subjected to a voltage equal to

$$U'_f = U_{max}\, n \sin k\theta \sin\omega t - U_{bias1}, \quad (2)$$

where

$$n = \frac{r_1}{r_1 + r_2 + r_{i1}};$$

$U_{bias\ 1}$ is the bias voltage at the first grid and is determined by the voltage drop across the resistor r_5.

After the signals have been amplified, the plate voltage will be

$$U_a = \mu_1 (U_m n \sin k\theta \sin\omega t - U_{bias1}) + \mu_2 [U_m m \sin\theta \sin(\omega t - \varphi) - U_{bias2}], \quad (3)$$

where μ_1, μ_2 are the gains for the two arms of the tube.

Figure 2 shows the waveshapes of the currents in the left and right halves of the tubes, as well as the waveshape of the over-all plate current for a constant mismatch angle; the figure corresponds to the case where the voltages U'_f and U'_c are in phase opposition. The curve abcd bounds the ordinates for the instantaneous value of the current in the right half of the tube; the curve e bounds the ordinates of the current in the left half of the tube, and the curve abfd bounds the ordinates of the resultant current.

If we approximate the transfer characteristics of the tube by a straight line, then we shall have a constant identical gain for both halves of the tube. In that case the ac component of plate voltage (its effective value) ΔU_a will be given by the following formula when the phase shift angle φ is neglected:

$$\Delta u_a = \mu\,(U'_m \sin k\theta + U''_m \sin\theta), \qquad (4)$$

where $U'_m = \frac{U_{mn}}{\sqrt{2}}$ is the effective value of the voltage at the grid g_1 arriving from the fine-control detector; U''_m is the effective value of the ac voltage component at the grid g_1, corresponding to operation of the left half of the tube.

The graph of the ac component of the plate current as a function of the mismatch angle θ is shown in Fig. 3.

If we design a network with a deep dip Δu_1 (this can be achieved by increasing the coefficient n), it follows that when the drive compensates for a large mismatch angle at the controller output, a smaller voltage will correspond to this mismatch angle range ($k\theta$ = 360° to 180°); this will cause braking of the controlled object.

This fact can be used in certain servodrives (drives which have a high overthrust speed, etc.) in order to reduce the compensation of large mismatch angles; i.e., the rate at which the controlled object arrives at the matched position is reduced.

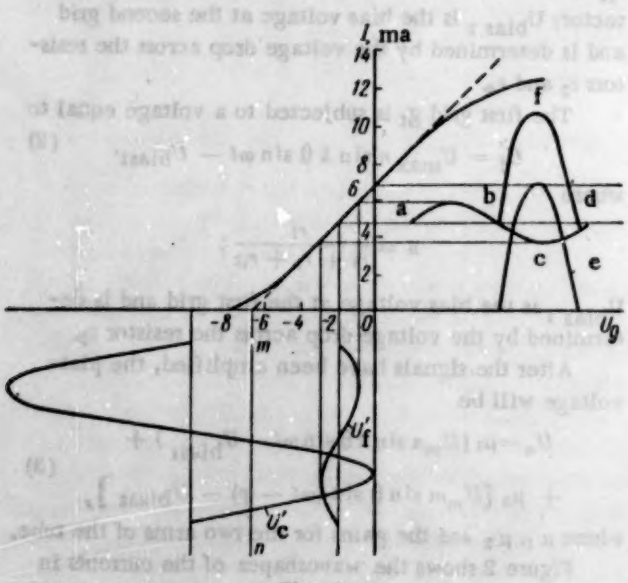

Fig. 2

The bias voltage at the first grid g_1 of the tube and the plate load resistance are chosen from the operating conditions of the amplifier based on the fine-control voltage; their computation is performed on the basis of the requirements imposed on the amplifier. The bias voltage at the second grid g_2 is determined by the required range over which operation must be based solely on the fine-control voltage and the tube cutoff voltage. The range over which the amplifier (drive) is operated by the fine-control signal only (θ_1) is somewhat greater than the required operational precision of the drive:

$$U_{bias2} = U_{co} + U_1, \quad U_1 = U_m m \sin\theta_1 \sin(\omega t - \varphi),$$

where U_{co} is the cutoff voltage of the tube and is determined from the transfer characteristic.

The resistors r_3 and r_4 (Fig. 1) are related by the following expressions:

$$\frac{r_3}{r_3 + r_4} = \frac{U_{bias1}}{U_{bias2}}, \qquad I_a (r_3 + r_4 + r_i + r_a) = U_a.$$

Here I_a is the dc component of the plate current, and r_i is the plate resistance of the tube.

From these relationships we obtain

$$r_4 = \left(\frac{U_a}{I_a} - r_i - r_a\right)\left(1 - \frac{U_{bias1}}{U_{bias2}}\right),$$

$$r_3 = r_4 \frac{U_{bias1}}{U_{bias2}}\left(1 - \frac{U_{bias1}}{U_{bias2}}\right)^{-1}.$$

The capacitor C (Fig. 1) which blocks dc current from the coarse-control detector coil must have a maximum capacitance in order to reduce the phase shift angle φ and increase the coefficient m; however, its magnitude is limited by physical size (in practice it can be equal to 2 μ f). The resistance r_5 is determined from the grid current conditions. In choosing the parameters of the network it is important to know the data for the voltage divider consisting of the resistors r_1 and r_2.

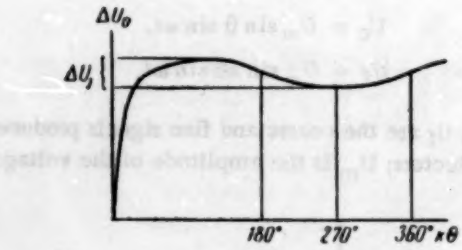

Fig. 3

Using $k\theta_2$ (≈ 270°) to denote the angle for which the ac component of plate voltage has its maximum dip (Fig. 3) due to phase opposition of the coarse and fine control voltages, it is possible to write

$$\mu\left(U''_m \sin\theta_2 - U_m \frac{n}{\sqrt{2}} \sin k\theta_2\right) = \Delta u,$$

where Δu is the voltage at the input of the last stage and corresponds to the beginning of saturation in the amplifier or in the drive as a whole.

From this we determine n:

$$n = (\Delta u + \mu U''_m \sin\theta_2)\frac{\sqrt{2}}{\mu U_m \sin k\theta_2}.$$

In designing and checking the network we use the following parameters: T is a dual "6N7S" triode;* r_1 = = 27 kohm; r_2 = 1 meg; r_3 = 1 kohm; r_4 = 4 kohm; r_5 = = 27 kohm; r_a = 20 kohm; C = 2μf.

The signals at the grids of the tube were supplied from "SS-405" selsyns, and the transfer number between selsyns was 20.

Notwithstanding its simplicity, the network analyzed above not only sums signals but also amplifies them.

* The specifications for the "6N7S" tube are: $\underline{E}_f$ = 6.3 v, $\underline{I}_f$ = 0.8 amp, $\underline{E}_p$ = + 300 v, $\underline{I}_p$ = 3.5 ma, $\underline{E}_{c_1}$ = −6 v, g_m = 1600 μmho, $\underline{r}_p$ = 22 k, $\underline{R}_L$ = 16 k, $\underline{P}_p$ = 6 w, $\underline{P}_{out}$ = = 4.2 w [Publisher's note].